Dissertation
submitted to the
Combined Faculties for the Natural Sciences and for Mathematics
of the Ruperto-Carola University of Heidelberg, Germany
for the degree of
Doctor of Natural Sciences

presented by

Priyanka Noel Fernandes

Master of Science

born in Mumbai, India

Oral-examination: 11.10.2016

Differences in antigen presentation between sporozoite and parasitised-erythrocyte infections uncovers divergent mechanisms in the development of experimental cerebral malaria

Referees: Prof. Dr. Michael Lanzer

Dr. Ann-Kristin Mueller

Hiermit erkläre ich, dass ich die vorliegende Arbeit von Juli 2011 bis August 2016 unter Anleitung von Dr. Ann-Kristin Mueller selbst durchgeführt habe und schriftlich ausgearbeitet habe. Ich habe mich keiner anderen Hilfmittel und Quellen bedient als den hier ausdrücklich erwähnten.

....

Datum Priyanka Fernandes

Table of contents

Summary

Cerebral malaria (CM) is one of the most severe manifestations of *Plasmodium falciparum* infections, characterised by seizures, coma and death within a short time period. The aetiology of the disease remains poorly understood and is limited by ethical constraints. A large body of research dedicated to CM has therefore focussed on delineating the mechanisms involved using the rodent model of malaria. Infection of mice with sporozoites or infected red blood cells (iRBCs) of *Pb*ANKA parasites recapitulates several features of CM including haemorrhaging, oedema and blood-brain barrier breakdown and is termed experimental CM (ECM).

The development of ECM relies on a complex series of interactions between the parasite and host. Although regarded as an immune-mediated pathology, sequestration of iRBCs is considered a central event for ECM to ensue, thus supporting the notion that ECM is purely the outcome of host-parasite interactions at the pathological blood stage. However, previous studies have shown that both surface antigens of iRBCs and the host's immune response differ between naturally transmitted (sporozoites) and blood-passaged parasites. This thesis aims at describing the role of a novel *Plasmodium* antigen in the development of ECM and outlining differences in ECM progression between naturally transmitted and blood-passaged parasites.

The antigen, *Pb*maLS_05 is expressed in both liver-stage- and blood-stage schizonts and localises to the apicoplast of individual merozoites. Deletion of the endogenous *Pb*maLS_05 gene had no effect on parasite viability, but abrogated the development of ECM in mice, after both sporozoite and iRBC infections. *PbmaLS*_05 (-) parasites displayed retarded growth rates in the blood and enhanced clearance by the spleen, both of which were more pronounced on the days when *Pb*ANKA wild type infected mice showed signs of ECM. The absence of ECM in *PbmaLS*_05 (-) infected mice was accompanied by reduced infiltration of activated $CD8^+$ T cells within the brain and reduced cross-presentation of a known parasite antigen (GAP50) by the brain endothelium, after iRBC but not sporozoite infection. Further investigations into sporozoite infections revealed an important role for *Pb*maLS_05 in the priming of $CD8^+$ T cells responsible for causing ECM. These data thus highlight the existence of multiple mechanisms leading up to the development of ECM relevant to sporozoite or iRBC

infections, with potential implications for vaccines or therapeutics designed to alleviate CM.

Zusammenfassung

Die zerebrale Malaria (CM) ist eine der schwerwiegendsten Auswirkungen einer *Plasmodium falciparum*-Infektion – klinisch auffällig durch das Auftreten von Krämpfen, Koma und Tod innerhalb einer kurzen Zeitspanne. Die Ursache der Erkrankung ist bislang immer noch wenig verstanden – limitiert durch ethische Einschränkungen bezüglich der Verfügbarkeit von humanem Patientenmaterial. Ein Großteil der Forschung auf dem Gebiet der CM konzentriert sich deshalb auf die Beschreibung der relevanten Mechanismen im Nagetiermodell der Malaria. Die Infektion von Mäusen mit Sporozoiten oder infizierten roten Blutkörperchen (iRBC) des Nagetier-Malaria-Parasitenstammes *Pb*ANKA rekapituliert einige Charakteristika der CM wie z.B. Einblutungen, Ödeme sowie den Zusammenbruch der Blut-Hirn-Schranke und wird daher als experimentelle zerebrale Malaria bezeichnet (ECM).

Die Entwicklung von ECM beruht auf einer komplexen Abfolge von Interaktionen zwischen Parasit und Wirt. Obwohl, als eine durch das Immunsystem vermittelte Pathologie angesehen, wird der Sequestrierung von iRBCs eine zentrale Rolle bei der Entwicklung von ECM zugeschrieben. Die Auffassung dadurch unterstützt, dass ECM alleinig das Ergebnis von Wirt-Parasit-Interaktionen ist, welche während des pathologischen Zyklus im Blut stattfinden. Allerdings konnte in Studien gezeigt werden, dass sich nach Injektion von Sporozoiten, welche in einer natürlichen Infektion übertragen werden bzw. von Blut-passagierten Parasiten sowohl die Oberflächenantigene auf iRBCs als auch die Immunantwort des Wirtes unterscheiden. Das Ziel dieser Arbeit war daher die Rolle eines neuartigen *Plasmodium*-Antigens im Bezug auf die Entwicklung von ECM zu beschreiben und zudem Unterschiede in der Progression von ECM nach Infektion mit (natürlich, übertragenen) Sporozoiten bzw. im Blut passagierten Parasiten aufzuzeigen.

Das Antigen *Pb*maLS_05 ist sowohl in Leberstadien- als auch Blutstadien-Schizonten exprimiert und lokalisiert im Apikoplasten in individuellen Merozoiten. Die Deletion des endogenen *Pb*maLS_05 Lokus (*Pb*maLS_05 (-)) hatte keinen Effekt auf die Lebensfähigkeit der Parasiten. Allerdings ist die Entwicklung von ECM in Nagetieren, sowohl nach Sporozoiten als auch nach iRBC Infektion, unterbunden. *PbmaLS*_05 (-) Parasiten zeigten verlangsamte Wachstumsraten im Blut und eine erhöhte Eliminierung

durch die Milz. Dies war besonders ausgeprägt an Tagen, an denen Mäuse, welche mit *Pb*ANKA WT Parasiten infiziert waren, Anzeichen von ECM gezeigt haben. Der Schutz vor ECM in *Pb*maLS_05 (-) infizierten Tieren ist assoziiert mit einer reduzierten Infiltration von aktivierten $CD8^+$ T-Zellen in das Gehirn und einer reduzierten *cross*-Präsentation eines bekannten Parasitenantigens (GAP50) durch Endothelzellen des Gehirns nach iRBC aber nicht nach Sporozoiten Infektion. Weitere Untersuchungen zum Mechanismus nach Sporozoiten-Infektion zeigten eine wichtige Rolle für *Pb*maLS_05 im *Priming* von $CD8^+$ T-Zellen, welche für die Entwicklung von ECM verantwortlich sind. Die Daten dieser Arbeit unterstreichen somit die Existenz von mehreren Mechanismen, welche zur Ausbildung von ECM führen, in Abhängigkeit von der Infektion von Sporozoiten oder iRBCs. Diese Erkenntnisse haben mögliche Auswirkungen auf die Entwicklung von Impfstoffen oder Medikamenten zur Behandlung der CM.

List of Abbreviations

ACP	Acyl carrier protein
AMA-1	Apical membrane antigen
APC	Antigen presenting cell
Apo	Apolipoprotein
B6	C57BL/6
BBB	Blood-Brain Barrier
BSA	Bovine Serum Albumin
CCL	Chemokine (C-C motif) ligand
CCR	C-C chemokine receptor
CD	Cluster of Differentiation
CD40L	Cluster of Differentiation 40 ligand
cDNA	Complimentary
CDPK6	Calcium-dependent protein kinase 6
CelTOS	Cell-traversal protein for ookinetes and sporozoites
CM	Cerebral Malaria
CNS	Central Nervous System
CPS	Chemoprophylaxis with sporozoites
CQ	Chloroquine
CSA	Chondroitin sulfate A
CSP	Circumsporozoite protein
CT	C-terminal
CTL	Cytotoxic Lymphocytes
CTLA-4	Cytotoxic T-Lymphocyte Associated Protein 4
CXCL10	C-X-C motif chemokine 10
CXCR3	C-X-C Motif Chemokine Receptor 3
DC	Dendritic Cell
DIC	Differential Interference Contrast
EC	Endothelial Cell
ECM	Experimental Cerebral Malaria
EGFP	Enhanced Green Fluorescent Protein
ELISpot	Enzyme-Linked ImmunoSpot
EPCR	Endothelial protein C receptor
EphA2	Ephrin type A receptor 2
EPO	Erythopoeitin
ETRAMPS	Early Transcribed Membrane Proteins
EXP-1	Exported Protein 1
FACS	Fluorescence-activated cell sorting
FCS	Fetal Calf Serum
G6PD	Glucose-6-phosphate dehydrogenase
GAP	Genetically attenuated Parasites
GAP50	glideosome associated protein 50
GPI	Glycosylphosphatidylinositols
GRASP	Golgi re-assembly stacking protein
h.p.i.	hours post infection
HCM	Human Cerebral Malaria
HRPII	Histidine-rich protein

HSP70	Heat Shock Protein 70
HSPG	Heparan Sulfate Proteoglycans
ICAM-1	ntercellular Adhesion Molecule 1)
IFA	Immunofluorescence Assay
IFN-γ	Interferon gamma
IgG	Immunoglobulin G
IL	Interleukin
iRBC	Infected red blood cell
KO	*Pb*maLS_05 (-)
L-FABP	Liver Fatty acid-binding protein
LFA-1	Lymphocyte Function-associated antigen 1
LS	Liver stage
maLS_05	Malaria Attenuated Liver Stage Antigen 05
MAPK	Mitogen-activated protein kinases
MHC	Major Histocompatibility complex
MIP-α	Macrophage inflammatory protein alpha
MRI	Magnetic resonance imaging
NF-κB	Nuclear Factor kappa B
NK	Natural Killer Cells
NKT	Natural Killer T Cells
NO	Nitric Oxide
NT	N-terminal
ORF	Open Reading Frame
PAMP	Pathogen-associated Molecular Patterns
Pb	*Plasmodium berghei*
PBS	Phosphate Buffered Saline
PC	Phospatidylcholines
Pf	*Plasmodium falciparum*
*Pf*EMP-1	Plasmodium falciparum erythrocyte membrane protein 1
PV	parasitophorous vacuole
PVM	parasitophorous vacuole membrane
RACE	Rapid Amplification of cDNA ends
RAS	Radiation-attenuated sporozoites
RBC	Red Blood Cell
RMCBS	Rapid Murine Coma and Behaviour Scale
ROS	Reactive Oxygen Species
SPECT	Sporozoite microneme protein essential for cell traversal
SP	Sulfadoxine-Pyrimethamine
SRB1	Scavenger receptor class B 1
SSP3	Sporozoite Surface Protein
T regs	Regulatory T cells
Th1 & Th2	T-helper 1 and 2
TLR	Toll-like receptor
TNF-α	Tumor Necrosis Factor alpha
TRAP	Thrombospondin-related anonymous protein
Tregs	Regulatory T cells
VEGF	Vascular endothelial growth factor
WB	Western Blotting
WT	*Pb*ANKA wild type

Chapter 1

Introduction

1.1 Cerebral malaria

Cerebral malaria is a term that is often associated with infections caused by *Plasmodium falciparum* parasites. In clinical terms, it is one of the most common non-traumatic encephalopathies, affecting about 2-3 million people annually, especially those living in tropical countries (1). Until the 1980s, any disorder of the central nervous system observed during infections with any *Plasmodia* species was widely regarded as CM by clinicians. However, the loose association of the term CM with CNS disorders was inaccurate, since it did not distinguish between other causes such as meningitis and mixed infections with *P.falciparum*. The definition of CM was therefore amended to "a state of persistent coma accompanied by the presence of *Plasmodium* infected erythrocytes in peripheral circulation, after other causes of encephalopathy such as viral or bacterial meningitis have been excluded and hypoglycaemia has been accounted for" (1, 2).

Both *Plasmodium falciparum* and *Plasmodium vivax* are responsible for the majority of malaria-related deaths in sub-Saharan Africa, Southern and South-east Asia. However, from all malaria infections, *Plasmodium falciparum* alone accounts for 80% mortality, mainly in children and travellers from malaria-naïve countries (3). Mortality is influenced by a number of factors such as age, endemic exposures, access to intensive medical care and transmission intensities, all of which are linked to differences in clinical presentation and pathology. For example, clinical features such as seizures, retinopathy, metabolic acidosis, hypoglycaemia and brain swelling are frequently observed in both children and adults (4, 5). However, incidences of neurological sequelae are less common in South Asian adults compared to African children, even though recovery from a coma is lower in these adults (6). In adults, CM is part of a severe systemic disease involving multiple organs, a feature that frequently accounts for increased mortality (7). CM in Southeast Asian adults alone accounted for 50% mortality when accompanied by renal failure and metabolic acidosis but averaged to 8% in the absence of organ dysfunction (1). Other symptoms like retinal haemorrhaging, pulmonary oedema or respiratory distress also develops in a fraction of patients (1, 8). In malaria-endemic areas however, children

gradually acquire mechanisms to limit severe disease and control parasite replication, due to which incidences of CM are rare in adults (9).

In contrast, children living in Sub-Saharan Africa, especially those below the age of five are more susceptible to developing CM. Younger children rarely develop renal failure or pulmonary oedema but typically present with fever, multiple and prolonged seizures, different patterns of neurological sequelae and other features of brain death (10, 11). Symptomatic features commonly include abnormal respiratory patterns, posture, motor dysfunction and retinopathy, all of which are believed to result from increased intra-cranial pressure and brain swelling observed with MRI **(Figure 1.1)** (12). Most deaths occur within the first 48 hours after admission to a hospital; however a sizeable proportion of children that survive develop neurological deficits such as cognitive impairment, paralysis, epilepsy, blindness and speech disorders (13, 14). It is therefore not surprising that cerebral malaria is regarded as one of the leading causes of neurodisability in children living in malaria endemic areas (15). Incidences of CM in older children are usually lower and the clinical pathophysiology is more comparable to that of adults.

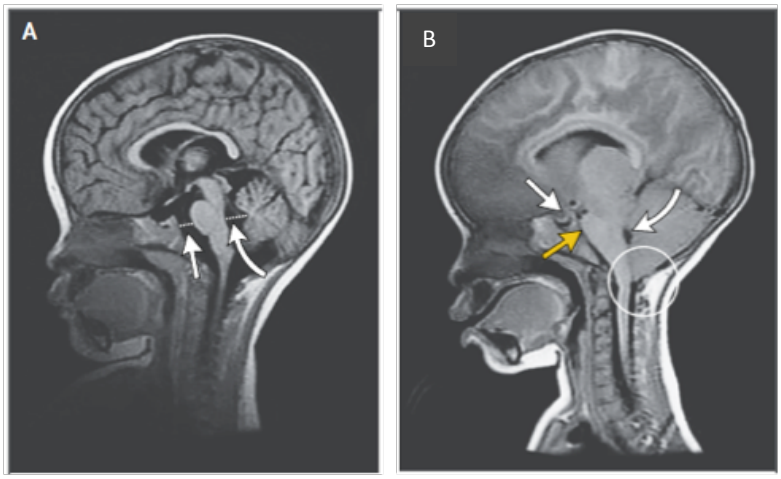

Figure 1.1 MRI imaging of cerebral malaria (12). Comparative MRI images of a child with a normal brain (A) and a child with cerebral malaria (B) show a severe increase in brain volume and loss of structural integrity in the latter.

Due to inconsistencies in clinical presentation and neuropathological manifestations between patients, the prognosis and treatment of CM remains a complex task. The management of clinical complications moreover depends on a thorough understanding of the disease, the mechanistic basis of which is lacking.

1.2 The pathogenesis of cerebral malaria

CM is part of a spectrum of complications caused by infection with parasites of the genus *Plasmodia.* There are five known species of *Plasmodium* that afflict humans, though the clinical manifestations of CM can exclusively be attributed to infections with *P. falciparum* parasites. Rare cases of cerebral symptoms arising from an infection with *P. vivax* have been reported (16-19), however mixed infections with *P. falciparum* cannot be excluded (20). The life cycle of *Plasmodium falciparum* parasites is complex and involves several different life cycle stages that are adapted to several different tissues.

1.2.1 The pre-erythrocytic stage

Though the manifestations of cerebral malaria are primarily caused by intra-erythrocytic stages of *P. falciparum* parasites, the initiation and spread of infection occurs through the bite of a female *Anopheles* mosquito. The phase between the bite of an infected mosquito and the intra-erythrocytic cycle constitutes the pre-erythrocytic stage of malaria infection, which is both clinically silent and represents an ideal target for vaccination strategies due to low parasite densities (21). An overwhelming part of information about the pre-erythrocytic phase of the parasite life cycle comes from studies using rodent parasite strains; although the notion that conserved mechanisms exist between both rodent and human malaria parasite strains, is generally accepted.

Gravid female mosquitoes rely on an occasional blood meal for the development of their eggs and in the process inoculate an average of ~50-100 *Plasmodium* sporozoites into the dermis of the host (22-24). *Plasmodium* sporozoites are motile in the skin and move in random trajectories (25, 26) traversing an array of dermal tissue before locating and invading blood vessels (25, 27). Even though motility serves to evade engulfment by phagocytic cells in the dermis (28) only about 50% of sporozoites deposited into the skin enter the blood stream, while a significant proportion end up in the lymphatic system or remain at the inoculation site **(Figure 1.2)** (29, 30). Sporozoites that enter the lymphatic system are cleared by immune cells while a proportion those left behind in the skin invade and mature into exo-erythrocytic forms within skin cells (31-33). It was shown that an immune response is elicited in both cases (34) that could partially contribute to cell-mediated immunity against subsequent infections.

Sporozoites that successfully enter the blood circulation are passively carried to the liver, where they sequester due to interactions between sporozoite surface proteins like CSP

and TRAP (35, 36), and HSPGs expressed as fenestrated protrusions by hepatocytes, stellate and Kupffer cells **(Figure 1.2)** (37, 38).

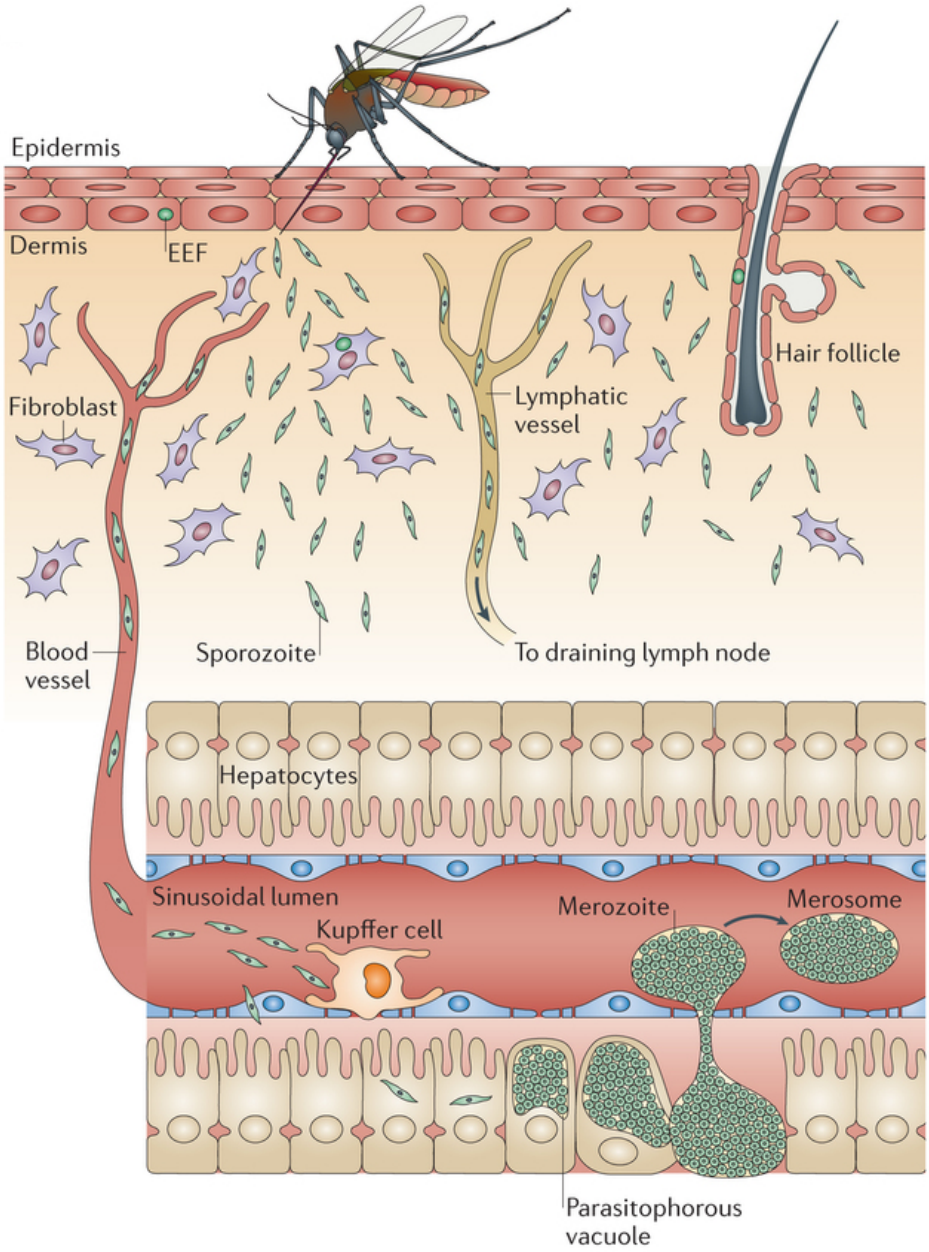

Figure 1.2 The pre-erythrocytic phase of the *Plasmodium* life cycle (28). The pre-erythrocytic stage involves several steps and barrier crossings. A fraction of sporozoites deposited into the dermis enter the blood stream and journey to the liver. An arrest within the sinudoidal lumen of the liver is mediated by several interactions between sporozoites and cells of the liver parenchyma. Sporozoites traverse through several hepatocytes before finally invading one within which they differentiate into merozoites that are then packaged into merosomes and released into the blood stream.

Due to these interactions, sporozoites glide along the endothelium, until they encounter a Kupffer cell that they use as a 'gateway' to hepatocytes (27, 39). Sporozoites traverse through Kupffer cells by employing several different proteins such as SPECT (40), CelTOS (41) and PL (42) which also play an important role in exiting the skin (43).

However, intravital imaging of wild-type sporozoites moreover has suggested that sporozoites use multiple pathways to cross the sinusoidal space (39), thus questioning the need for passage through Kupffer cells (43). Those that go through the sinusoidal barrier and across the space of Disse, trans-migrate through several hepatocytes, in a process termed as 'cell wounding', before finally invading and developing within a hepatocyte (44). Recent evidence has suggested that sporozoites use independent pathways for transmigration and productive invasion of hepatocytes, with the former requiring the formation of a transient vacuole while the latter employing a parasitophorous vacuole (45). Several key players in hepatocyte invasion have been identified over the years, including host receptors like tetraspanin CD81 (46), SRB1 (47) and EphA2 (48) along with parasite molecules such as AMA-1, CSP and TRAP (38, 49-51). However, evidence for direct interaction between host receptors and their corresponding parasite molecule is missing (52).

Sporozoites that actively invade hepatocytes through receptor-ligand interactions recruit host-cell actin to the site of invasion (53, 54). Commitment to invasion is followed by the formation of a parasitophorous vacuole that occurs through invagination of the host-cell plasma membrane (27, 30), aided by discharge of sporozoite rhoptry proteins (46, 55). The association of the host-cell cytoskeleton with the parasitophorous vacuole membrane results in passive translocation of the parasite to the peri-nuclear region of the host hepatocyte, though the exact reason for this event remains unclear (30). In order to prevent degradation by host cell lysosomes, parasites remodel the PV and stay hidden (53) whilst hijacking a plethora of host pathways to support their development, including the host apoptotic machinery (56-58). Within the protected enclosures of the PVM, parasites undergo several rounds of nuclear division paralleled with branching and division of the parasite apicoplast and mitochondria (59). To accommodate the growing parasite, the PVM expands by incorporation of host cell lipids like phosphatidylcholine (60). Insertion of different parasitic proteins such as ETRAMPS (61) and EXP-1 (62) into the PVM further supports its structure and fuels parasite growth through interactions with and incorporation of liver-fatty acid binding protein (63), ApoH (64) and other host cell lipids. Nuclear division terminates with the formation of thousands of merozoites, each containing a single apicoplast and mitochondrium, that are released into the host cell cytosol upon PVM rupture (65). Merozoites packaged into vesicles called merosomes bud off into the sinusoidal lumen (66) wrapped in a host cell-derived membrane that protects them from phagocytosis **(Figure 1.2)** (67, 68). After reaching

the pulmonary capillaries, these merosomes eventually disintegrate and release free merozoites into the blood stream (69).

1.2.2 The intra-erythrocytic stage

The intra-erythrocytic stage is perhaps the only stage in the entire parasite life cycle that has been extensively investigated. Free merozoites released into the bloodstream upon merosome rupture drift passively until they randomly collide with a red blood cell (70). *P. falciparum* parasites infect RBCs of all ages in circulation (71) by exploiting multiple ligand-receptor interactions to achieve successful invasion (72, 73). RBC invasion is an active process and occurs through a tight junction that causes an invagination of the host-cell plasma membrane that further envelops the invading merozoite to form the PV (74). Within the PV, *Plasmodium* parasites undergo extensive morphological changes while developing from ring to trophozite followed by schizogony to form new merozoites **(Figure 1.3)** (75).

Intra-erythrocytic parasites rely heavily on host cell haemoglobin and serum amino acids, proteins and lipids (76) to sustain growth and multiplication (77). Acquisition of serum components is achieved by the introduction of transporters in the RBC membrane (77) that help the parasite tap into the extracellular milieu. Parasites also export proteins coded by antigenically variable families like the *var* genes RIFINs and STEVORs to the RBC surface, that function to mask the infected RBC from immune surveillance (78). RIFINS additionally mediate a process of spontaneous adhesion to uninfected RBCs, called 'rosetting' which enhances the infection of new RBCs (79).

Such modifications to the RBC membrane reduce the deformability of an infected cell and mark it for destruction and removal by the spleen (80, 81). In order to circumvent splenic clearance, parasites additionally express polymorphic adhesins such as *Pf*EMP-1 on the RBC surface in electron dense structures termed 'knobs', which mediate cytoadherence to endothelial cells and sequestration within different organs (78). Knobs are also expressed on the surface of other *Plasmodium* strains like *P. vivax, P. malariae* and *P. brasilianum* but do not always play a role in sequestration (82, 83). In contrast, certain rodent strains of *Plasmodium* sequester in spite of the absence of knobs (84). Typically, trophozoite and schizont stages of the parasite sequester away from circulation until differentiation is complete and new merozoites are released into the blood stream, which initiate the next round of replication.

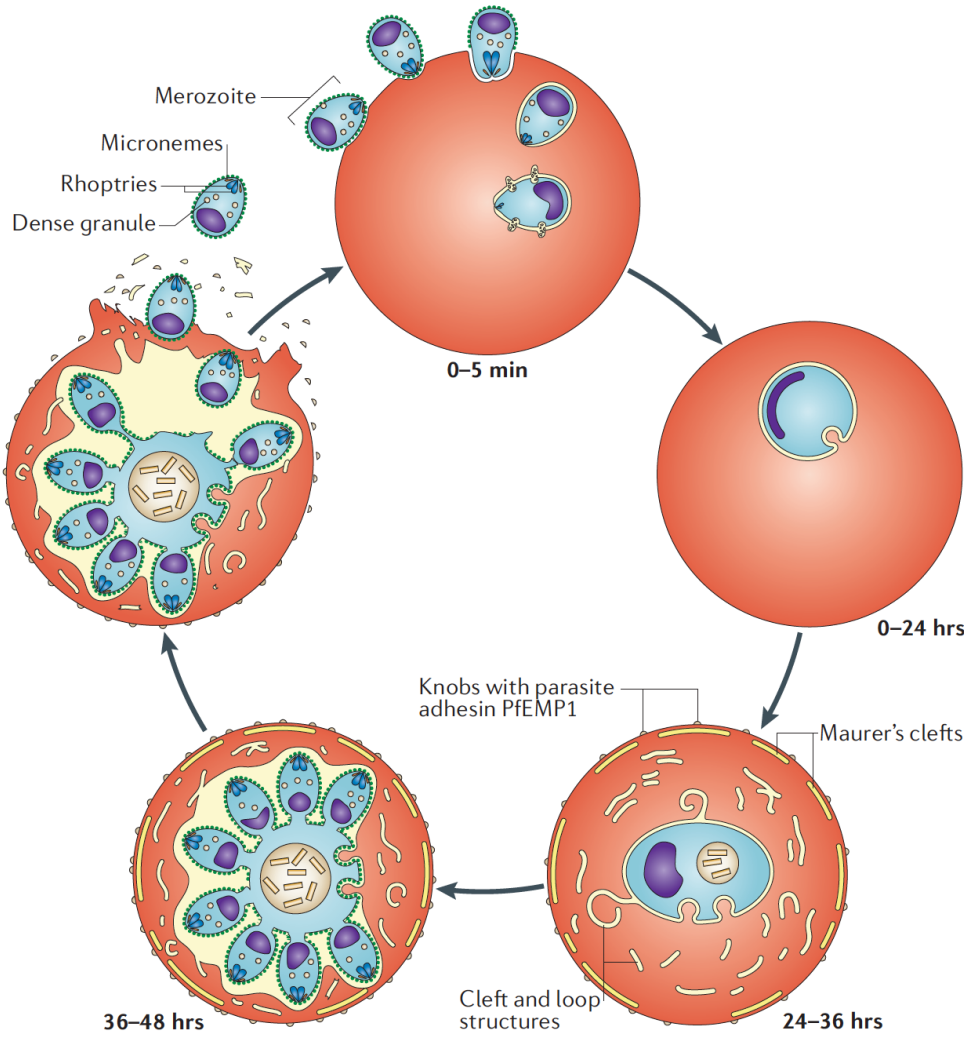

Figure 1.3 Stages of the *Plasmodium* intra-erythrocytic cycle (85). Invasion of an erythocyte is a chance event that occurs in a matter of minutes after the release of merozoites. Attachment is followed by re-orientation and invasion. Invaded merozoites form rings (0-24 hrs),which progress to trophozoites (24-36 hrs) and schizonts (36-48 hrs), which upon rupture release more merozoites that continue the cycle. Remodelling of the RBC involves several changes to the RBC membrane and cytoplasm including the insertion of *Pf*EMP-1 and other adhesins into knob like structures.

While the majority of merozoites re-enter the asexual cell cycle, a small fraction enter the sexual cycle and terminally differentiate into male and female gametocytes (86). In contrast to trophozoites and schizonts, immature stages of *P.falciparum* gametocytes sequester away from peripheral circulation in different organs like the brain, spleen and gut and in particular within the bone marrow (87, 88). An *Anopheles* mosquito while feeding on an infected host eventually takes up the circulating mature gametocytes that mate to form a zygote within its midgut (89, 90). Zygotes differentiate into motile ookinetes that traverse the midgut epithelium and form oocysts between the basal lamina and midgut epithelium (91). Sporozoites are formed within the oocyst and then upon

oocyst rupture passively transported by the haemolymph to the salivary gland, where they invade and are ready to be transmitted during the next infectious bite **(Figure 1.4)**.

These sequential events pertaining to intra-erythrocytic development and sequestration are primarily responsible for the severe disease pathology associated with malaria, the most striking one of which is Human Cerebal Malaria.

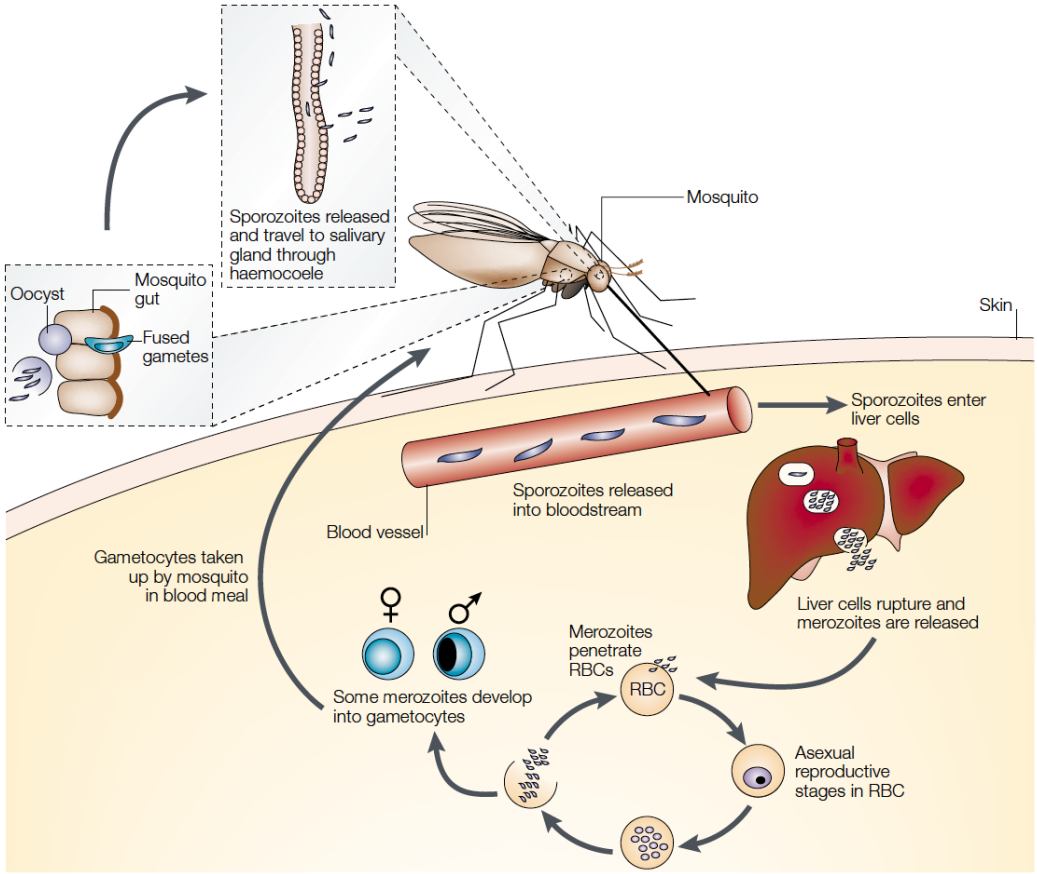

Figure 1.4 Transmission stages from host to mosquito (92). A fraction of intra-erythrocytic parasites terminally differentiate into male and female gametocytes and are taken up by a feeding mosquito. Within the mosquito midgut, these gameocytes mate to form a zygote that differentiates into a motile ookinete. Ookinetes traverse the midgut barrier to form an oocyst on the basal part of midgut epithelium. Sporozoites formed within the oocyst are released into the haemolymph upon rupture of the oocyst wall and transported to the salivary gland where they accumulate; ready to be transmitted during the next blood meal.

1.2.2.1 Human Cerebral Malaria (HCM)

Human Cerebral Malaria is a severe pathology that accounts for about 1% of all *P.falciparum* related deaths and is linked to the sequestration of late stages of *P.falciparum* parasites within the microvasculatures of the brain. It is widely regarded as a multi-faceted process that is influenced by both parasites and immune status of the host.

Several hypotheses regarding the pathogenesis of HCM have been proposed, with little or no consensus.

One of the complications of HCM is the heterogeneity in pathology that precludes comparisons between different populations. Incidences of HCM in endemic areas are uncommon in children experiencing their first clinical episode of malaria, but instead higher in those experiencing their second or third round of infection and who have developed some level of semi-immunity (93, 94). In contrast, adult travellers from malaria-naïve countries are more susceptible to developing CM compared to children, even though immunity develops much faster in adults (95). The cause for this variation in susceptibilities between children and adults is not well understood, but immuno-epidemiological evidences suggest that a concert of innate and adaptive immune responses might be responsible for initiation or protection from cerebral symptoms (96).

Several lines of evidence have suggested that the outcome of severe pathology relies on an individual's ability to regulate the inflammatory response to infection. High levels of circulating pro-inflammatory cytokines like IFN-γ, TNF-α and IL-6 are linked to CM in both children and adults (97, 98), while insufficient levels prevent parasite clearance and cause hyperparasitaemia-induced complications (96). Cytokines are however considered a poor predictor of disease severity in African children since TNF-α levels do not always correlate with disease severity (99, 100). Another line of reasoning proposes the involvement of anti-parasitic immunity and cross-reactive T cells that are primed in response to antigens from other pathogens which are mimicked by *Plasmodium* (101). It is hypothesised that children from malaria-endemic areas, are at a higher risk of developing CM only after the second or third round of infection due to an overriding pro-inflammatory response that is triggered by T cells primed during the first exposure. However, with each subsequent infection, anti-parasitic immunity is developed that contributes to protection and lowers the risk of CM, as seen in older children and adults. In contrast, adults from non-immune or malaria-free areas are more susceptible to CM because of the accumulation of cross-reactive T cells primed by exposures to other pathogens. Non-immune children experiencing their first infection on the other hand have a smaller pool of cross-reactive T cells and are thus less prone to developing CM (101) **(Figure 1.5)**. Ironically, any immunity acquired to severe pathology is short-lived and lost in the absence of exposure (102, 103), thereby complicating efforts to determine the exact correlates of protection.

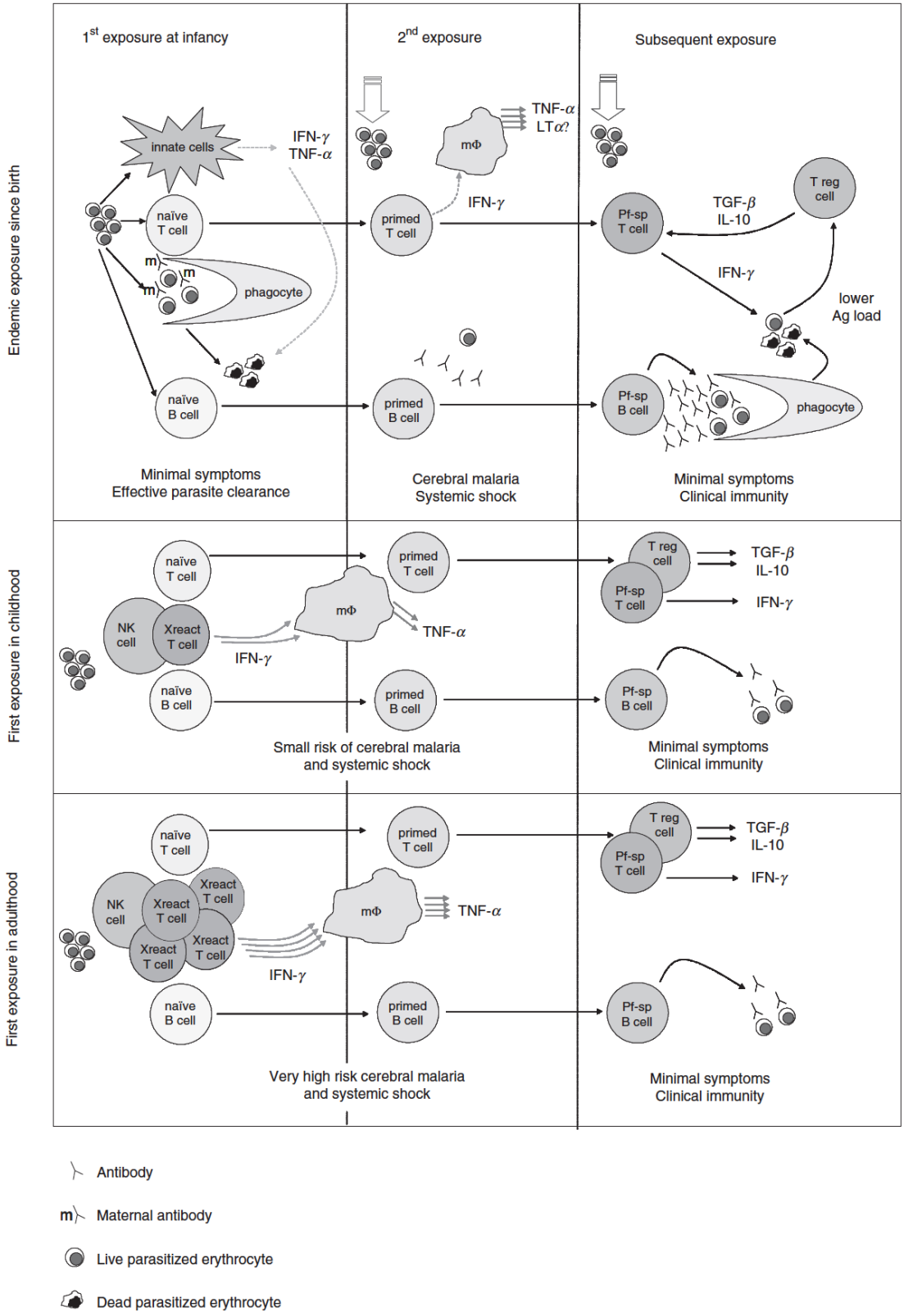

Figure 1.5 A hypothetical model describing the development of clinical immunity to *P.falciparum* malaria, depending upon the age at first exposure (9). The proposed model describes the development of clinical immunity with respect to age and exposure. It is hypothesised that children living in malaria-endemic areas are less prone to developing severe cerebral pathology due to the subdued pro-inflammatory response and lack of parasite-specific T cells that are primed in response to a malarial infection. Upon re-infection, these T cells secrete

high levels of pro-inflammatory cytokines that trigger the development of CM. With each subsequent infection, anti-parasitic immunity is developed that helps curb the pro-inflammatory response and prevents the development of cerebral symptoms, thus contributing to protection as seen in older children and malaria-endemic adults. In contrast, non-immune adults from malaria-free regions lack protective immunity and are therefore more susceptible. These adults additionally accrue a pool of cross-reactive T cells primed by non-malaria pathogens that are capable of contributing to the development of CM. Non-immune children however, have a smaller pool of cross-reactive T cells and are hence at a lower risk of developing CM.

Most of what is known about HCM has been gathered from post-mortem studies, which provide a restricted view about the syndrome. One common finding in most autopsy reports is occlusion of brain capillaries caused by sequestered parasites which are considered the underlying cause of localised inflammation, haemorrhaging, hypoxia and neuronal death (104). One of the hallmarks of CM is in fact the engorgement of capillaries and venules due to plugging of microvessels by both infected and uninfected erythrocytes **(Figure 1.6)** (87, 105). However, post-mortem studies on Malawian children showed evidence of leucocytes and platelets instead of parasites within the brains (106, 107). Although anti-malarial treatment was thought to account for the absence of parasites in the brains of these children, studies from India and Thailand reported similar findings (108-111) thereby suggesting that other factors responsible for CM exist.

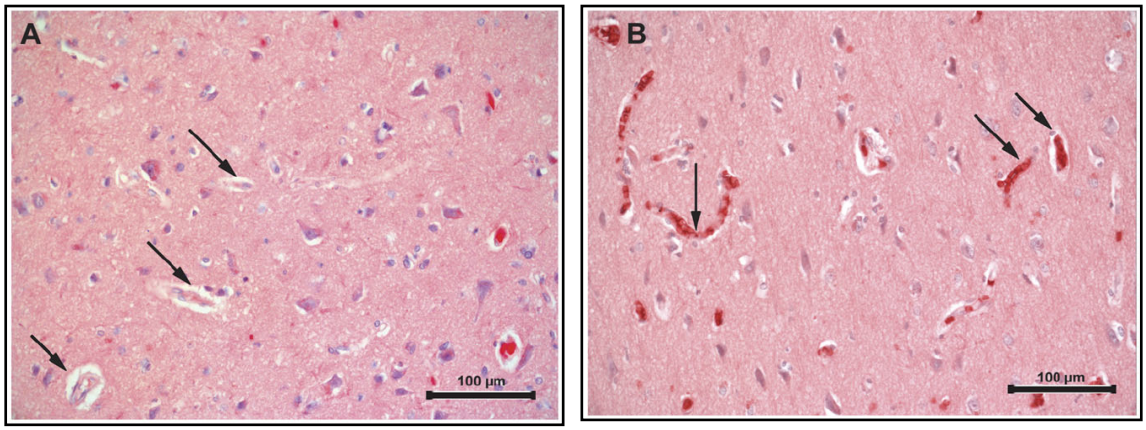

Figure 1.6 Histological sections of brain tissue of patients infected with malaria (105). Brain tissue sections of patients infected with *P.falciparum* malaria stained with glycophorin A and haematoxylin, show blood vessels (indicated by arrows) that are not plugged by erythrocytes (A) versus vessels that are congested due to sequestration of infected and uninfected erythrocytes (B).

Parasites modify the iRBC membrane in multiple ways at the cost of reducing its flexibility during circulation, which favours binding to the endothelium (112). Infected erythrocytes can bind a number of endothelial cell receptors like CD36, CSA and ICAM-1 (113) with varying specificities (114), though the exact reason for this differential

preference is unknown. One plausible explanation could be to enhance the probability of binding ECs in different regions of the body and thus the requirement of binding to different receptors. This is in agreement with the observation that variation of surface adhesins on iRBCs promotes binding to ECs in different organs and thus contributes to organ-specific sequestration (115). Indeed parasites isolated from the placenta of pregnant women bound CSA, which is abundantly expressed in the placenta, with higher affinity compared to CD36 (116-118). iRBCs predominantly bind CD36 in peripheral organs, but the lack of up-regulation of CD36 expression on brain ECs during a malaria infection (119) has questioned its validity. Instead, it is suggested that platelets and microparticles in the brain might express CD36 and indirectly facilitate binding of iRBCs to the endothelium (120, 121), though this has not yet been demonstrated. On the contrary, ICAM-1 is significantly up regulated on brain-endothelial cells (122) and expression levels were shown to correlate with the risk of CM (119). In fact, post mortem sections of CM patients have often correlated ICAM-1 expression to sequestered parasites within the brain (122).

iRBCs bind to ICAM-1 and trigger a signalling cascade involving the MAPK pathway, cytokine production, expression of proteins like P-selectin, oxidative stress and ROS production which subsequently contribute to the loosening of tight junctions (123-125). Alternatively, iRBC adhesion could directly induce endothelial cell apoptosis and permit an influx of fluids and plasma proteins into the perivascular space of the brain parenchyma leading to cerebral oedema (126, 127). In post-mortem studies from Vietnam and Malawi, direct adhesion of iRBCs to ECs was shown to compromise the integrity of the blood-brain-barrier through loss of tight junction proteins occludin and vinculin (128, 129). However, localised occlusions and loosening of the tight junction are not always sufficient to cause brain swelling and coma seen in CM (130, 131).

Numerous studies argue that both inflammation and cytoadherence contribute to BBB breakdown, albeit with varying contributions. Components of the immune system like platelets (108), leucocytes (132), neutrophils (133) also play a role through secretion of chemokines and cytokines. Indeed, expression levels of pro-inflammatory cytokines such as TNF-α, IFN-γ and IL-1β are higher in HCM patients and were shown to activate ECs, resulting in vascular permeability (134, 135). Cytokines such as TNF-α increase ICAM-1 expression on endothelial cells, thereby inducing an activation loop that further enhances sequestration of parasites (136-138). Other factors including the endothelial

protein C pathway receptors (139), histidine rich protein II (140), parasite glycosylphosphatidylinositol (141) and haemozoin were also shown to play a role in BBB permeabilisation (142). However, the exact contribution of different leucocyte subsets in HCM cannot be determined *in vivo*.

Although parasite sequestration in the brain is considered an important event in HCM, there is emerging data supporting a role for the spleen in HCM pathogenesis. However, any direct evidence linking the spleen to pathological changes in the brain is missing. The spleen plays a vital role in the clearance of damaged RBCs from circulation and retention of iRBCs during a malaria infection and during anti-malarial therapy (143). These functions are however is reduced in splectomised individuals (144, 145) compared to those with an intact spleen. In the absence of the spleen, iRBC clearance is partially taken over by other organs like the liver, kidneys and intestines, but this is insufficient to reduce the circulating parasite burden. The spleen was also suggested to influence sequestration and antigen expression on the surface of iRBCs, in addition to clearance. This conclusion was derived due to observation that the peripheral blood of splenectomised individuals almost always contained mature forms of iRBCs, Moreover, the data was also consistent with experiments on squirrel monkeys infected with *P. falciparum* where differences in surface antigen expression were observed between splenectomised and spleen intact hosts (146, 147). Although these results would imply that the spleen directly modifies sequestration through an influence on surface antigen presentation, a study from naïve individuals splenectomised before infection, found that surface antigen expression of iRBCs was similar to those from spleen-intact individuals and incidences of CM were unchanged (148, 149). Ironically, parasites sequester to avoid splenic clearance, by varying their surface adhesins, which is the primary cause of chronic infections and organ dysfunction. Sequestration within the spleen also leads to remodelling of the splenic architecture (150) thus fostering retention of uninfected RBCs, splenomegaly and consequently anaemia. The exact role of the spleen in malaria is therefore uncertain; however these data indicate that the spleen plays a dual role in protection and pathology, consequently either exacerbating or mitigating instances of cerebral malaria.

In summary, numerous *in vitro* investigations have examined multiple host and parasite molecules involved in the pathogenesis of CM. However, few have actually studied the interplay of these factors and the mechanisms leading to BBB disruption.

1.2.2.2 Experimental Cerebral Malaria (ECM)

Studies delineating the factors involved in HCM are restricted to post-mortem samples and *in vitro* experiments. Due to apparent limitations and ethical constraints of studying CM in humans, re-construction of the series of events and mechanisms responsible for CM is preferentially done through experimental animal models.

Both primate and rodent models of HCM reproduce certain aspects of CM (151), though primate models are the preferred choice in terms of sequestration pathology, which is closest to the human situation. However, limitations in terms of cost-effectiveness have restricted the use of primates to study CM. In spite of the long-standing debate questioning the validity of the mouse model, infection of C57BL/6 mice with *P.berghei* ANKA (152) is widely accepted as the best available tool to study CM (153). Other models of CM such as infection with *P.berghei* K173 are also available, though the use of *Pb*K173 is limited due to the dose-dependent occurrence of CM in susceptible mice (151).

Infection of B6 mice with *Pb*A recapitulates several features of HCM like paralysis, convulsions, haemorrhaging (154, 155), brain swelling (156), retinopathy (157), and coma in a relatively short period of time (7-10 days) and is termed as experimental cerebral malaria (ECM) (158). Experimental evidence has shown that both iRBCs (154, 159-161) and leucocytes (162, 163) accumulate within the brains of ECM mice, in higher proportions compared to those without ECM. While parasite sequestration is less prominent in the case of ECM, studies have proven that drug treatment of infected mice just prior to the onset of neurological symptoms, abrogates ECM (160, 164). Moreover, differences in sequestration patterns between HCM and ECM can be attributed to the method used for tissue preparation; i.e. perfusion of mice is a rather routine procedure, however individuals that have succumbed to HCM are never perfused before organ isolation.

As with humans, genetic variability between mice can alter susceptibility to ECM, evident from differences between the Th1 biased-ECM susceptible (C57Bl/6J, CBA) and Th2 biased-ECM resistant (Balb/c, A/J) mice. In fact, Th1 or pro-inflammatory cytokines are of paramount importance to ECM pathology. Indeed, ECM development can be accelerated in the Th1-biased mouse through treatment with phenylhydrazine that increases the production of cytokines like IFN-γ and TNF-α (165), or restored in Balb/c mice, which are Th2-biased, through the induction of pro-inflammatory cytokines (166,

167). ECM outcome is also influenced by factors such as dosage (168), parasite clone (169) and stage of parasite used for infection (sporozoites versus iRBCs) (170, 171). Susceptibility also changes according to age with older mice being more resistant to developing cerebral symptoms compared to younger ones (161).

Accumulating evidences supporting the similarities between HCM and ECM, have thus justified the use of the murine model to study the complex process of CM. Moreover, the availability of new tools and genetically manipulated mice has advanced our understanding of the steps involved in the development of cerebral pathology. Based on the current available literature about ECM, the following series of events are thought to occur **(Figure 1.7)** and likely conserved in both ECM and HCM.

(1) Priming in the spleen. The spleen is central to ECM pathogenesis and plays a key role in priming immune cells that are responsible for BBB damage. Indeed, splenectomised mice are protected from ECM and have lower levels of $CD4^+$ (172) and $CD8^+$ (173) T cell infiltrates within the brain (174). During the early stages of infection, $CD11c^{high}$ dendritic cells in the spleen efficiently present parasite material from dead or dying parasites to resident $CD4^+$ and $CD8^+$ T cells (175). Although several DC populations are involved, specific depletion of the $CD8\alpha^+$ $Clec9A^+$ DC subset was found to abrogate the development of ECM (173). DCs differentiate in response to the cytokine Flt3L (176, 177) that is also responsible for increasing the number of splenic $CD11c^{high}$ $CD8^+$ DCs and phagocytosis of iRBCs (176).

(2) Parasite sequestration. Late blood stages of *Pb*A parasites sequester in an organ-specific manner, through antigenic variation of surface receptors and by immune-mediated mechanisms (174). Like the *var* genes in humans, *bir* genes code for variant surface proteins in *Pb*A parasites and might therefore play a role in both sequestration and cytoadherence (178). A recent study highlighted similarities in the virulence machinery between *P.falciparum* and *P.berghei* ANKA parasites, thus postulating conserved mechanisms of endothelial cell activation in both (180). Sequestered parasites release inflammatory ligands such as GPI and haemozoin, which activate DCs through Toll-like receptors 2 and 9 respectively (181, 182).

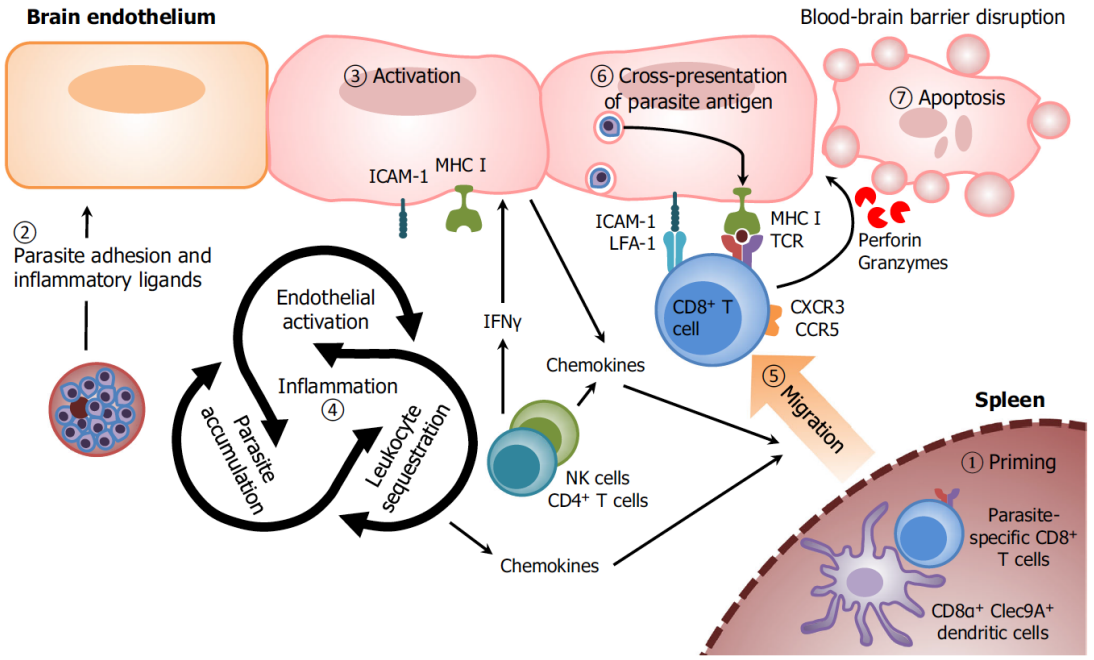

Figure 1.7. Schematic of the sequential steps in the development of ECM pathology (179). The development of ECM begins with the priming of $CD4^+$ and $CD8^+$ T cells within the spleen by $CD8\alpha^+$ $Clec9A^+$ DCs that have phagocytosed parasite material from sequestered or dead parasites. Parasite sequestration together with inflammatory parasite ligands like GPI and haemozoin activate the endothelium. ECs up-regulate receptors like ICAM-1, MHC class I and class II in response and secrete chemokines and cytokines. Leucocytes and platelets that are recruited to the site of inflammation become activated and secrete pro-inflammatory cytokines, which further triggers the upregulation of receptors on ECs. The triad of sequestration, EC activation and cytokine secretion by leucocytes induces a positive feedback loop that triggers a state of systemic inflammation in the host. Both inflammation and IFN-γ produced by NK cells trigger T cells that are primed within the spleen to express chemokine receptors like CXCR3 and CCR5 and migrate towards the brain and other sites of inflammation, where they adhere to ECs *via* ICAM-1. Upon recognition of parasite antigens cross-presented by the brain endothelium *via* MHC class I molecules, $CD8^+$ T cells release perforin and granzyme B, which induces apoptosis of the EC and consequently permeabilisation of the BBB. (This legend has been adapted from Howland, S.W. *et. al.* (179))

(3) Activation of the endothelium

EC activation is a gradual process that appears to be conserved between ECM and HCM. The combination of sequestered parasites, GPI and haemozoin activate ECs, which secrete chemokines like CXCL10 (183), which then up-regulate ICAM-1, MHC class I and class II molecules (184). Resident macrophages respond by secreting chemokines like MIP-1α and CCL5 that up-regulates the expression of chemokine receptors such as CCR2, CCR5 and CXCR3 (179) on monocytes and T cells, triggering their migration to the site of EC activation. Leucocyte subsets like monocytes (185), macrophages (163), NK (186) cells, T cells (186, 187) or DCs (173) and platelets (188, 189) were all reported to accumulate in higher numbers in the brains of ECM mice compared to those without

ECM symptoms. In contrast to the depletion of T cells, depletion of monocytes, neutrophils and platelets just before the onset of cerebral pathology does not prevent ECM (190, 191), suggesting they might rather play a role during the early stages of infection through cytokine and chemokine production (191-193). Recruited leucocytes and platelets secrete pro-inflammatory cytokines like IFN-γ and TNF-α which induce a positive feedback loop that further up-regulates adhesion receptors on ECs and promotes the sequestration of iRBCs and leucocytes (194, 195). Interestingly, IFN-γ in conjunction with $CD8^+$ T cells was shown to mediate sequestration of iRBCs within different tissues, in a time-dependent manner (196).

Endothelial activation is followed by the release of VWF multimers that recruit platelets, iRBCs and monocytes (197), of which platelets were shown to directly cause EC damage (198). Sequestered macrophages potentially undergo a respiratory burst to release nitric oxide that could damage the endothelial barrier, though by unclear mechanisms (199-201).

(4) Systemic inflammation.

Monocytes that infiltrate the brain adhere to endothelial cells *via* CD40L (202) and engender the secretion of pro-inflammatory cytokines like IFN-γ (168, 203, 204), TNF-α (162) and lymphotoxin-α (184, 205) that are central to the ECM pathology. Though the exact source of IFN-γ is unclear, studies have demonstrated that NK cells infiltrating the brain tissue during the early stages of infection are the primary producers of IFN-γ and this role is later taken over by $CD4^+$ T cells (186). Recent studies highlighted that IL-12Rß2 but not IL-12 exerts an indirect effect on IFN-γ, TNF-α and lymphotoxin-α (206), thereby influencing ECM. Conversely, anti-inflammatory cytokines like IL-10 were shown to deter ECM immunopathogenesis (207), thus suggesting that the progression of ECM hinges upon a delicate balance of pro- and anti-inflammatory cytokines maintained by regulatory T cells (Tregs) (208).

The cyclical events of sequestration followed by endothelial activation and cytokine-chemokine secretion within different organs eventually contribute to an overall state of systemic inflammation in the host.

(5) Migration to the brain

The migration of T cells to the brain is a key event in ECM immunopathogenesis. Upon

stimulation with IFN-γ, splenic $CD8^+$ T cells express CD69, CD11a and CD54 in addition to chemokine receptors like CXCR3 and CCR5, and migrate out of the spleen towards the brain and other organs *via* chemotaxis (209, 210). Indeed CCR5 and CXCR3 deficient mice feature reduced $CD8^+$ T cells in the brain and are partially protected from ECM (211, 212). Migration of $CD8^+$ T cells to the brain microvasculature mainly relies on IFN-γ secreted by both NK cells (213) and $CD4^+$ T cells (186) and relies on CXCL9 and CXCL10 expression. The antigen-specificity of brain infiltrating $CD8^+$ T cells was recently determined by sequencing of the Vβ8 segment of $CD8^+$ T cells, which also resulted in the identification of dominant immunogenic epitopes contributing to ECM development (209, 210).

(6) Cross-presentaion of parasite antigens

ECs can also act as antigen presenting cells and cross-present antigens to $CD8^+$ T cells within the brain microvasculature (214, 215). Indeed, two studies identified parasite-specific epitopes that were cross-presented by the brain endothelium in ECM susceptible mice (209, 210). In contrast, brain microvessels from mice infected with non-ECM causing parasite strains such as *Pb*NK65 were incapable of efficient cross-presentation both *in vitro* (209) and *in vivo* (216). Cross-presentation of parasite antigens in particular was deemed responsible for the arrest of pathogenic $CD8^+$ T cells within the brain, an event that was again unique to ECM causing parasite strains (216).

(7) Blood-brain-barrier permeabilisation

$CD8^+$ T cells adhere to ICAM-1 on activated ECs *via* LFA-1 (217). Upon recognition of cross-presented antigens, these $CD8^+$ T cells exert their cytotoxic effect by secreting molecules like IFN-γ, Granzyme B (218) and perforin (219), all of which are a primary requirement for ECM pathogenesis since mice deficient for either component are protected from ECM. The release of these cytotoxic molecules together contributes to cytolysis, apoptosis, permeabilisation of the endothelial cell barrier and subsequently coma and death.

1.3 Mechanisms of protection against cerebral malaria

Although the advancement of cerebral symptoms relies on the spatio-temporal interplay of numerous host and parasite molecules, several genetic polymorphisms and environmental factors are know to perturb this process and thus disrupt the progression of CM.

1.3.1 Protection against human cerebral malaria

Variations in susceptibility to HCM are common for *P. falciparum* infections, but the underlying mechanisms are not well described. Evolutionary studies often align with the view that malaria parasites co-evolved with the human race, which is not surprising given that most metabolic disorders and genetic polymorphisms of red blood cells including thalassemias and haemoglobinopathies are frequently found in malaria endemic regions and confer protection against CM (220, 221). Erythrocyte polymorphisms interfering with remodelling of the red blood cytoskeleton were found to reduce transport of adhesins like *Pf*EMP-1 to the red blood cell surface and subsequently abolish rosetting and cytoadherence (222-224). Likewise, individuals deficient for glucose-6 phosphate dehydrogenase or pyruvate kinase feature reduced parasitaemias and are protected from severe disease (225).

In addition to erythrocyte polymorphisms, mutations within EC receptors such as ICAM-1 and CD36, including allelic variations of cytokines like TNF-α and IL-10 are all known to contribute towards protection from CM (226). However, not all polymorphisms contribute to protection, as observed by a lack of association between EPCR variants and protection from severe disease in a cohort of Tanzanian children (227). Moreover, ample variations observed within populations suggest that protection may rather depend upon a combination of factors (228).

In addition to genetic polymorphisms, naturally acquired immunity also offers protection against CM. Older children and adults from malaria endemic areas gradually accrue antibodies to blood stage antigens after years of repeated exposure. These antibodies protect from clinical disease, but do not confer sterile immunity. Antibodies to different variants of *Pf*EMP-1 for example (229) are thought to interfere with rosetting and parasite sequestration and thus indirectly contribute to protection (230, 231). Antibodies specific to other parasite antigens such as MSP-1 were instead shown to contribute to protection through opsonisation of merozoites and stimulation of ROS production (232) or simply through enhanced clearance of iRBCs by phagocytic cells (233). In other studies with African children, high levels of erythropoietin (120) (120) and VEGF were found to correlate with reduced risk of neurological sequelae (234). EPO has a neuroprotective effect and was therefore proposed as an adjunct therapy for CM (235). However, a recent study showed that increased levels of plasma EPO correlated with increased mortality of African children, thus disproving the therapeutic use of EPO (236).

Interventions such as the RTS,S malaria vaccine designed to prevent *Plasmodium* parasites from entering and multiplying within the liver, does not confer sterile protection in vaccinated individuals but instead conferred partial protection against cerebral symptoms. In spite of a lack of understanding about the mechanism of protection, studies have hypothesised that antibodies against CSP (237) reduce the number of sporozoites entering and developing within the liver, leading to a delayed release of merozoites, giving rise to sub-microscopic parasitaemias and an opportunity for the host to gradually acquire immunity to blood stage infection (238-240). A similar mechanism of protection was also proposed to occur in Tanzanian children given preventive treatment with anti-malarials like sulfadoxine-pyrimethamine (241, 242). While these data would suggest that a delay in the initial blood stage growth increases the odds of developing an immune response against CM, the mechanisms by which this might occur remain undetermined.

While the above data indicates plausible mechanisms of protection, it does not explain why some individuals are more susceptible than others. Moreover, addressing intervention strategies that prevent CM requires a proper understanding about the correlates of protection.

1.3.2 Protection against experimental cerebral malaria

Studies about the disruption of CM immunopathogenesis are replete with examples from rodent models of ECM and several mechanisms of protection have been proposed with reference to interventions against HCM.

Although similar genetic polymorphisms linked to protection in HCM cannot be found in mice, mice deficient for critical genes such as CCR5, IFN-γ and TNF-α or depleted of $CD4^+$ T cells, $CD8^+$ T cells, etc. are all protected from ECM (243). Loss of TLR7 signalling also confers partial protection against ECM through alterations in the cytokine profile resulting in a shift towards anti-inflammatory cytokines (244). Treatment of mice with anti-malarials like chloroquine also produces the same effect, though by inhibition of TLR-9 and MHC-II expression on DCs, which leads to a severe decline in Th1 cytokines like IFN-γ and TNF-α (245). Similarly, administration of IL-33 (246), EPO (247, 248), iron (249), *Agaricus blazei* (250), Cyclosporin A(251) and even activated charcoal (252) prevented the development of ECM through downregulation of the Th1 response by different mechanisms. Both IL-33 (246) and EPO (247, 248) trigger the expansion of regulatory T cells that are responsible for protection against ECM. In

contrast, administration of iron dextran protected mice from ECM, by reducing CXCR3 expression on T cells, thus curbing their migration to the brain. Moreover, the accumulation of T cell within the spleen was associated with a decrease in both NK cells and Tregs (249). A study by Haque *et al.* demonstrated that artificial expansion of T regs *in vivo* protected mice against ECM by mediating a reduction in both parasite sequestration frequencies of $CD4^+$ and $CD8^+$ T cells in the brains of infected mice. Protection was moreover found to rely on CTLA-4 and IL-2, instead of IL-10 (253). Another study however showed that depletion of Tregs through administration of anti-CD25 monoclonal antibody prevents the development of ECM (254), thus suggesting a paradoxical role for Tregs in ECM immunopathogenesis (255, 256). Interestingly, a study by Liu, Y. *et. al.* proposed a role for IL-10 producing B regulatory cells in protection against cerebral pathology in mice (257). Therefore, further investigations are required to dissect the exact role of regulatory cells in preventing immune-mediated cerebral pathology.

Co-infection of mice with *Pb*A and *Pb*XAT (151, 258), Filaria (259) or *Schistosoma japonicum* (260) also confers protection against ECM through an early induction of IL-10. Protection in case of the latter was found to associate with increased levels of Th2 cytokines like IL-4, IL-5, TGF-β and reduced numbers of CD4 and CD8 T cells, both within the spleen and brains of infected mice (260). In contrast, co-infection of mice with *Pb*K173 or treatment of infected mice with soluble *Toxoplasma gondii* antigens (261) triggers an early peak of IFN-γ instead of IL-10, but also protects against ECM (151, 258). It is likely that an early IFN-γ peak triggers the secretion of IL-12 that could potentially reduce parasitaemia and sequestration, thereby mediating protection against ECM (261).

In addition to modulating the host response, interventions specifically targeting the parasite have also been shown to confer protection against cerebral symptoms. For example, the administration of chloroquine just before the onset of cerebral symptoms ablates ECM by reducing the parasitaemia rather than through immunmodulatory mechanisms (160). Interestingly, interventions targeting the parasite within the liver have also been shown to delay blood-stage growth kinetics, which eventually translates into protection from cerebral symptoms. Infection of mice with sporozoites deficient for *Plasmodium*-specific protein that plays a role in liver merozoite formation (79) features a delay in merozoite egress from the liver thus reproducing an 'RTS, S' like effect that

abrogates the development of ECM (262). Similarly, immunisation of mice with a single dose of irradiated sporozoites (Pfeil, J. *et al.* unpublished) or partial attenuation of intra-hepatic parasite stages *via* treatment with isopentaquine (263) contributes to protection against ECM and is associated with early T cell activation and IL-10 production within the liver and spleen and in the latter (263). The effect of delayed blood stage growth on ECM outcome was also shown for parasites lacking plasmepsin-4 that were all protected from ECM (264).

In summary, one could conclude from the examples above that both timing of pro-inflammatory cytokine secretion and blood stage growth kinetics of the parasite are critical to the development of ECM. Thus delaying blood stage growth could prevent the development of a robust pro-inflammatory response leading to blood-brain-barrier breakdown, while permitting the development of antibody responses that contribute to protection against ECM. Similarly, an early IFN-γ driven environment could help control infection (265) and promote the proliferation of Tregs that secrete IL-10 and other Th2 cytokines (260), which steers the immune system into a Th2-biased state. Alternatively, Th2 cytokines could reduce the activation of antigen-specific T cells within the spleen and subsequently their migration to the brain and other organs, thus affecting ECM progression. These results therefore highlight the potential of therapeutic measures targeting the window of transition from 'liver to blood-stage of development' that could offer protection against CM.

1.4 The aim of this study

Vaccination strategies against malaria rarely focus on the alleviation of cerebral symptoms, but rather target the clinically silent pre-erythrocytic stage to achieve sterile protective immunity. Pitfalls from the RTS,S story have highlighted the importance of vaccines targeting multiple stages of the parasite life cycle and more specifically those antigens that are shared by pre-erythrocytic and intra-erythrocytic stages. This concept is supported by the success of immunisation with sporozoites under CQ cover (CPS) which is by far considered the best method of conferring sterile protection against re-infection (266, 267). CQ specifically targets intra-erythrocytic stages of the parasite, whilst permitting complete intra-hepatic development (268) to confer sterile protection. Moreover, a study in 1997 suggested that vaccination strategies that curtail exposure to blood stages might inadvertently prevent the boosting of protective blood-stage immunity and thereby contribute to an increase in morbidity (269). Current vaccination

strategies are therefore adapted to incorporate antigens expressed in multiple stages of the parasite life cycle, or rather antigens that are shared among different life cycle stages of the parasite (270) in an attempt to induce both innate and adaptive immune responses.

The focus of this study was thus the characterisation of a *Plasmodium*-specific antigen, maLS_05 (malaria attenuated liver stage antigen 5) that was identified in liver stages of *P.falciparum* RAS and hypothesised to play a role in sterile protection (Frank, R. *et al.*, unpublished). Preliminary results from the rodent model however, suggested that *Pb*maLS_05 is critical to the development of ECM. The aim of this study was thus amended to functional characterisation of *Plasmodium berghei* maLS_05 (*Pb*maLS_05) in the development of ECM.

In addition to functional characterisation, this study aims at delineating the mechanisms of ECM development between the different modes of infection; i.e. sporozoites versus iRBC infections. More importantly, this study intends to highlight critical differences in ECM progression between the two modes of infection, which potentially has profound implications for vaccination or therapeutic strategies designed to alleviate cerebral malaria.

Chapter 2

Materials & Methods

2.1 Materials

2.1.1 Computer Software

ABI 7500 Software v2.0.5	Applied Biosystems
AutoQuant X	Media Cybernetics
CellQuest 6.0 Pro	BD Biosciences
EndNote X4.0.2	Thomson Reuters
ImageJ 2.0	Open sourceware
ImageStudio 4.0	Li-Cor
Microsoft Office for Mac 2008	Microsoft Corporation
Prism 5.0 for Mac OS X	GraphPad Software, Inc
Serial Cloner 2.6.1	Franck Perez, SerialBasics
Volocity 6.3	Perkin Elmer

2.1.2 Laboratory equipment

ABI 7500 Real-Time PCR Cycler	Applied Biosystems
Analytical scales BL510	Sartorius
Autoclave Systec	GmbH, Wettenberg
BD FACS Canto I	BD Biosciences
Blot Scanner	Li-Cor
Centrifuge 5415 R	Eppendorf
Eclipse Ti-E Inverted Microscope	Nikon
Electrophoresis System Horizon 11.14	Whatman Inc.
ELISpot/Fluoro Spot Reader	AID GmbH
Freezer -20^0 C	Liebherr
Freezer -80^0 C	Thermo Scientific
Fridges	Liebherr
GeneAmp PCR System 9700	Applied Biosystems
Haemocytometer (Neubauer)	Labotec, Labor-Technik
Heat block thermomixer comfort	Eppendorf

Hera Cell Incubator	Heraeus Instruments
Ice machine	ZIEGRA Isernhagen
ImagEM X2 EM-CCD camera	Hamamatsu Photonics
Innova 4300 Incubator Shaker	Eppendorf
Intenslight C-HGFIE Fibre illuminator	Nikon
Light optical microscope Axioskop	Zeiss
Light optical microscope, Axiostar plus	Zeiss
Light optical microscope, Axiovert 25	Zeiss
Liquid nitrogen tank	CBS
MasterCycler Gradient	Eppendorf
Megafuge 1.0R	Heraeus Instruments
Microwave oven	Sharp
Mosquito cages	BioQuip Products Inc
NanoDrop ND-1000	Thermo Fischer Scientific
pH-meter 7110	Inolab
Photometer	Eppendorf
Pipettes (Single and multi-channel)	Abimed
Sterile work bench Gelaire X	Flow Laboratories
XCell SureLock Mini-Cell Electrophoresis System	Invitrogen
Ultra*VIEW* VoX 3D live cell imaging system	Perkin Elmer
Vortex Genie 2	Scientific Industries Roth
Water Bath	GFL

2.1.3 Disposables

96-well cell culture plate	Sarstedt
96-well round bottom plates	Greiner Bio-one
96-well Multi-Screen Filter plates	Merck, Millipore
14 ml polystyrene round bottom tubes	Greiner Bio-one
8-well chamber slides	Nunc Corporation
Aluminum foil	Roth
Cell strainer (70 µm nylon)	Falcon, Corning
Falcon tubes (15 ml, 50 ml)	Sarstedt
Glass bottom culture dishes	Mattek Corporation
Gloves (Latex)	Semper Guard

Immersion oil	Waldeck
Eppendorf tubes (0.5ml, 1.5 ml)	Eppendorf
Object slides	Marienfeld
Microscope cover slips	Marienfeld
Needles BD Discardit II (0.4 mm x 19 mm; 0.6 mm x 30 mm; 0.9 mm x 40 mm)	BD
NuPAGE Novex 4-12% Bis-Tris Pre-cast Gels	Invitrogen
Nunc Lab-Tek II Chamber Slide System	Thermo Scientific
Parafilm	Pechiney Plastic Packaging
Petri dishes (145 x 20mm; 94 x 16mm)	Sarstedt
Pipettes (1 ml, 5 ml, 10 ml, 25 ml)	Sarstedt
Syringe BD Discardit II (U-100 Insulin, 1 ml, 5 ml, 20 ml)	Sarstedt
Sterile filter Millipore bottle	Starstedt
Thermo-Fast 96 PCR Detection Plate	Thermo Scientific
WesternSure Pen	Li-Cor

2.1.4 Chemicals

All chemicals were purchased from Applichem, Gibco, Merck, Roth, and Sigma, unless specified otherwise.

Bacto Agar	Difco, BD
Bacto Tryptone	Difco, BD
Bacto Peptone	Difco, BD
Collagenase Type 4	Worthington
DNase I	Roche
Complete Protease Inhibitor	Roche
Easycoll Density 1.124 g/ml	Biochrom AG
Fetal Bovine Serum (FBS)	Invitrogen
Giemsa (0,4%, w/v)	Roth
Heparin	Rathiopharm
Ketamine (10 %)	Bremer Pharma GmbH
MEM NEAA 100x solution	Gibco Invitrogen,
NuPAGE MOPS SDS Running Buffer (20 X)	Invitrogen
Nuclease Free Water	Ambion

Nycodenz	Axis Shield
Sea salt	Alnatura
Sodium pyruvate 100 mM solution	Gibco Invitrogen
Streptavidin-ALP	Mabtech
QIAzol Lysis Reagent	Qiagen
Xylazine (Xylariem®)	Ecuphar GmbH

2.1.5 Kits

5' RACE and 3' RACE Systems for Rapid Amplification of cDNA ends	Invitrogen
Amaxa Human T Cell Nucleofector Kit	Lonza
First Strand cDNA synthesis Kit	Thermo Scientific
ECL Plus Western Lightning	Perkin Elmer
Power SYBR Green PCR Master Mix	Applied Biosystems
QIAquick Gel Extraction Kit	QIAGEN
QIAprep Spin Miniprep Kit	QIAGEN
QIAquick PCR Purification Kit	QIAGEN
QIAamp DNA Mini Blood Kit	QIAGEN
RNeasy Mini Kit	Qiagen
TURBO DNA-free Kit	Ambion

2.1.6 Antibodies

Name	Dilution/ Concentration	Clone	Application	Manufacturer
α-CD4-PerCpCy5.5	1:100 (0.2 mg/ml)	RM4/5	FACS	eBioscience
α-CD8 PE-Cy7	1:100 (0.2 mg/ml)	53-6.7	FACS	eBioscience
α-CD16/CD32	1:100 (1.0 mg/ml)	93	FACS	eBioscience
α-IFN-γ APC-Cy7	1:100 (0.2 mg/ml)	XMG1.2	FACS	BD Pharmingen
α-Pb HSP70 (Mouse)	1:300	Hybridoma supernatant	IFA/WB	Pesce *et al,* 2008 (271)
Alexa Fluor 488 (Goat α-Mouse)	1:300	-	IFA	Invitrogen
Alexa Fluor 546 (Goat α-Mouse)	1:300	-	IFA	Invitrogen
Mitotracker Red CMX-Ros	1:500	-	IFA	Invitrogen

Hoechst	1:10000	33342	IFA	Invitrogen
α-GFP (Rabbit anti-Mouse)	1:1000	-	WB	Roche
Rabbit anti-mouse POD	1:10000	-	WB	Dianova
α-CD3 mAb	1:1000	CD3-2	ELISpot	Mabtech
α-mouse IFN-γ	1:100 (10 µg/ml)	rat/XMG1.2	ELISpot	eBioscience
α-IFN-γ, biotinylated	1:100 (5 µg/ml)	rat/R4-GA2	ELISpot	eBioscience

2.1.7 Peptides

Predicted CD8 T cell epitopes for *Pb*maLS_05 and the Pb1 epitope of GAP50 (209) were synthesized as peptides by JPT Peptide Technologies GmbH. The peptides were dissolved in DMSO to a final stock concentration of 20 mM, aliquoted and stored at -80 °C.

Name	Sequence	Concentration
Pb 1 (*Pb*GAP50)	SQLLNAKYL	1 µM
*Pb*maLS_05_K8L	KLDYYEKL	1 µM
*Pb*maLS_05_I8I	ILYFYNKI	1 µM
*Pb*maLS_05_E8L	ENIEFEYL	1 µM
maLSA_1568 (Db)	TSLENLKPM	1 µM
maLSA_395 (Kb)	SIFLYWIKL	1 µM
maLSA_64 (Kb)	VVYFFYTNV	1 µM
maLS05_827_8mer	LTYVFNTI	1 µM
maLS05_147_9mer	SVIKNDENL	1 µM
maLS05_1562_9mer	ASNENKTSL	1 µM

2.1.8 Antibiotics

Name	Concentration	Manufacturer
Ampicillin	100 mg/ml in ddH_2O	Carl Roth
Azithromycin	25 mg/ml in ddH_2O	Azi-TEVA (Apotheke)
Gentamicin	50 mg/ml	Gibco
Tetracyclin	5 mg/ml in 70 % EtOH	Carl Roth
Penicillin	100 mg/ml in ddH_2O	Sigma-Aldrich
Antibiotic-Antimycotic (100X)	1:100	Gibco

2.1.9 Enzymes and molecular ladders

All restriction enzymes and ladders were purchased from New England Biolabs.

2.1.10 Biologicals

2.1.10.1 Bacterial strain

Escherichia coli XL1 blue	Stratagene, Agilent Technologies Sales

2.1.10.2 Parasite strain

Plasmodium berghei ANKA cl15cy1	Hall *et al.*, 2005 (272)

2.1.10.3 Mosquito strain

Anopheles stephensi	Max Planck Institute for Infection Biology, Berlin

2.1.10.4 Cell lines

HuH-7 human hepatoma cell line	Nakabayashi *et al.*, 1982 (273) Kindly provided by AG Bartenschlager (University Hospital Heidelberg)

2.1.10.5 Mice strains

Naval Medical Research Institute (NMRI), outbred mice	Janvier, France
C57BL6/J Rj, inbred mice	Janvier, Paris, France

2.1.10.6 Anaesthetic

Ketamine/ Xylazine (K/X)	1 ml Ketamine 150 µl Xylazine 2.85 ml 1x PBS

2.1.11 Buffers

2.1.11.1 Immunological experiments

10x PBS, pH 7.0	50 tablets in 1L ddH_2O
CBA buffer	100 ml 1x PBS

	0.05 % Tween 20 2 tablets of complete protease inhibitor cocktail (Roche)
MACS buffer	1x PBS 1% FCS 2mM EDTA
Permeabilisation buffer (intra-cellular staining)	0.1% BSA 0.3% Saponin 1x PBS
Red cell lysis buffer	1L ddH_2O 8.26 g NH4Cl 1 g KHCO3 0.037 g EDTA

2.1.11.2 Immunofluorescence Assays

Wash buffer	1% FCS 1x PBS
Blocking buffer	10% FCS 1x PBS

2.1.11.3 SDS-PAGE

RIPA buffer	50 mM Tris HCl (pH 7.5) 150 mM NaCl 5 mM EDTA 50 mM NaF 0.5 % Sodium deoxycholate 0.1 % SDS 1% Triton X-100 Store at 4 ^{0}C. Add 0.25 µl 2mM DTT and 20 µl Protease Inhibitor cocktail to 500 µl RIPA buffer, just before use.
Novex Transfer buffer (25x)	300mM Tris Base

	2.4 M Glycine
	20% Methanol
	ddH_2O
TBS, pH 7.4	50mM Tris
	150mM NaCl
	1x PBS
TBST	TBS
	0.1% Tween 20
Stripping buffer	62.5mM Tris, pH 6.8
	2% SDS
	100mM 2-Mercaptoethanol
Blocking buffer	5% Milk Powder
	1x PBS

2.1.12 Media and solutions

2.1.12.1 Gradients

Easycoll gradient (Working stock)	9 ml Easycoll
	1 ml 10x PBS (Sterile)
30% Easycoll (Brain)	3% Working stock
	7% RPMI
Nycodenz	110.4 g Nycodenz powder
	5 mM Tris/HCl, pH 7.5
	3 mM KCl
	0.3 mM EDTA, pH 8.0
	Filled up to 400 ml with ddH_2O
	Autoclaved, stored at 4 °C
55 % Nycodenz	5.5 ml Nycodenz
	4.5 ml 1x PBS

2.1.12.2 Bacterial culture

LB Medium	10 g/L trypton
	5 g/Lyeast extract

	10 g/L NaCl Autoclaved
LB Agar	15 g agar 1L LB medium
Freezing solution	500 µl bacterial culture 500 µl 30 % glycerol Stored at -80 ^{0}C

2.1.12.3 Parasite culture

Transfection medium (Schizonts)	160 ml RPMI 40 ml FCS (US certified), heat-inactivated (56 °C /30 min.) 40 µl gentamicin Sterile filtered and prepared fresh before use
Freezing solution (*P. berghei*)	10 % w/v glycerine in Alsever's solution (Sigma) Stored at 4°C
Pyrimethamine	7 mg/ml in DMSO Stored at 4°C

2.1.12.4 Cell culture

Cell culture medium	DMEM (Gibco) 10% FCS 1% Anti-Anti
Cell culture medium (Imaging)	DMEM High Glucose (without sodium pyruvate and phenol red) 25mM HEPES 10% FCS 1% Antibiotic-Antimycotic
Freezing solution	100 µl FCS 100 µl DMSO 800 µl cell suspension

2.1.12.5 Immunological experiments

Complete Culture Medium	RPMI (Life Technologies) 10 % FCS 5 ml 100x MEM NEAA (Gibco) 5 ml 100mM sodium pyruvate (Gibco) 5 ml penicillin / streptomycin 10 µl heparin
Brain infiltrating lymphocyte medium	0.5mg/ml Collagenase 10µg/ml DNAse I 1x PBS Sterile filtered

2.1.13 Vectors

Name	**Use**
PB300mycmCherry-CT (274)	*PbmaLS_05* (-) (Knockout vector)
b3D+ (275)	*Pb*maLS_05 CT EGFP (C-terminal tagging)
b3D (provided by Andrew Waters, Glasgow University)	*Pb*maLS_05 NT mCherry (N-terminal tagging)

2.1.14 Oligonucleotides

All primers were ordered as custom DNA oligonucleotides from Invitrogen and dissolved in ddH_2O to a final concentration of 100µM, aliquoted and stored at -20^{0}C.

2.1.14.1 *PbmaLS*_05 (-) vector primers

PbAgA_5'UTR	
Forward (*Sac II*)	5'-ATC CGC GGG GCA TTA TTA GAT GTC ATA GGA GCG-3'
Reverse (*Nde I*)	5'-ATA CAT ATG GGA TTA AAT ATA CAC ACG CAC AAC G-3'
PbAgA_3'UTR	
Forward (*Hind III*)	5'- ATT AAG CTT CGA GTA TTG CTT ACG TTT AAA TTG ATA GAG-3'
Reverse (*Xho I*)	5'- ATC TCG AGG CCC TAA ATA GGA ATA ATA ATG

	CAA AAT GC-3'
PbAgA_Seq_5'UTR	With mCherry_tag_rev as the reverse primer
Forward	5'-CGG AAA GCA GCA ATA ACA CTA CTA C-3'
Reverse	5'-GAT CCT TAC TTG TAC AGC-3'
PbAgA_Seq_3' UTR	With *Tg*DHFR/TS_rev as the reverse primer
Forward	5'- CGG CGA AAT TAT ATT GCT ACC GT-3'
Reverse	5'-GCA GTT GAT TTG TTT GAA AGA ATG TC-3'
PbAgA_RT	
Forward	5'-GCA AAG GCG GAG AAA TAC C-3'
Reverse	5'-CAC CCG TAG TAG CAT CTT CC-3'

2.1.14.2 *Pb*maLS_05 CT EGFP tagging vector

PbAgA_3'UTR	
Forward (*Hind III*)	5'-ATA AGC TTC GAG TAT TGC TTA CGT TTA AAT TGA TAG AG-3'
Reverse (*Kpn I*)	5'-ATG GTA CCG CCC TAA ATA GGA ATA ATA ATG CAA AAT GC-3'
CT_EGFP_5' end	With 5' UTR big tag rev as the reverse primer
Forward (*Sac II*)	5'-ATC CGC GGC GCA ATT GCA AGA AAT TGC TAT GT-3'
Reverse (*Xba I*)	5'-ATA TCT AGA ATA GTG TTT CGT TTT TTT TAA AAT CAT ATT GGC C-3'
EGFP	
Forward (*Spe I*)	5'-GCA CTA GTG CCG CCG CCG TGA GCA AGG GCG AGG AGC TG-3'
Reverse (*Bam HI*)	5'-GCG GAT CCT TAC TTG TAC AGC TCG TCC ATG CCG AG-3'
5' tag_sequencing	With b3D+ rev as the reverse primer
Forward	5'-GCA AAA GAT TCT TTA TGG ATA ATA GGG G-3'
Reverse	5'-CCT TGC TCA TTT ACC TGC TAA TAC GAT TGC-3'
3' sequencing	With TgDHFR/TS rev as the reverse primer
Forward	5'-CGG CGA AAT TAT ATT GCT ACC GT-3'

Reverse	5'-GCA GTT GAT TTG TTT GAA AGA ATG TC-3'

2.1.14.3 *Pb*maLS_05 NT mCherry tagging vector

PbAgA_NT Prom PI	
Forward (*Kpn I*)	5'-GCG GTA CCC CAC GTG CAC ATC AAT TTA TTC GTT CAT TAAC-3'
Reverse (*Hind III*)	5'-GCA AGC TTG CGT ACA CTT TAT AAT CTC ACA CTA TAC TTC-3'
PbAgA_NT Prom PII	
Forward (*BamHI*)	5'-GCG GAT CCG AAG TAT AGT GTG AGA TTA TAA AGT GTA CGC-3'
Reverse (*Spe I*)	5'-GCA CTA GTT TAA ACA CGC ACT TTA TAT CGA TAT ATT TTA CTC-3'
NT_mCherry	
Forward (*Spe I*)	5'-GCA CTA GTA AAA TGG TGA GCA AGG GCG AGG-3'
Reverse (*Xba I*)	5'-GCT CTA GAT GCT GCT GCC TTG TAC AGC TCG TCC ATG CC-3'
maLS_05_ORF	
Forward (*Xba I*)	5'- GCT CTA GAG ATA ATA ATG CAG ATG GGA AAT CAA AAG G-3'
Reverse (*Sac II*)	5'-GCC CGC GGC GTA ATA TAC CAT TAA GCA TTT TTG ACA GTT C-3'
5' integration	With *Tg*DHFR/TS as the reverse primer
Forward	5'-GGG CTA GAT TAT ATA GCG GAA AAT TTG-3'
Reverse	5'-GCA GTT GAT TTG TTT GAA AGA ATG TC-3'
3' integration	With NT_mCherry as the forward primer
Forward (*Spe I*)	5'-GCA CTA GTA AAA TGG TGA GCA AGG GCG AGG-3'
Reverse	5'-GAA ATA TTT TCG ACC CAT TTA GCA TTA GTT C-3'

2.1.14.4 Transcriptional analysis

Exon 1 (P1)	
1003_forward	5'-GCG GTG GAA GAC GGA ATC AAG AAG G-3'
1864_reverse	5'-GAG GGG AAA GGG AAT ATA TAG C-3'
Exon 1-2 (P2)	
maLS_05_p1_ forward	5'-GCT ATA TAT TCC CTT TCC CCT CTT ATT TAT AGC-3'
2455_reverse	5'-CAA TTG GTA ATA CTT GTT CAA CTC-3'
Exon 2-3 (P3)	
maLS_05_qRT-p2_forward	5'-GCA ACT TCC ACA ATG TGC TCA TG-3'
maLS_05_p3_reverse	5'-CGT AAA AGT CCC ATT CTA GAA ACT CCT GC-3'
Exon 3-4 (P4)	
Circ_forward	5'-CAA CAC GCT TTA GAA ATG AGG ACG-3'
5299_reverse	5'-CGT AAA CTA TCA CTA CCA CCT TC-3'
Exon 4 (P5)	
maLS_05_qRT-p4_forward	5'-CTG GTA GTG CAT CGC CAA TTT TAG-3'
maLS_05_p4_reverse	5'-GCA CTT GAG ATT GGT ATG GGC AAA TAA TAC C-3'

2.1.14.5 Quantitative Reverse Transcriptase Real Time analysis (qRRT-PCR)

Mouse GAPDH	
Forward	5'-TTG ATG GCA ACA ATC TCC AC-3'
Reverse	5'-CGT CCC GTA GAC AAA ATG GT-3'
***Pb* 18S rRNA**	
Forward	5'-AAG CAT TAA ATA AAG CGA ATA CAT CCT TAC-3'
Reverse	5'-GGA GAT TGG TTT TGA CGT TTA TGT G-3'

2.1.14.6 Rapid Amplification of cDNA ends

5' RACE	
GSP_reverse	5'-CCA TTA AGC ATT TTT GAC AGT TCT C-3'
Nested_GSP_reverse	5'-GCG TCA TCA TCA AGA ATG GAA ACG AG-3'

Nested_2GSP_reverse	5'- GAA ATT CGT GTT TTT CAC CAA TTA CAT TTG-3'
New_GSP_reverse	5'-GCT TAA TGG TAT ATT ACG TTC TTC-3'
3' RACE	
GSP_forward	5'-CGC AAT TGC AAG AAA TTG CTA TGT-3'
Nested_GSP_ forward	5'-GAA GCA CCA AAG ATG AAA ACA TCG-3'

2.2 Methods

2.2.1 Molecular biology methods

2.2.1.1 Isolation of RNA

Total RNA was isolated from mixed blood stages, blood stage schizonts, mid-gut and salivary gland sporozoites and *in vitro* pre-erythrocytic stages harvested at 24, 48 and 63 hours post infection, using the RNAeasy kit according to the manufacturer's instructions (Qiagen). All samples were lysed in 350 µl RLT buffer containing 3.5 µl β-mercaptoethanol. Following extraction, the RNA was dissolved in nuclease-free water and subjected to treatment with the TURBO DNAse Kit, to remove any contaminating DNA. The DNAse treated RNA was then stored at -80 °C.

Organs of experimental mice infected with either *Pb*ANKA WT or *PbmaLS*_05 (-) parasites were harvested after intra-cardial perfusion with 1x PBS. Isolated spleens and brains were homogenized in 2 and 3 ml of TRIZOL respectively and RNA extracted according to the manufacturer's instructions. The isolated RNA was DNAse treated as previously described, and stored at -80 °C.

The purity of RNA samples was measured on a photometer and integrity ascertained by 260/280 values.

2.2.1.2 Reverse Transcriptase PCR

cDNA was synthesized from total RNA using a mixture of random and oligo dT primers and MMulV reverse transcriptase enzyme according to instructions provided in the First Strand cDNA synthesis kit (Thermo Scientific). Reverse transcribed cDNA was aliquoted and stored at -20 °C. Transcriptional analysis for all stages of the parasite life cycle was performed using different primers designed to bind at 55 °C. A minus RT reaction was also performed in parallel to detect any presence of contaminating DNA.

2.2.1.3 Quantitative Real-time PCR

Quantification of parasite load in the spleen and brain was done as previously described (276). WT and KO infected mice were sacrificed around day 8 after injection of sporozoites, and day 5 p.i. with iRBC when WT mice developed clinical signs of ECM. RNA isolated from individual organs was reverse transcribed into cDNA. Equal amounts of cDNA were mixed with Power SYBR green PCR mastermix and transcript levels were measured on the ABI 7500 thermocycler. Parasite transcripts were measured using *P. berghei* 18S rRNA and mouse GAPDH primers **(2.1.14.5)**. All samples were analysed in duplicate wells in a total volume of 13 µl using the standard program of initial denaturation at 95 °C for 10 minutes, denaturation at 95 °C for 15 s, annealing at 55 °C for 15 s and extension at 60 °C for 45 s for 40 cycles. The data acquired was analysed on the program accompanying the ABI 7500 cycle. All transcript levels were normalized to mouse GAPDH and relative copy numbers were determined *via* the $2^{-\Delta\Delta CT}$ method.

2.2.1.4 5' and 3' RACE

The 5' RACE and 3' RACE system for Rapid Amplification of cDNA ends was used to determine the transcription initiation site and transcription end site, respectively. 1µg of RNA from blood stage schizonts and sporozoites was used to perform the RACE with gene-specific primers **(2.1.14.5)** according to the manufacturer's instructions. The results were confirmed by a nested PCR and the product sequenced.

2.2.1.5 SDS PAGE and Western Blotting

Western blot analysis was performed as previously described (16). Purified parasites were lysed in RIPA buffer (containing 4% Protease Inhibitor Cocktail and 0.05% 2M DTT) and stored at -80^0C. Parasitic stages were lysed in RIPA and stored at -20 °C. Blood stages were lysed in saponin buffer, washed once with 1x PBS and resuspended in RIPA, to avoid contamination with haemoglobin. Protein quantification was done using Bradfords assay after which 10µg of parasite protein was mixed with 1x sample buffer and boiled for 5 minutes at 95 °C. The sample was cooled on ice for 3-5 minutes and centrifuged briefly at maximum speed for 30 seconds. Parasite proteins were separated on a pre-cast 4-12% gradient gel, in MOPS buffer for 1 hour at 200V. On completion of the run, the proteins were blotted onto a PVDF membrane, in transfer buffer without methanol for 3 hours at 30V. Residual proteins on the gel were detected with Coomassie staining for 10 minutes on a shaker, followed by de-staining with tap water. The

membrane was then blocked for 1 hour at RT with 5% milk powder prepared in TBST buffer, and then kept in blocking buffer containing primary antibody, overnight at 4 °C. After washing, the membrane was incubated for 1 hour at RT with the secondary antibody prepared in blocking buffer. Following three washes with TBST, the membrane was air dried briefly to enable marking of the ladder with a chemiluminescent marker. The membrane was then incubated with the Perkin Elmer substrate kit according to the manufacturer's instructions, for 5 minutes on a rotor. Signals were visualized using the Li-Cor Blot Scanner and images analysed with ImageStudio 4.0.

2.2.1.6 Cloning of *PbmaLS*_05 knockout construct

Targeted replacement of the *PbmaLS*_05 genomic locus was done by double homologous recombination. A 546 bp fragment from the 5' UTR and a 509 bp fragment from the 3' UTR of the PBANKA_140100 gene were amplified from *P.berghei* ANKA genomic DNA (gDNA) and both fragments cloned into a Pb300 myc-mCherry vector. The resulting plasmid was linearised with enzymes *Sac II* & *Xho I*, gel extracted and used for targeted replacement of the endogenous *PbmaLS*_05 with a selection cassette **(Appendix Fig.6.1A)**. Blood stage schizonts purified from a density gradient were transfected with the linearised construct by electroporation using the Amaxa nucleofactor kit (Lonza), and then intravenously injected into NMRI mice. Transfected parasites were selected by addition of pyrimethamine to the drinking water (277). Primer pairs flanking the integration sites as shown in the diagram below **(Fig. 2.1)** were used to confirm stable integration into the parasite genome. Clonal populations of *PbmaLS*_05 (-) parasites were generated by limiting dilution and injection into mice. Absence of a wild type population was verified by genotyping of gDNA and RT-PCRs amplifying different fragments of the PBANKA_140100 wild type locus.

2.2.1.7 Cloning of *Pb*maLS_05 CT EGFP tagging construct

The tagging construct was designed to introduce an EGFP tag at the C-terminal of *Pb*maLS_05 using the double homologous crossover strategy. A 523 bp fragment corresponding to the 3' end of the *Pb*maLS_05 open reading frame (ORF) without the stop codon and a 509 bp fragment from the 3' UTR region were amplified from *P.berghei* ANKA genomic DNA, using primers listed in **(2.1.14.2)**. Both PCR fragments were then cloned into a b3D+ EGFP vector upstream of the EGFP **(Appendix Fig. 6.1B).**

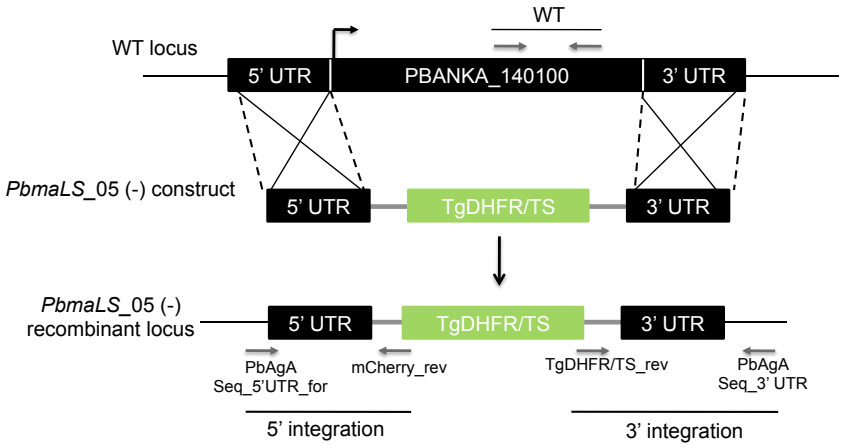

Figure 2.1 *PbmaLS_05* (-) targeting construct with primer pairs to determine integration.

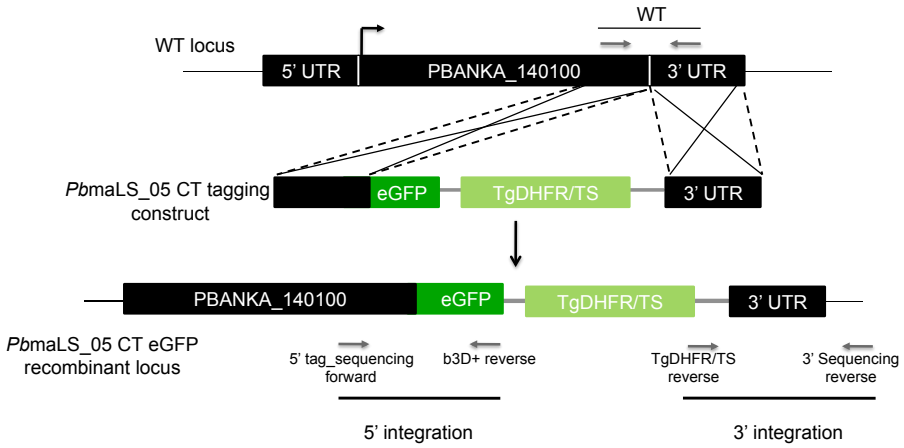

Figure 2.2 *Pb*maLS_05 CT EGFP tagging construct with primer pairs to determine integration.

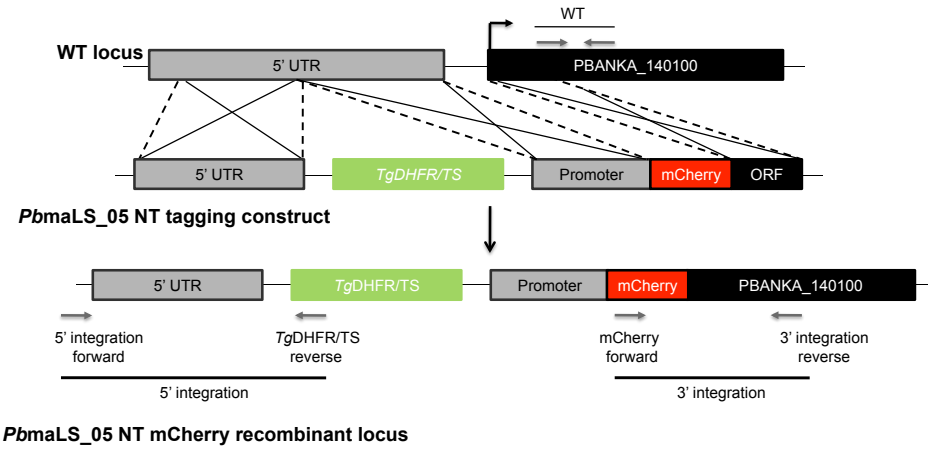

Figure 2.3 *Pb*maLS_05 NT mCherry tagging construct with primer pairs to determine integration.

The resulting plasmid was linearised by an overnight digest with enzymes *Sac II* & *Kpn I*, gel extracted and transfected into purified blood stage schizonts. The selection and cloning procedures were carried out as previously described **(2.2.1.6)**. Stable integration

was confirmed using primers that bound upstream of the integration site and downstream of the stop codon **(Fig. 2.2)**. Expression of EGFP was analysed by live fluorescence microscopy **(Fig. 3.4)**.

2.2.1.8 Cloning of *Pb*maLS_05 NT mCherry tagging construct

The NT tagging construct was designed to introduce an mCherry tag at the N-terminal end of *Pb*maLS_05 by the double homologous crossover strategy. A 656 bp fragment corresponding to one half of the promoter region of *Pb*maLS_05, a 1184 bp fragment corresponding to the second half of the *Pb*maLS_05 promoter, the 404 bp of the *Pb*maLS_05 ORF excluding the ATG along with an mCherry tag were amplified using the primers listed in **(2.1.14.3)** and cloned into a b3D vector as shown in the diagram **(Appendix Fig. 6.1C)**. The resulting plasmid was linearised by an overnight digest with enzymes *Sac II* & *Kpn I* and transfected into purified blood stage schizonts. The selection and cloning procedures were carried out as previously described **(2.2.1.6)**. Stable integration was confirmed using primers flanking the integration sites **(Fig. 2.3)**. Expression of mCherry was analysed by live fluorescence microscopy **(Appendix Fig. 6.5C)**.

2.2.1.9 Cloning into a pGEM-T easy Vector for Sequencing

PCR fragments were cloned into the multiple cloning site of a pGEM-T easy vector according to the manufacturers' instructions (Promega). The vector was transformed into *E.coli* bacteria, cultured overnight and purified using the Plasmid mini-prep kit (Qiagen). The plasmid was sequenced using the T7 and SP6 primers (GATC).

2.2.2 Mosquito methods

2.2.2.1 *Anopheles* breeding

Anopheles mosquitoes were bred at 28 °C with 80% humidity. The eggs deposited on a filter paper by gravid female *Anopheles stephensi* mosquitoes were collected, washed once with 70% ethanol, twice with 0.1% salt solution and transferred to trays filled with 3-4 L of 0.1% salt solution. After 2-3 days, the hatched larvae were split into 15 trays containing fresh salt water and cat food pellets (brekkies), and left to develop into pupae for 7 days. Adults emerging from trays containing pupae were collected 2 days later, transferred to cages and fed on cotton pads soaked in 0.1% salt solution and 10% sucrose solution supplemented with 20 μg PABA. After an infectious blood meal (described below), the mosquitoes were transferred to an incubator maintained at 21 °C,

80% humidity and a 12-hour light/dark cycle. Fresh eggs were collected 3-4 days after the blood meal, to maintain the mosquito cycle.

2.2.2.2 *Anopheles* infection

Mice infected with *P. berghei* parasites were examined for presence of exflagellating gametocytes **(section 2.2.2.3)**, then anaesthetized and fed upon by naïve mosquitoes. Feeding was permitted for 12-15 minutes and twice within a 48-hour period. Infected mosquitoes were then kept at 21 °C and 80 % humidity.

2.2.2.3 Determination of prevalence

5-10 female mosquitoes were dissected 10 days post blood meal and their mid-guts isolated in RPMI/3% BSA. The mid-guts were placed on a glass slide, cover with a cover slip and examined under a 40x objective of a light field microscope with phase contrast, for the presence of oocysts. Prevalence was determined from the number of infected mid-guts, i.e. mid-guts positive for oocysts.

2.2.2.4 Sporozoite isolation and quantification

Sporozoites were isolated from mid-guts and salivary glands of infected mosquitoes on day 14 and 17 respectively. Mid-guts or salivary glands were crushed using a pestle in a 1.5 ml eppendorf tube containing RPMI/ 3% BSA and centrifuged for 3 minutes at 1000 rpm at 4 °C. After 3 repetitions, the supernatant from each step was pooled and sporozoites counted in the four large squares of a Neubauer haemocytometer. The total number of sporozoites per ml was estimated by the following formula:

Total number of sporozoites counted in 4 large squares / 4 x dilution factor x 10000.

2.2.3 Cell biological methods

2.2.3.1 Culture of human hepatocarcinoma cell line

Human hepatocarcinoma (HuH7) cells were maintained at 37 °C and 5% CO_2 in DMEM culture medium supplemented with 10% FCS and 1% antibiotic cocktail. Cells were cultured in 25 cm^2 gas-permeable culture flasks until confluent and split twice a week, depending on requirement. Splitting was done by aspiration of medium, washing with HBSS and incubation with 1-3 ml trypsin-EDTA for 10 minutes at 37 °C. Trypsinisation was stopped by the addition of 7-10 ml pre-warmed culture medium and the cell suspension transferred to a 15 ml falcon tube. After pelleting the cells by centrifugation

at 1000 rpm for 2 minutes, the supernatant was discarded and cells re-suspended in complete medium. An aliquot of the suspension was then transferred to a new flask and maintained at 37 °C. Frozen stocks were prepared by resuspending the cells in freezing solution (80% cell suspension, 10% DMSO, 10% FCS) and storage at -80 °C.

Viability was determined by mixing 1 part cell suspension with 10 parts trypan blue (10% solution). Live cells were counted in the four large squares of a Neubauer's chamber and calculated using the formula: Viable cells counted/4 x dilution factor x 10000 per ml.

2.2.3.2 Preparation of pre-erythrocytic stages for RNA isolation

25000 HuH7 cells were plated in an 8-well Lab-Tek and allowed to differentiate into a monolayer for 24 hours. Pre-erythrocytic stages were obtained by infecting adherent cells with sporozoites isolated from salivary glands of infected mosquitoes. After 90 minutes of invasion time, the excess sporozoites were aspirated and the wells replaced with fresh medium. The cells were harvested at 24, 48 and 63 hours post inoculation, lysed in RLT buffer and stored at -80 °C until RNA isolation.

2.2.4 Microscopy methods

2.2.4.1 Determination of parasitaemia and exflagellation

A drop of blood obtained after pricking the tip of the tail of mice was smeared on to a glass slide; air-dried, fixed with 100 % methanol and stained with 10 % Giemsa solution. Stained smears were observed under an oil immersion objective (100x) of a light microscope and the total number of parasites and red blood cells counted. Parasitaemia was expressed as % parasitized red blood cells.

To check for exflagellation, a drop of tail vein blood was placed on a glass slide, covered with a glass cover slip and incubated at room temperature for 10 minutes. Exflagellation of microgametocytes occurs upon drop in temperature, change in pH or upon simulation with xantheneuric acid. The slide was then observed under a 40x objective of a light microscope with phase contrast, and checked for exflagellating centres.

2.2.4.2 Sporozoite motility

Gliding motility patterns of salivary gland sporozoites were assessed by addition of sporozoites to a glass bottom 96-well plate pre-coated with 3% BSA-RPMI and incubation at 37 °C. The sporozoites were allowed to adhere for 10 minutes and an

image was recorded every 3 seconds thereafter for 5 minutes, using a light microscope with phase contrast. Several movies were recorded over different sections of the well and later analysed using the ImageJ software.

In order to visualize trails of CSP, the sporozoites were allowed to glide on a slide pre-coated with 3% BSA at 37 °C and then fixed with 4% PFA for 20 minutes at room temperature followed by blocking with 10% FCS in PBS for 30 minutes. The wells were incubated with 1:300 α-CSP antibody for 45 minutes at 37 °C, followed by three washes with 1% FCS in PBS, after which the wells were incubated with 1:300 Goat anti-mouse secondary antibody coupled to Alexa Fluor 488, for 45 minutes a 37 °C. The nucleus was stained with 1:10000 Hoechst during the last 5 minutes of incubation with the secondary antibody. After 3-5 washes, the wells were mounted in 30 % glycerol, covered with a cover slip and sealed with nail polish.

2.2.4.3 Pre-erythrocytic stages

8000 HuH7 cells were plated in a Matek lab dish for 24 hours and infected with 10^5 *Pb*maLS_05 CT EGFP sporozoites for 2 hours at 37 °C. After aspiration of excess sporozoites, fresh medium was added to the wells and the infected cells placed in an incubator. Intra-hepatic stages were visualized live at 24, 48 and 58 hours post infection, using a spinning disc confocal microscope.

For the azithromycin treatment, 250 mg tablets were dissolved in ddH_2O and then pre-diluted 1:100 in complete DMEM. 6 µl of the pre-diluted solution was then added to 1.5 ml to achieve a final concentration of 1 µM. Liver stages were treated 24 hours post infection to minimize apoptosis of parasitic stages and the medium with antibiotic refreshed once daily until imaging.

Merosomes were carefully aspirated 72 hours post infection from wells containing infected hepatocytes, spun down at 1200 rpm for 5 minutes in an eppendorf tube and then re-suspended in plain DMEM (without FCS) containing Hoechst and Mito-tracker, for 20 minutes at 37 °C. After an additional spin, the merosomes were re-suspended in complete DMEM for imaging. Care was taken to leave a small volume of solution in the eppendorf tube, both times after the spin, so as to avoid rupturing of the merosomes.

An hour before imaging, the medium in the wells was replaced with imaging medium containing 1:10000 Hoechst and 50nM Mitotracker. The parasites were imaged live in a

pre-incubated chamber at 37 °C with 5 % CO_2 over an oil immersion objective of a Spinning disc confocal microscope. Stacked images with a z spacing of 0.5 μm were recorded using the Volocity software. The images were analysed using ImageJ and deconvolved using AutoQuant X software. Deconvolution was done using a calculated point spread function, with 35 iterations and noise reduction. The contrast was enhanced for some images using ImageJ.

In order to assess parasite growth at 24, 48 and 63 hours p.i., intra-hepatic development was stopped and fixed by the addition of ice-cold methanol for 10 minutes, at room temperature. The cells were then washed twice with 1% FCS in PBS and blocked with 10% FCS in PBS. Liver stages were visualized using 1:100 of hybridoma cell culture supernatant containing anti-Hsp70 antibody, followed by three washes and the addition of 1:300 Alexa Fluor 488 goat anti-mouse secondary antibody. The nucleus was stained using 1:10000 Hoechst that was added to the secondary antibody solution. The cells were washed thrice and then mounted in 30% glycerol, sealed with a coverslip and nail polish and imaged using a fluorescence microscope (Zeiss). Images were analysed using ImageJ.

2.2.5 Rodent methods

2.2.5.1 Ethics statement

All experimental animal procedures were performed in accordance with standard guidelines as set by regulations concerning FELASA category B and GV-SOLAS. Animal experiments were approved by the German authorities (Regierungspräsidium Karlsruhe, Germany), 1 8 Abs. 1 Tierschutzgesetz (TierSchG) under the license G-260/12 and G-258/12.

2.2.5.2 Mice & Parasites

6-8 week old female C57BL/6 and NMRI mice were purchased from Janvier, France and kept under specific pathogen free (SPF) conditions at the animal facility (IBF) of the University of Heidelberg.

Blood stage parasites of *Pb*ANKA (clone 15Cy1) and *PbmaLS*_05 (-) were passaged in NMRI mice by the injection of cryopreserved stabilates prepared in Alsever's solution. C57BL/6 mice were either inoculated intravenously with 10^4 salivary gland sporozoites or through bites of infectious mosquitoes. Alternatively, 10^6 iRBCs were injected intravenously into the tail vein of mice. Pre-patency was determined by the first

appearance of parasites in the blood and parasitaemia monitored daily by Giemsa-stained blood smears.

2.2.5.3 Anaesthesia

Mice infected with parasites for the blood meal were injected intraperitoneally with 80 µl of Ketamine/Xylazine for the first blood meal and 100 µl for the second blood meal. All experimental mice were sacrificed after the second blood meal.

2.2.5.4 Evans Blue staining and RMCBS

Mice were monitored for signs of ECM every day using the rapid murine coma and behaviour scale (RMCBS) as previously described (278) **(Appendix Fig. 6.2)**, and euthanized when signs of cerebral pathology were evident. The extent of permeabilisation of the blood-brain barrier was determined by the injection of Evans Blue, a non-toxic dye that is widely used to study endothelial and cellular membrane permeability (279). Mice were sacrificed 1 hour after an intravenous injection of 150 µl 2% Evans blue, then perfused intra-cardially with 20 ml PBS and the brains isolated.

2.2.6 MRI

The baseline scan for infected mice was performed on day 2-post injection with sporozoites and day 0 post injection with iRBCs. MRI was performed on a 9.4 T small animal scanner (BioSpec 94/20 USR, Bruker Biospin GbmH, Ettlingen, Germany) using a volume resonator for transmission and a 4-channel-phased-array surface receiver coil. Anaesthesia was induced per inhalation using 2 % and maintained with 1-1.5 % isoflurane. Mice were placed prone in a fixed position to monitor body temperature and respiration. MRI scans were performed on day 5 p.i. for iRBC infected mice (WT n=6, KO n=7), and day 7 for sporozoite infected mice (WT n=6, KO n=7). The MR imaging protocol included 3D T1-weighted imaging (TR/TE=5/1.9ms, FA=8.5°, 156µm isotropic resolution), T2*-weighted flow compensated gradient echo imaging (TR/TE=50/18ms, FA=12°, 80µm isotropic resolution) and 2D T2-weighted imaging covering the rostral part of the brain from the olfactory bulb to the lateral ventricles (TR/TE=2000/22ms, slices=12, slice thickness=0.7mm).

Image processing was undertaken in Amira 5.4 (FEI, Visualization Sciences Group). Brain volume was assessed semi-automatically on 3D T1-w datasets. Microhemorrhages were analyzed on T2*w images, edema on T2-w images and T2*w images. Grading of

disease severity into mild (=1), moderate (=2) and severe (=3) was performed as previously published. Faint oedema or less than 5 micro-haemorrhages were given a score of 0.5

2.2.7 Histology

Spleens were carefully harvested after perfusion and placed in 4% PFA. All organs were cut into 10 µm thick coronal sections using a cryotome (Leica Microsystems, Vienna, Austria) and then directly mounted onto SuperFrost/Plus slides (Microm International, Walldorf, Germany). After staining with H&E (Thermo Fisher Scientific, Waltham, MA) and Giemsa (Thermo Fisher Scientific), the slides were blinded and three randomly selected sections per coronal plane were subjected to histological analysis. Examinations were done on an Olympus BX45 research microscope (Olympus, Tokyo, Japan).

2.2.8 Immunological methods

2.2.8.1 Isolation of Splenocytes

Experimental mice were sacrificed and perfused intracardially with 20 ml 1x PBS. The spleens were removed and homogenized in 3 ml complete medium, over a 70 µm cell strainer using a plunger from a 5 ml syringe. An additional 7 ml of medium was used to flush out the residual cells and the entire suspension transferred to a 15 ml falcon. The cell pellet obtained after centrifugation for 5 minutes at 1500 rpm, 4 °C, was treated with 3 ml RBC lysis buffer, for 6 minutes on ice. Cell lysis was stopped by the addition of 7 ml of fresh medium and the suspension centrifuged again. The resulting cell pellet was resuspended in 2-4 ml volume of fresh medium. The cells were diluted 1:400 in trypan blue and viable cells counted using a haemocytometer. 100 µl of the cell suspension was used for flow cytometry or pipetted into a 96-well plate and stimulated *ex vivo* with peptides **(2.2.8.3)**.

2.2.8.2 Isolation of brain infiltrating lymphocytes

After intracardial perfusion with 1x PBS, the brains were isolated from sacrificed mice and digested in 10 ml PBS containing 0.05% collagenase IV and 0.001% DNAse I, for 45 minutes at room temperature. After incubation, the brains were homogenised through a 70 µm cell strainer using the plunger from a 5 ml syringe. The cell suspension obtained was transferred to a 15 ml falcon along with the residual cells that were flushed with 2 ml of MACS buffer, and centrifuged at 500 rpm for 30 seconds to pellet the large debris. The supernatant was carefully layered over 10 ml of 30% percoll solution and centrifuged

for 10 minutes at 1900 x g, without brake. The pellet fraction consisting of brain infiltrating lymphocytes and erythrocytes was then treated with 500 µl of RBC lysis buffer for 6 minutes on ice. Lysis was terminated by addition of 1 ml of fresh medium and the entire suspension centrifuged at 1500 rpm for 8 minutes. The cell pellet obtained was resuspended in 250 µl of complete medium and viable cells quantified by the trypan blue exclusion method. After assessing viability, 100 µl of the cell suspension was processed for flow cytometry or plated for *ex vivo* stimulation with peptides **(2.2.8.3)**. Cell counts were determined using a Neubauer's chamber.

2.2.8.3 *Ex vivo* stimulation with GAP50 peptide

Isolated lymphocytes from brains, spleens and livers were resuspended in complete medium and stimulated *ex vivo* with 1 µM GAP50 peptide (Pb1 epitope, (209)). Briefly, 100 µl of cell suspension was plated in duplicate sets of stimulated and un-stimulated wells, in a round-bottom 96 well plate. 100 µl of stimulus containing 2µM GAP50 peptide, prepared in complete medium was added to the stimulated wells, to achieve a final concentration of 1 µM. Both stimulated and un-stimulated cells were cultured in the presence of 10 µg/ml Brefeldin A for 5 hours, at 37 °C, 5% CO_2 and 95% humidity. After incubation, stimulation was stopped and cells stained for flow cytometry (**2.2.8.4).**

2.2.8.4 Flow cytometry

Lymphocyte populations from spleens and brains of infected and naïve mice were isolated and plated in a 96-well plate and stimulated with 1 µM GAP50, for 5 hours at 37 °C. After 5 hours of incubation, the cells were pelleted, washed once with 100 µl 1x PBS to discard any traces of stimulus and then stained with α-CD8-PE Cy7 and α-CD4-PerCp Cy5.5 antibodies on ice, for 20 minutes in the dark. The cells were then fixed with 2% PFA for 15 minutes and stained for intra-cellular markers with α-IFN-γ APC-Cy7 in permeabilisation buffer. After 20 minutes incubation on ice, the cells were washed once with 1x PBS, fixed with 1% PFA, washed again and re-suspended in 100 µl PBS for FACS measurements (FACS Canto I). The data was analysed using FlowJo (Version 10). The gating strategy for lymphocytes, T cells and IFN-γ^+ $CD8^+$ T cells are described in **Appendix Fig. 6.7.**

2.2.8.5 ELISpot assay

All steps till the addition of secondary antibody were performed under sterile conditions. Multi-Screen Filter plates were briefly pre-wetted with sterile 35% ethanol in PBS and washed thrice with 1X PBS. The plates were then coated with 50 µl purified IFN- γ (10 µg/ml in 1X PBS), sealed and incubated overnight at 4 °C. After 24 hours, the plates were washed 3-4 times with 150 µl 1X PBS and then blocked with 200 µl RPMI complete medium for at least 2 hours at 37 °C.

Splenocytes isolated from naïve mice were used as donor APCs in the range of 10^5 per well. One set of splenocytes were pulsed with a pool of maLS_05 peptides (final concentration 10 µM), or GAP50 (10 µM) or un-pulsed (DMSO control), for 1 hour at 37 °C, with intermittent shaking. After 1 hour, the cells were washed once with 8 ml of RMPI complete medium, centrifuged at 1500 rpm for 5 mins and re-suspended in 2 ml medium. After re-counting, the volume was adjusted to obtain 10^5 cells per 50 µl suspension. Splenocytes and brain infiltrating lymphocytes were isolated and quantified from naïve, *Pb*ANKA and *PbmaLS*_05 (-) infected mice, as described in sections 2.2.8.1 and 2.2.8.2. 0.2 x 10^6 effector cells (brain and spleen lymphocytes) were added to each well in a total volume of 100 µl, together with 50 µl of pulsed or un-pulsed APCs. An additional set of wells stimulated with α-CD3 antibody and un-pulsed APCs, served as positive controls. After incubation for 22-24 hours at 37 °C, the plates were washed 8-10 times with 150 µl PBS/0.05% tween 20 and then incubated with 50 µl of biotinylated anti-IFN-γ antibody (5 µg/ml in PBS/0.2% BSA) for 2 hours at room temperature. The plates were then washed 6 times with PBS/0.05% tween 20 and twice with PBS, followed by incubation with 50 µl streptavidin-ALP (1:1000 in PBS) for 1 hour at room temperature. The plates were washed thrice with PBS/0.05% tween 20 followed by 3 washes with PBS. Spots were visualized subsequently by the addition of substrate solution (AP Conjugate Substrate Kit, Biorad) according to the manufacturer's instructions. After incubation for 15 minutes at room temperature, the reaction was terminated by 10 washes under running ddH_2O. The plates were allowed to dry overnight at room temperature and spots counted using an ELISpot plate reader.

2.2.8.6 Statistical analyses

Statistical significance was determined using the GraphPad Prism software (GraphPad Software V 5.0, La Jolla, CA). Differences were analysed by mean of nonparametric tests

(One way ANOVA followed by either Kruskal-Wallis or Bonferonni post-hoc adjustment) or Student's t test. Asterisks indicate significance; where *** is $p<0.0001$, ** is $p<0.001$ and * is $p<0.01$.

Chapter 3

Results

3.1 *PfmaLS*_05 (PF3D7_1302500) is an up-regulated transcript in *in-vitro* liver stages of *P. falciparum* RAS

PF3D7_1302500 (*Pf*maLS_05) was identified as an enriched transcript in liver stages of *P. falciparum* radiation attenuated sporozoites (*Pf*RAS-LS). It was selected after a suppression subtractive hybridisation screen (SSH) that compared *Pf*RAS-LS to liver stages of wild type *P. falciparum* (*Pf*WT-LS) (280). *Pf*maLS_05 is highly conserved in all *Plasmodium* species and was hypothesised to play a role in protective immunity that has been observed with RAS immunisations (281, 282).

3.2 *PfmaLS*_05 is conserved in all *Plasmodium* species both at the genomic and proteomic level

*PfmaLS*_05 is a *Plasmodium* specific gene with an unknown function. A sequence alignment (ClustalW, EBI) of *P. falciparum* (PF3D7_1302500) with *P. knowlesii* (PKH_140100), *P. berghei* (PBANKA_140100), *P. yoelii yoelii 17XL* (PY17X_1402600) and *P. yoelii yoelii XNL* (PY02854 and PY02855) showed that the gene was well conserved in all *Plasmodium* species **(Appendix Fig. 6.3)**. The genomic sequences of *PfmaLS*_05 and *PbmaLS*_05 are about 70.05 % identical to one other **(Fig. 3.1A)** while their protein sequences are about 49 % similar (IP of *Pf*maLS_05 is 8.46 versus IP of *Pb*maLS_05 which is 9.16) **(Fig. 3.1B).** In *P. yoelii yoelii 17XNL* the *Pf*ma*LS*_05 gene is split into two open reading frames with each corresponding to one half of the *Pf*maLS_05 gene. The function of all the orthologues of *Pf*maLS_05 is unknown except for PY02854, which has been annotated as a SEN-1 related protein (PlasmoDB). To determine the function of maLS_05 in the complete parasite life cycle, I functionally characterised the rodent orthologue, PBANKA_140100 (*Pb*maLS_05).

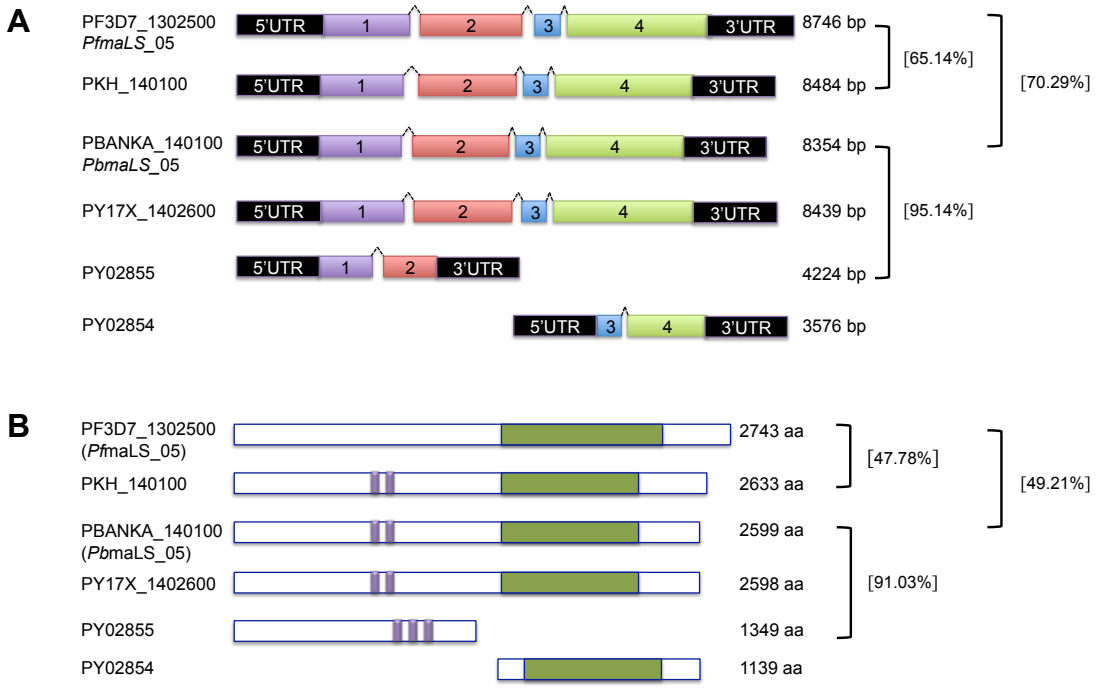

Figure 3.1 *Pf*maLS_05 is well conserved in all *Plasmodium* species. (A) Alignments for gene sequences of *P. falciparum* (PF3D7_1302500), *P. knowlesi* (PKH_140100), *P. berghei* (PBANKA_140100), *P. yoelii yoelii 17X* (PY17X_1402600), *P. yoelii yoelii 17XNL* (PY02854 and PY02855) was done using the ClustalW tool from EMBL-EBI. **(B)** Alignments for protein sequences of PF3D7_1302500, PKH_140100, PBANKA_140100, PY17X_1402600, PY02855 and PY02854 are as shown together with % sequence similarity in brackets. All orthologues of *Pf*maLS_05 contain conserved predicted domains (transmembrane domains are shown in purple and the P loop containing nucleoside triphosphate hydrolase is shown in green).

3.3 Spliced variants of *PbmaLS*_05 are present in different stages of the parasite life cycle

I first performed a transcriptional analysis for *PbmaLS*_05 using cDNA prepared from all developmental stages of the parasite life cycle. *PbmaLS*_05 has a predicted mRNA size of 7800 bp, which precluded amplification of the full-length transcript. I therefore designed RT-PCR primers that spanned across the full gene and amplified fragments of about 500-800 bp in size **(Fig 3.2A)**. I could detect transcripts for all primer pairs in all stages of the parasite life cycle, except mid-gut sporozoites and liver stages at 24 h.p.i. **(Fig. 3.2B)**. The transcript from liver stages harvested 24 h.p.i. was the shortest consisting of fragments from exon 1 and exon 2 alone. In contrast, I did not detect any transcripts for primers amplifying the region over exon 2 and exon 3 in mid-gut sporozoites, indicating a splicing event within either exon **(Fig. 3.2B)**. These results indicated differential splicing of the full-length *PbmaLS*_05 mRNA in different stages of the parasite life cycle. For convenience, I termed the full-length transcript ORF a, the transcript isolated from

mid-gut sporozoites ORF b and the transcript isolated from liver stages 24 h.p.i ORF c **(Fig. 3.2C)**.

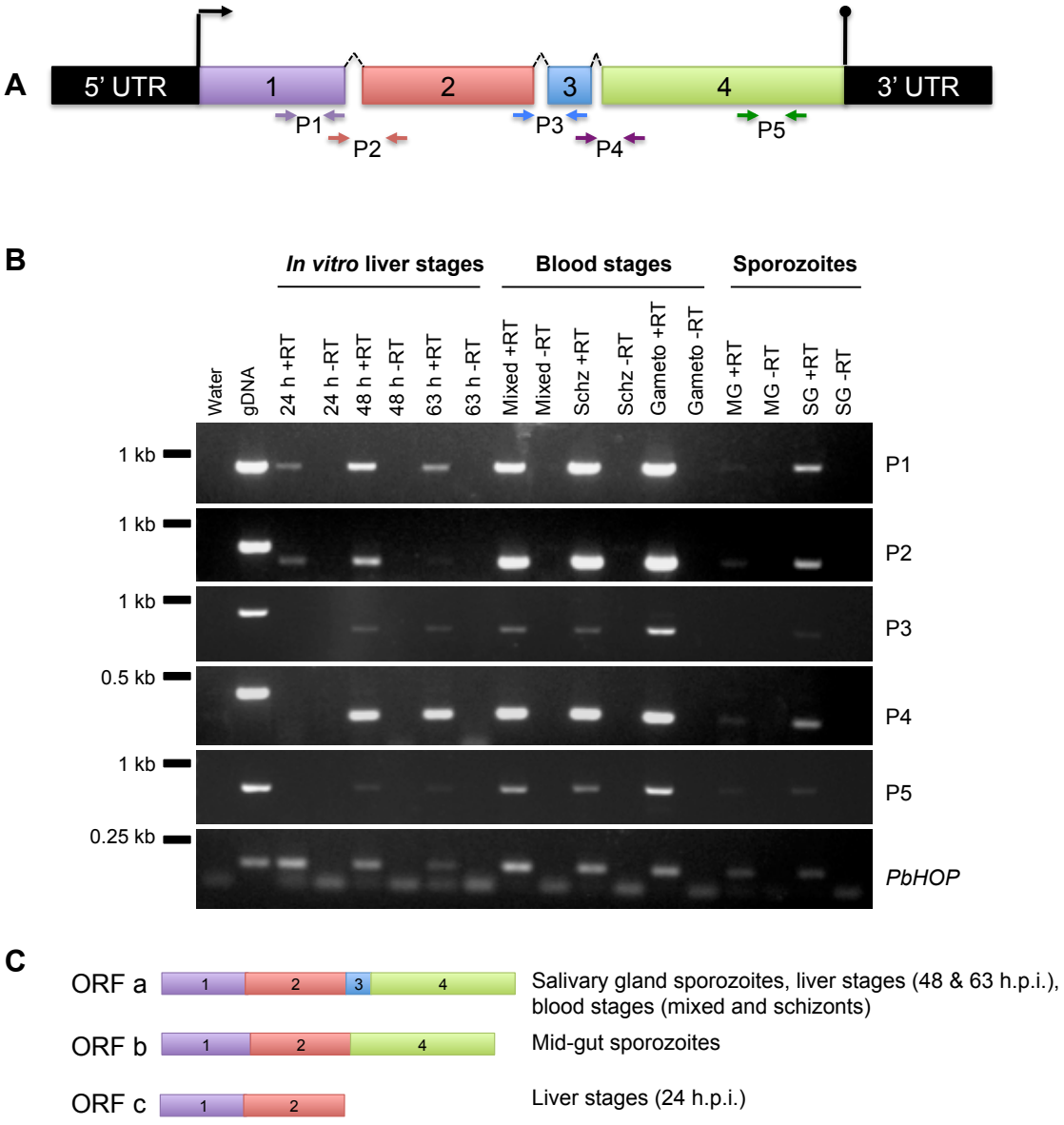

Figure 3.2. *PbmaLS*_05 is alternatively spliced in different stages of the parasite life cycle. **(A)** RT-PCR primers were designed to amplify 500-800 bp fragments from different regions of the full length *PbmaLS*_05 gene. **(B)** PCR analysis for sporozoites (salivary gland; SG and mid-gut; MG), liver stages (24, 48 and 63 h.p.i.) and blood stages (mixed, schizonts; Schz and gametocytes; Gameto) of the parasite life cycle, revealed the presence of distinct alternatively spliced variants in mid-gut sporozoites and early liver stages (24 h.p.i.). A housekeeper, *Pb*HOP was used to exclude genomic DNA contamination and test the integrity of the isolated RNA. **(C)** Schematics of the three isoforms observed for *Pb*maLS_05 are shown.

I used the 5' and 3' RACE method to verify the results of the RT-PCR and determine the exact length of the alternatively spliced isoforms. However attempts to identify the transcriptional initiation and termination sites were unsuccessful due to the length of the cDNA and presence of multiple polyadenine stretches **(Fig. 3.2D).**

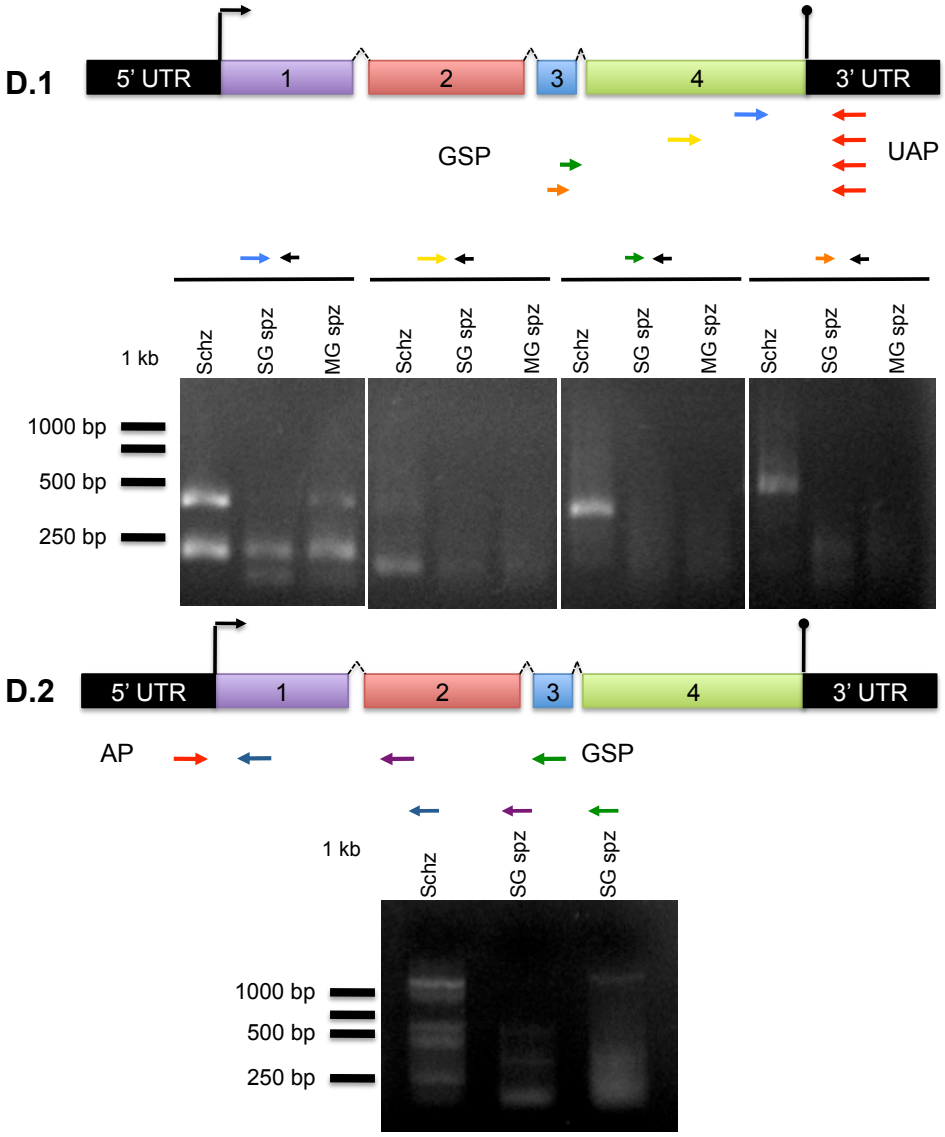

Figure 3.2. *PbmaLS_05* is alternatively spliced in different stages of the parasite life cycle. **(D)** Amplification of the 3' and 5' ends of the *PbmaLS_05* gene from different life cycle stages (schizonts; schz, midgut sporozoites; MG spz and salivary gland sporozoites; SG spz) was done using the kit protocol, according to the manufacturers instructions. Gene-specific primer pairs were designed to bind up-stream of the universal adaptor primer (UAP, 3' RACE) **(D.1)** or downstream of the adaptor primer (AP, 5' RACE) **(D.2)** and amplify fragments of about 500-1000 bp. In-spite of repeated attempts, the transcriptional start and termination sites could not be determined for either of the isoforms.

3.4 The full length *Pb*maLS_05 localises to the apicoplast in blood- and liver-stage schizonts

I decided to mainly focus on characterisation the full-length transcript, ORF a, since it was present in most stages of the parasitic life cycle. To investigate if the full-length *Pb*maLS_05 was translated into a functional protein, I introduced a single C-terminal EGFP at the 3' end of ORF a **(Fig. 2.2)**. Clonal populations of transfected *Pb*maLS_05

EGFP parasites were isolated **(Fig. 3.3)** and then passaged throughout the life cycle, to determine sub-cellular localisation and expression patterns.

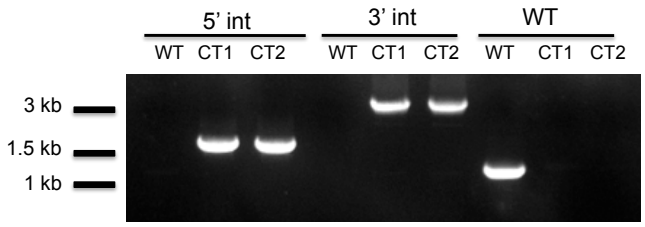

Figure 3.3 C-terminal tagging strategy and cloning of *Pb*maLS_05 EGFP parasites. *Pb*maLS_05 EGFP parasites were generated by a double homologous crossover strategy that introduced a single EGFP tag at the C-terminal end of *Pb*maLS_05. *Pb*maLS_05 EGFP transfected parasites were cloned out using limiting dilution. Stable integration of the tagging construct was confirmed by PCR using primers flanking the integration sites and live microscopy. Clonal populations of *Pb*maLS_05 EGFP parasites were passaged through the life cycle and analysed for *Pb*maLS_05 expression.

In accordance with the transcriptional data, I observed expression of the full-length *Pb*maLS_05 only in late liver stages (48 and 63 h.p.i) and blood stages (rings, gametocytes and schizonts) respectively **(Fig. 3.4).** There was no observable expression in salivary gland sporozoites, mid-gut sporozoites and early liver stages (24 h.p.i.) **(Fig. 3.4)** which could either be attributed to an alternative splicing event or absence of translation of *Pb*maLS_05 in these stages. Unfortunately, neither the full-length protein nor the truncated versions were detectable *via* Western Blot using a GFP antibody **(Appendix Fig. 6.4)**. The localisation and expression pattern of *Pb*maLS_05 in late liver stages, observed through live imaging, was branched-like during the cytomere stage but distinctly more punctuate in liver stage- and blood stage schizonts, reminiscent to what has previously been observed for parasite apicoplast and mitochondria (59) **(Fig. 3.4)**. I therefore co-stained liver stage schizonts, merosomes and blood stage schizonts with a mitochondrial marker but only observed partial co-localisation of the *Pb*maLS_05 protein with the mitochondria **(Fig. 3.5)**.

To determine if *Pb*maLS_05 localised to the apicoplast or mitochondria, I treated *Pb*maLS_05 EGFP liver stage parasites with azithromycin, a drug that specifically inhibits biogenesis of the apicoplast (283, 284). The branched pattern previously observed for *Pb*maLS_05 in late liver stages was not visible after azithromycin treatment, even though the mitochondrial structure was retained **(Fig. 3.5)**. These data suggested that *Pb*maLS_05 localises to the apicoplast.

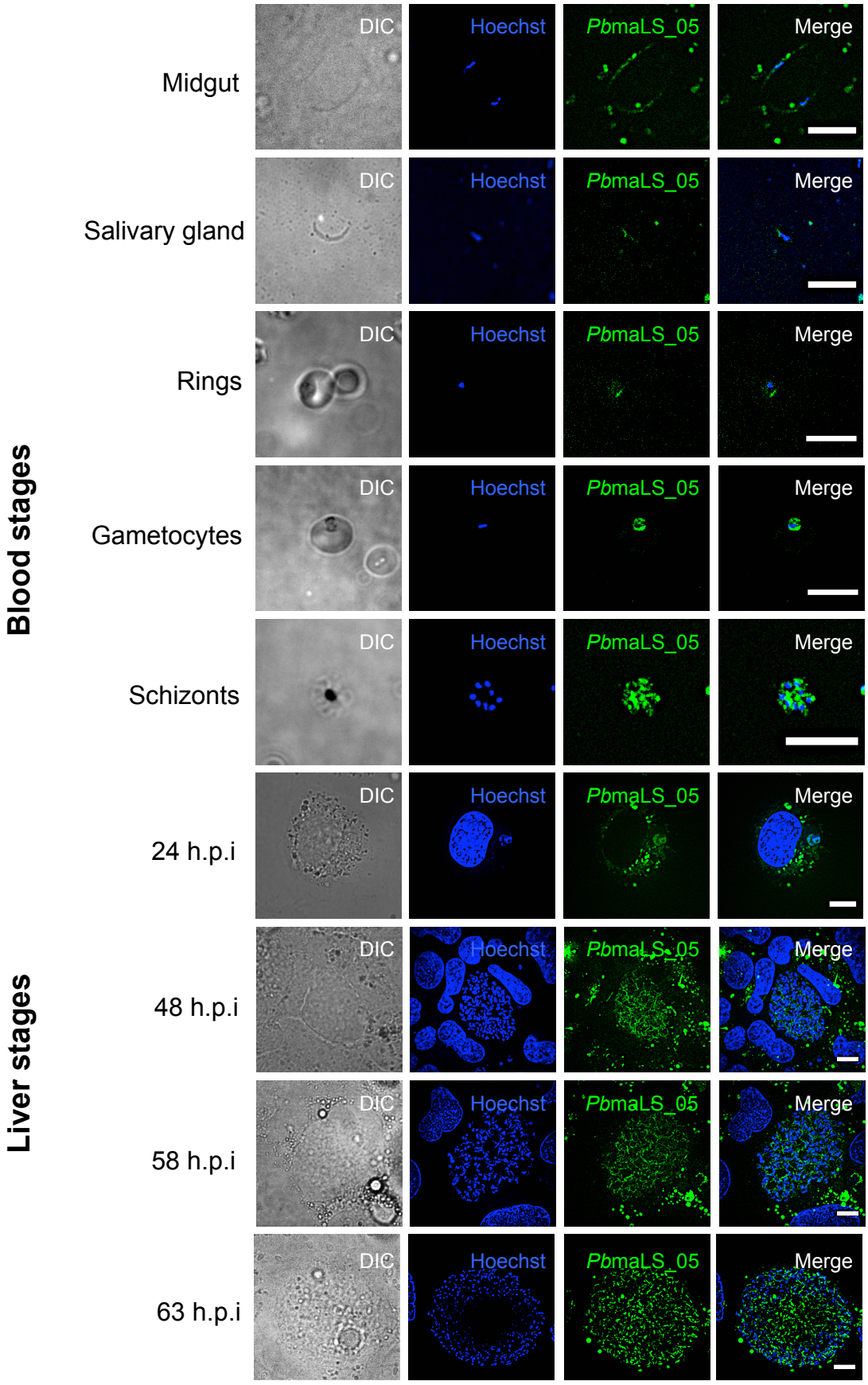

Figure 3.4 Expression analysis of *Pb*maLS_05 in the complete parasite life cycle. *Pb*maLS_05 is expressed in blood stages and late liver stages as observed by live imaging of *Pb*maLS_05 EGFP parasites using a spinning disc confocal microscope. The nuclei were stained with Hoechst. Expression of *Pb*maLS_05 was exclusively observed in blood stages and late liver

stages (48, 58 and 63 h.p.i.). No expression above background was detected in sporozoites and early liver stages (24 h.p.i), at least through live imaging. Scale bar = 10 μm.

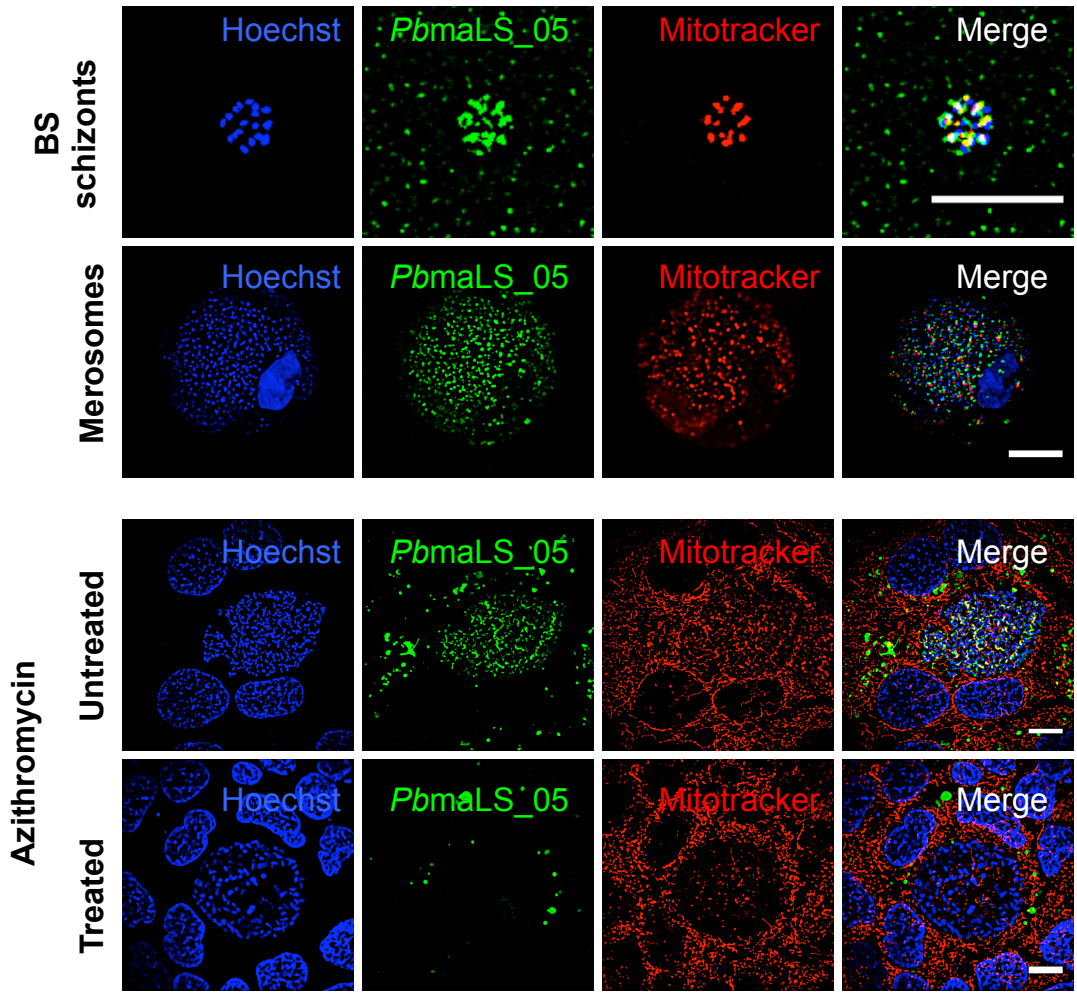

Figure 3.5 *Pb*maLS_05 localises to the apicoplast of liver and blood stage schizonts. The expression pattern of *Pb*maLS_05 was distinctly more punctuate in blood stage schizonts and merosomes. Co-staining of these parasitic stages with Mitotracker suggested partial or no co-localisation with the mitochondria. To check if *Pb*maLS_05 localised to the apicoplast, I treated *Pb*maLS_05 EGFP liver stages with 1 μM azithromycin. The treament abolished the branched structure previously observed in untreated liver stage schizonts, thus confirming that *Pb*maLS_05 indeed localises to the apicoplast. Scale bar = 10 μm; for merosomes scale bar = 80 μm.

In an attempt to visualise the expression of the alternatively spliced isoforms, I additionally generated a transgenic parasite line where I tagged *Pb*maLS_05 N-terminally with an mCherry tag **(Fig. 2.3)**. Clonal *Pb*maLS_05 NT mCherry parasites were isolated after transfection and limiting dilution **(Appendix Fig. 6.5A).** However, I could not observe any detectable level of expression in both sporozoites and early liver stages (24 h.p.i.). Moreover, the branching pattern previously observed with the CT EGFP tag was lost in liver-stage and blood stage schizonts and was replaced by a distinct punctuate

pattern, probably suggesting mis-folding or mis-localisation of the *Pb*maLS_05 protein **(Appendix Fig. 6.5B)**.

3.5 *Pb*maLS_05 influences sporozoite motility *in vitro* but has no effect on pre-patency *in vivo*

To characterise the role of *Pb*maLS_05 in parasite development in the entire life cycle, I replaced the full-length *Pb*maLS_05 with a selectable marker by a double homologous crossover strategy **(Fig. 2.1)**. Clonal lines of *PbmaLS*_05 (-) (KO) parasites were obtained from independent transfections **(Fig. 3.6A).** RT-PCR primers amplifying different fragments of the full-length ORF were used to verify the absence of any residual WT transcript **(Fig. 3.6B)**. Since deletion of the endogenous *Pb*maLS_05 did not affect parasite viability of the clones, I concluded that the gene was dispensable for blood stage development.

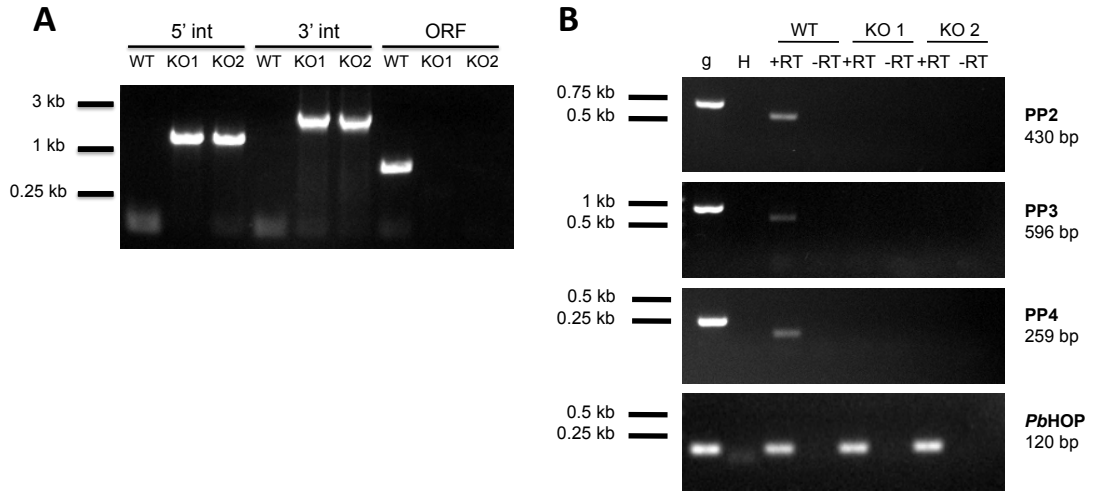

Figure 3.6 Deletion of the endogenous *Pb*maLS_05 and generation of clonal *PbmaLS*_05 (-) parasites. The endogenous *PbmaLS*_05 locus was targeted by homologous recombination with a linearised plasmid consisting of 500 bp fragments from both the 5' and 3' UTR, flanking a *Toxoplasma gondii* DHFR/TS cassette. **(A)** PCR primers flanking the integration sites for both 5' and 3' ends were used to confirm stable integration of the *PbmaLS*_05 (-) construct. Absence of a WT signal in the PCR amplifying a 500 bp fragment of the WT genomic locus verified the presence of clonal populations of *PbmaLS*_05 (-) parasites. **(B)** Absence of any residual WT transcript was verified by RT-PCR on blood stage schizont cDNA.

To investigate if deletion of *Pb*maLS_05 influenced sporozoite development in the mosquito, I infected mosquitoes with WT or KO parasites and then quantified sporozoite numbers from mid-guts and salivary glands on days 14 and 17 p.i. respectively. Although mid-gut sporozoite numbers were comparable between WT and KO infected mosquitoes (WT, 74289±30328 and KO, 54631±22303), the number of salivary gland sporozoites isolated from KO infected mosquitoes was significantly reduced when

compared to those infected with WT (KO, 10609±1421 and WT, 21079±2723, Student's t test, **p<0.001) **(Fig. 3.7A)**. Similar results were obtained with a second independent clone of *PbmaLS*_05 (-) (WT, 49622±9907 and KO, 32463±6512 midgut sporozoite numbers); (WT, 13066±2427 and KO, 4518±1267 salivary gland sporozoite numbers) **(Fig. 3.7A)**.

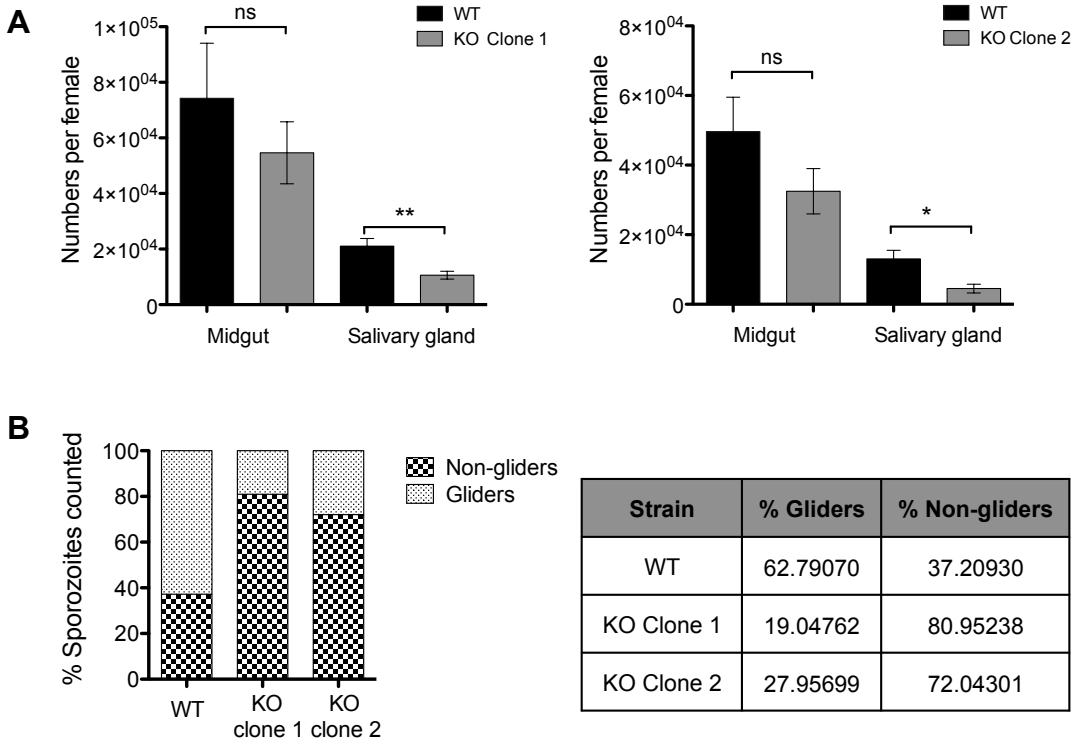

Strain	% Gliders	% Non-gliders
WT	62.79070	37.20930
KO Clone 1	19.04762	80.95238
KO Clone 2	27.95699	72.04301

Figure 3.7 Deletion of *Pb*maLS_05 has an influence on salivary gland invasion and gliding motility. (A) Mosquitoes fed with KO parasites have significantly lower numbers of salivary gland sporozoites in comparison to WT, in spite of comparable infectivity in the mid-gut. Sporozoites were quantified from midguts (day 14 p.i.) and isolated salivary glands (17-21 days p.i) and numbers represented as mean (+/- SEM) of (n) independent experiments [n=5 for KO Clone 1 and n=3 for KO Clone 2]. Statistical significance was determined by the Student's t test (**p<0.001; ns, not significant). **(B)** Quantification of CSP trails by an immunofluorescence assay showed that a higher percentage of *PbmaLS*_05 (-) sporozoites do not glide.

Isolated salivary gland sporozoites glide in concentric circles on a BSA-coated surface *in vitro*, an ability that is used to characterise and investigate defects in motility. I therefore decided to test if the KO sporozoites that successfully invaded the salivary glands were capable of normal motility. To this end, I isolated sporozoites from salivary glands of WT and KO infected mosquitoes and added them to slides coated with 3% BSA in RPMI. After 30 minutes of gliding, I visualised and counted motile and non-motile sporozoites by staining of their CSP trails using immunofluorescent methods.

Quantification of CSP trails revealed a significant reduction in the percentage of gliders (sporozoites with a trail) for the KO in comparison to WT **(Fig. 3.7B)**. However, I never observed any expression of *Pb*maLS_05 in salivary gland sporozoites, based on live imaging of *Pb*maLS_05 EGFP parasites, thus questioning a direct role for *Pb*maLS_05 in salivary gland sporozoite motility.

I then looked at the behaviour of these isolated sporozoites on a BSA-coated slide. Live imaging for 30 minutes suggested that the majority of KO sporozoites were incapable of adhering and gliding, unlike WT sporozoites **(Fig. 3.8A).** This phenotype was consistent even after 30 minutes of gliding, in contrast to WT sporozoites, which adhered within 10 minutes of addition to BSA-coated slides. Interestingly, the few KO sporozoites that were motile had comparable speeds to those of WT sporozoites **(Fig. 3.8B).**

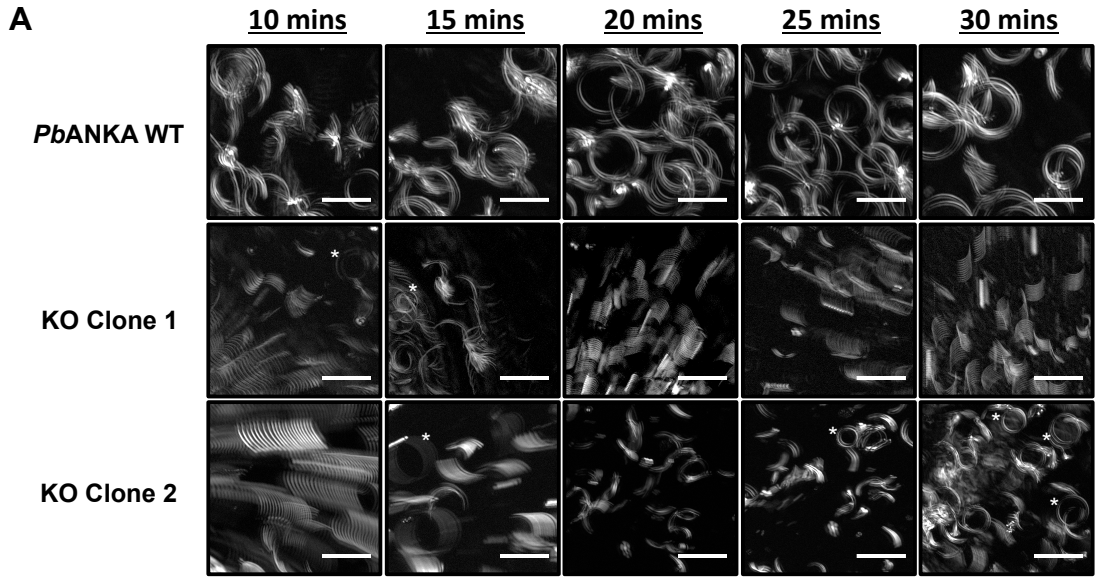

Figure 3.8 The majority of *PbmaLS*_05 (-) sporozoites display an adhesion defect *in vitro*, but the minority that can glide have comparable speeds to wild type sporozoites. (A) Sporozoites isolated from salivary glands of WT and KO infected mosquitoes were added to wells coated with RPMI/3% BSA and allowed to settle for 10 minutes. After 10 minutes, the sporozoites were observed live under a microscope and images recorded every 3 seconds for 5 minutes. While the majority of KO sporozoites did not adhere and glide even after 30 minutes, a majority of WT sporozoites were attached and gliding after the first 10 minutes. Asterisks highlight the few KO sporozoites that managed to adhere and glide. The images represented are Z projections of 20 frames from each time point. Scale bar = 10µm. **(B)** Recording of live images of WT and KO sporozoite motility *in vitro* and quantification of the total distance covered by the sporozoites in 3 minutes suggested that the reduced numbers of KO sporozoites that can attach and glide have comparable speeds to WT sporozoites. The Student's t test was used to determine statistical significance (ns, not significant).

In the next step, I decided to investigate if the *in vitro* motility defect of KO sporozoites also affected their ability to infect hepatocytes. I therefore added sporozoites isolated from salivary glands of infected mosquitoes to an *in vitro* confluent layer of cultured hepatoma cells. After 90 minutes of invasion time, I aspirated the excess sporozoites and fixed the cells at various time points after invasion for immunofluorescent staining of parasitic HSP70. Successful invasion was quantified through the number of liver stages, while measurement of size was used to compare intra-hepatic development between WT and KO parasites. Surprisingly, neither invasion nor development within hepatocytes was affected since both numbers and sizes of liver stages were comparable between WT and KO parasites **(Fig. 3.9A &B)**.

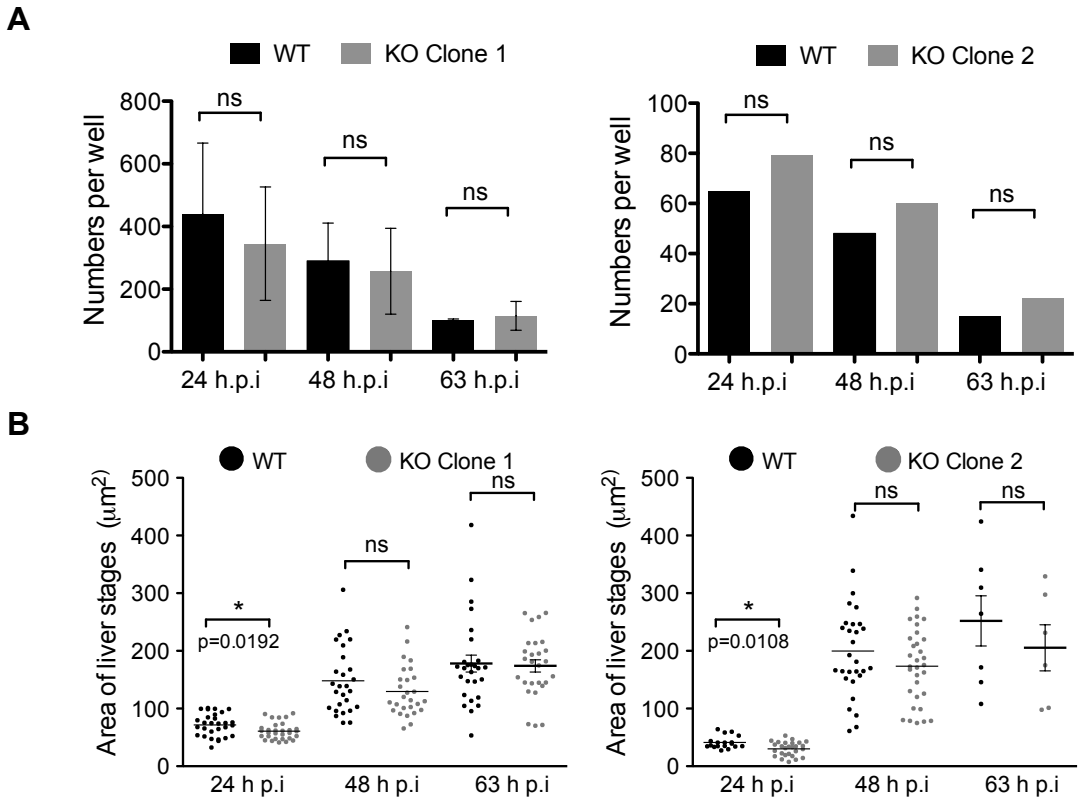

Figure 3.9 *PbmaLS*_05 (-) parasites develop normally within hepatocytes, in spite of the *in vitro* defect in gliding motility. (A) HuH7 cells were cultured in an 8-well labtek for 24 hours and infected with 10^4 WT or KO sporozoites. The cells were fixed, 24, 48 and 63 hours post invasion respectively, and stained with α-Hsp70 (green) and hoechst (blue) to visualise and quantify the intra-hepatic stages, by fluorescence microscopy. There was no difference in liver stage numbers between WT and KO parasites, suggesting no defect in invasion of hepatocytes. **(B)** Liver stage sizes were measured using the ImageJ plugin. There was also no difference in liver stage sizes thus suggesting comparable intra-hepatic development between WT and KO parasites. The Student's t test was used to determine statistical significance (*$p<0.01$; ns, not significant). Scale bar = 10 µm.

The motility of salivary gland sporozoites is important for salivary gland invasion and within the skin where sporozoites traverse tissues to find a blood vessel. To examine if the observed *in vitro* defect in motility translated into a complete block in infectivity *in vivo,* I inoculated mice with sporozoites of either WT or KO by subcutaneous or intravenous injections, or through natural transmission, i.e. by bites of infectious mosquitoes. Interestingly, all KO infected mice became pre-patent on the same day as those infected with WT sporozoites, regardless of the route of infection used **(Table 1)**. The data suggested that *Pb*maLS_05 is not essential for infectivity *in vivo*. Moreover, the absence of any difference in pre-patency supported previous *in vitro* observations where comparable intra-hepatic development was observed between WT and KO parasites. I therefore concluded that deletion of *Pb*maLS_05 influences salivary gland invasion but had no effect on sporozoite motility and infectivity.

Route of infection	WT Pre-patency d.p.i (n= no. of mice)	KO clone 1 Pre-patency d.p.i (n= no. of mice)	KO clone 2 Pre-patency d.p.i (n= no. of mice)
Intravenous	3-4 (n=17)	3-4 (n=15)	3-4 (n=6)
Natural transmission (Mosquito bite)	3 (n=14)	3 (n=7)	3 (n=7)
Sub-cutaneous	4-5 (n=14)	5 (n=7)	4-5 (n=7)

Table 1. Mice infected through various routes with *PbmaLS*_05 (-) sporozoites showed the same pre-patency as *Pb*ANKA WT infected ones. C57Bl/6 mice were infected with 10,000 sporozoites of WT or KO either intravenously, subcutaneously or the natural route of transmission, i.e. infectious bites of 10 mosquitoes. The mice were monitored for blood stage parasites from 3 days on post infection (d.p.i.) by microscopic examination of blood smears and pre-patency calculated as the number of days until the mice became blood stage positive. Experiments performed with *PbmaLS*_05 (-) clones from independent transfections showed the same result.

3.6 *PbmaLS*_05 (-) infected mice do not develop experimental cerebral malaria after sporozoite infection

C57BL/6 mice infected with *P. berghei* ANKA develop a severe cerebral pathology known as experimental cerebral malaria (ECM) that is characterised by disease symptoms like convulsions, paralysis, coma and eventually death (158). The cumulative mortality is about 90% and typically occurs between day 6 and 14 post infection, with low

parasitaemias. Mice that do not succumb to ECM eventually develop hyperparasitaemia and anaemia, and die around the third or fourth week after infection (162). Therefore, it was interesting to observe that even though deletion of the endogenous *Pb*maLS_05 had no effect on parasite viability, none of the mice infected with KO sporozoites developed severe cerebral symptoms unlike WT infected mice that succumbed to ECM between day 7-10 post-injection **(Table 2)**.

Route of infection	**WT**		**KO clone1**		**KO clone 2**	
	No. of mice	ECM (%)	No. of mice	ECM (%)	No. of mice	ECM (%)
Intravenous	17	100	15	0	6	0
Natural transmission (Mosquito bite)	14	85.58	7	0	7	0
Sub-cutaneous	14	78.57	7	0	7	0

Table 2. Mice infected with *PbmaLS*_05 (-) sporozoites do not develop ECM. C57BL/6 mice were infected with KO sporozoites failed to develop cerebral symptoms of ECM compared to mice infected with WT sporozoites, which succumbed to ECM between day 7-10 post-infection. This phenotype was consistent regardless of the route of infection used.

Moreover, there was no difference in pre-patency, and all KO infected mice eventually developed hyper-parasitaemia and succumbed to anaemia 23-24 days post-injection **(Fig. 3.10A)**. Apart from clinical signs of ECM, all WT infected mice received an RMCBS score of 8 or below, with reduced body weight **(Fig. 3.10B)** and blue brains **(Fig. 3.10C)**, thus confirming permeabilisation of the blood brain barrier (BBB). In contrast, all KO infected mice received a minimum score of 15 **(Fig. 3.10B)** and had brains comparable to naïve mice thus confirming the presence of an intact BBB **(Fig. 3.10C)**.

The development of ECM relies upon an intact host immune response and the ability of parasites to grow and sequester in different organs. I therefore first looked at the growth kinetics of both parasite lines in the blood. There was no significant difference in the parasitaemia for both KO and WT infected mice during the initial days of infection **(Fig. 3.11)**. However, over the course of infection, the growth rate of KO parasites in the blood reduced gradually, reaching significantly lower levels on those days when WT mice displayed signs of ECM **(Fig. 3.11)**.

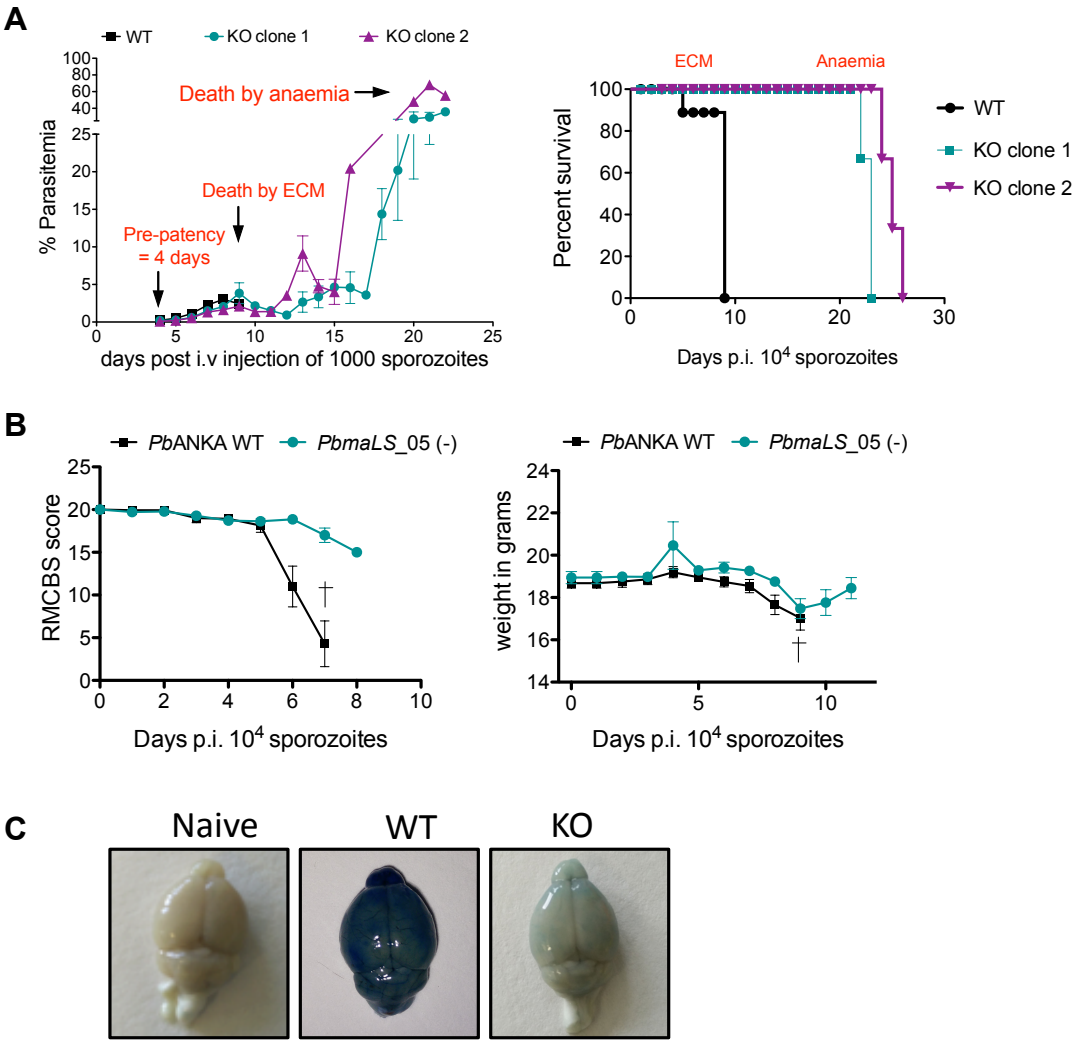

Figure 3.10. *PbmaLS*_05 (-) infected mice have an intact blood brain barrier and do not succumb to ECM in spite of no difference in prepatency compared to WT infected mice. **(A)** C57BL/6 mice infected with KO sporozoites die from hyperparasitaemia induced anaemia around day 22-24 post infection, in contrast to mice infected with WT sporozoites that succumb to ECM around day 7-10 post infection. **(B)** The extent of ECM pathology was assessed by the RMCBS scale based on the clinical signs displayed by WT and KO infected mice. In contrast to the KO infected mice, all WT infected mice received a score of 8 or less. **(C)** The integrity of the blood brain barrier was checked by injection of Evans Blue. While WT infected mice displayed blue brains signifying vascular leakage, all KO infected mice has intact blood brain barriers, comparable to naïve mice, consistent with the non-ECM phenotype.

3.7 Parasite load is higher in the spleens of *PbmaLS*_05 (-) infected mice, but is comparable to *Pb*ANKA WT in the brain, after sporozoite infection

Parasitaemia, both in blood and peripheral tissues has been shown to influence the outcome of ECM (160). To investigate the reason for reduction in parasite numbers in the blood of KO infected mice on day 8 p.i., I measured parasite load in the brains and spleens of mice injected with either WT or KO sporozoites, by qRRT-PCR. Both groups of mice were sacrificed when WT mice showed ECM symptoms and their organs

harvested after perfusion. Relative quantification of parasite 18S rRNA transcripts from the spleen revealed significantly higher levels of parasite transcripts in KO infected mice. However, there was no difference in transcript numbers between the brains of KO and WT infected mice, in spite of the difference in ECM outcome **(Fig. 3.12A)**. Histological sections of the spleen confirmed the presence of higher parasite load within the spleens of KO infected mice compared to WT **(Fig. 3.12B)**.

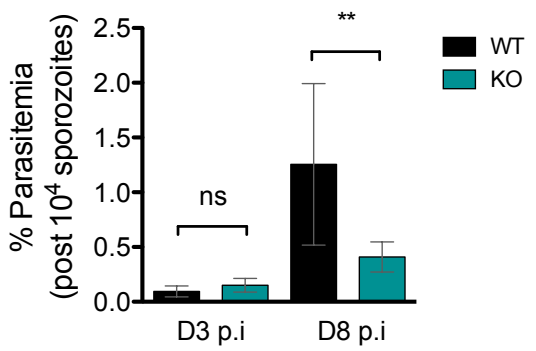

Figure 3.11. The difference in peripheral parasitaemias between *Pb*ANKA WT and *PbmaLS*_05 (-) infected mice is significant on the days when WT mice show symptoms of ECM. Parasite growth kinetics in the blood of infected mice was tracked by daily blood smears. A comparison between WT and KO infected mice showed similar starting parasitaemias (3 d.p.i.), consistent with no delay in pre-patency. However, on days when WT mice displayed signs of ECM (8 d.p.i.), the KO infected mice had significantly lower levels of parasites in the blood. The Student's t test was used to determine statistical significance, followed by post hoc Man Whitney U test or Welch correction depending on the distribution characteristics of the data (**p<.001; ns, not significant). Normal distribution was determined using the Shapiro-Wilk test.

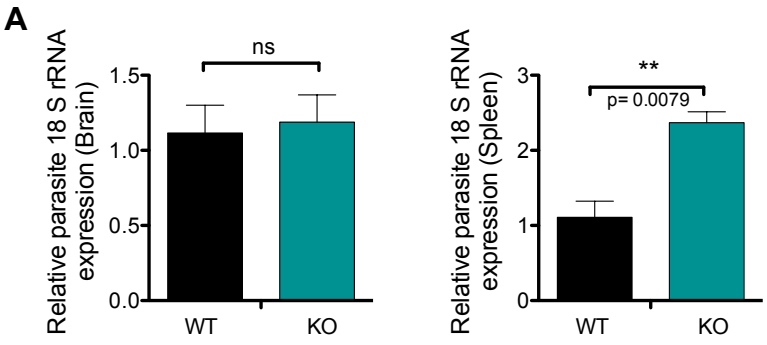

Figure 3.12. Parasite load for KO and WT infected mice are comparable in the brain but differ significantly in the spleen. (A) Groups of 5 C57BL/6 mice were intravenously injected with 10^4 WT or KO sporozoites and sacrificed on days when WT mice developed ECM. Brains and spleens were harvested and homogenised in trizol for RNA isolation. Parasite 18S rRNA transcripts were quantified by qRRT-PCR and normalised to mouse GAPDH. Based on relative expression, KO infected mice had comparable parasite 18S rRNA transcript numbers in the brain, but significantly higher numbers of parasite transcripts in the spleen, when compared to WT infected mice. (Student's t test, **p<0.001; ns, not significant)

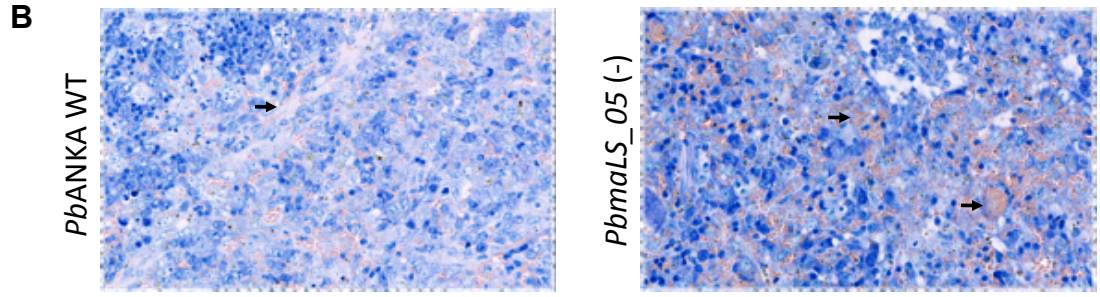

Figure 3.12. Parasite load for KO and WT infected mice are comparable in the brain but differ significantly in the spleen. (B) Histological analysis of the spleens of WT and KO infected mice showed significant amounts of RBC (stained red and indicated by arrowheads) and WBC (stained blue) infiltrates for the KO spleens.

3.8 Modified host-parasite interactions at the blood stage abrogate ECM in *PbmaLS*_05 (-) infected mice

Though widely regarded as a blood stage response, modulations in parasite development in the liver have been shown to alter the outcome of ECM (263). I therefore decided to investigate if the abrogation of ECM was because of an immune response developed at the liver stage. To do so, I bypassed the liver phase and injected mice with infected red blood cells (iRBCs), a routinely used method to induce ECM in mice (186, 190, 285). Strikingly, none of the KO infected mice developed severe cerebral symptoms like WT infected mice that succumbed to ECM around day 5 p.i. **(Fig. 3.13A, Table 3).**

Group	Intravenous injection	Number of mice	ECM	% Survival
WT	Sporozoites	22	21	4.54
	iRBC	**18**	**17**	**5.55**
KO Clone 1	Sporozoites	20	0	100
	iRBC	**11**	**0**	**100**
KO Clone 2	Sporozoites	8	0	100
	iRBC	**6**	**0**	**100**

Table 3. *PbmaLS*_05 (-) infected mice do not develop ECM even after injection of infected red blood cells. C57BL/6 mice were intravenously injected with 10^6 infected red blood cells (iRBC) of either WT or KO parasites. Consistent with the phenotype observed after sporozoite injection, all mice infected with KO iRBCs did not develop ECM unlike WT infected mice.

Moreover, the peripheral parasitaemia in the KO infected mice was again significantly lower compared to those infected with WT iRBCs, especially on the days when WT mice succumbed to ECM **(Fig. 3.13B)**. This was paralleled with reduced RMCBS scores for

WT infected mice, even though no difference in body weight was observed between WT and KO infected mice **(Fig. 3.13C)**.

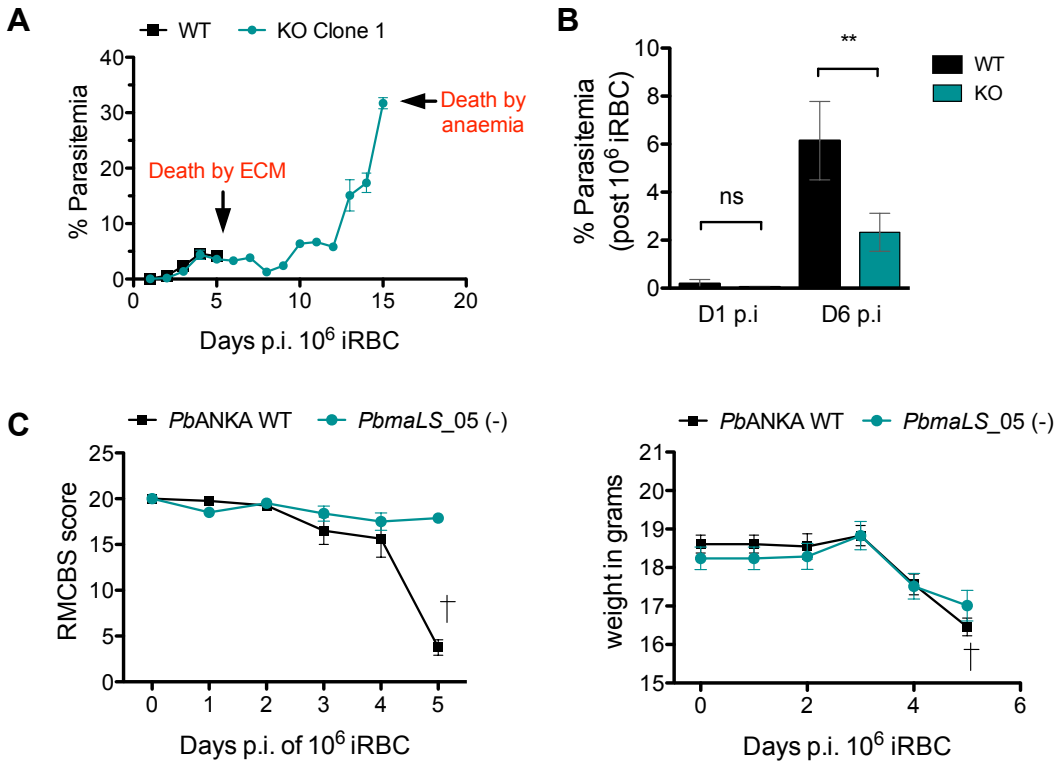

Figure 3.13 *PbmaLS*_05 (-) infected mice do not succumb to ECM even after injection of infected red blood cells. (A) C57BL/6 mice were infected with 10^6 iRBCs of either WT or KO parasites and observed for clinical signs of ECM. In contrast to WT mice which developed severe cerebral signs of ECM and died around day 5 p.i., all KO infected mice survived and died from hyperparasitaemia associated anaemia between day 19-22 p.i. **(B)** A comparison of the parasitaemias of WT and KO infected mice again showed similar starting parasitaemias, but significantly lower levels of parasites in the blood of KO infected mice, when WT infected mice developed ECM. The Student's t test was used to determine statistical significance, followed by post hoc Man Whitney U test or Welch correction depending on the distribution characteristics of the data (**p<0.001; ns, not significant). Normal distribution was determined using the Shapiro-Wilk test. **(C)** All infected mice were scored daily according to RMCBS parameters, including body weight. While the RMCBS scores practically remained unchanged for the KO infected mice, no differences in body weight were observed between WT and KO infected mice, even on the days when WT mice developed ECM.

Interestingly, the number of parasite 18S rRNA transcripts were significantly lower in the brains of KO infected mice compared to mice infected with WT iRBCs **(Fig. 3.14)**, while the number of parasite transcripts in the spleen were comparable for both groups of infected mice. These results further supported the conclusion that the observed non-ECM phenotype in KO infected mice was due to a modification in host-parasite interactions at the blood stage rather than a liver-mediated immune response. More importantly, these results highlighted differences between sporozoite and iRBC induced infections.

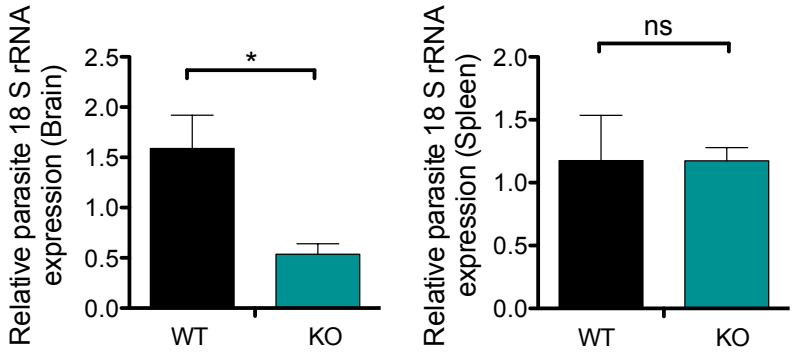

Figure 3.14. Measurement of parasite load in brains and spleens after iRBC injection shows no difference between *PbmaLS*_05 (-) and *Pb*ANKA WT infected mice. Groups of 5 C57BL/6 mice were intravenously injected with 10^6 iRBCs of WT or KO and sacrificed around day 5 p.i. when WT mice displayed signs of ECM. Relative quantification of parasite 18S rRNA transcripts by qRRT-PCR suggested comparable parasite loads in the spleens of KO and WT infected mice but lower parasite load in the brains of KO infected mice (Student's t test, *$p<0.01$; ns, not significant).

3.9 The immune response in mice infected with KO parasites is comparable to a WT infection after sporozoite injection but differs significantly after an iRBCs infection

ECM is an immune pathology that mainly originates in the spleen due to phagocytosis of both sequestered and dying parasites by DCs that prime pathogenic $CD4^+$ and $CD8^+$ T cells involved in blood-brain-barrier disruption (173). Due to increased clearance of a significant proportion of KO parasites after sporozoite infection, I hypothesised that altered priming/activation status of T cells within the spleens of KO mice might account for a different T cell response and difference in ECM outcome. To investigate T cell activity, I quantified $CD4^+$ and $CD8^+$ T cells isolated from spleens and brains of mice infected with either WT or KO sporozoites and found no difference between both groups **(Fig. 3.15A)**. I then evaluated the ability of these isolated T cells to recognise the Pb1 epitope of GAP50, by measurement of IFN-γ expression in response to *ex vivo* stimulation with a parasite specific peptide (Pb 1 epitope of GAP50) (209). In spite of the difference in disease outcome, I did not observe any significant difference in either numbers or activation status of $CD4^+$ and $CD8^+$ T cells isolated from WT and KO infected mice **(Fig. 3.15B)**. In contrast, both $CD4^+$ and $CD8^+$ T cell numbers were significantly lower in the brains and spleens of KO infected mice after iRBC injection (**Fig. 3.16A)**. Moreover, the number of GAP50 specific IFN-γ^+ $CD8^+$ T cells within the brains of KO infected mice was also significantly reduced, an observation that is

consistent with several other studies involving other non-ECM causing parasite strains **(Fig. 3.16B)**.

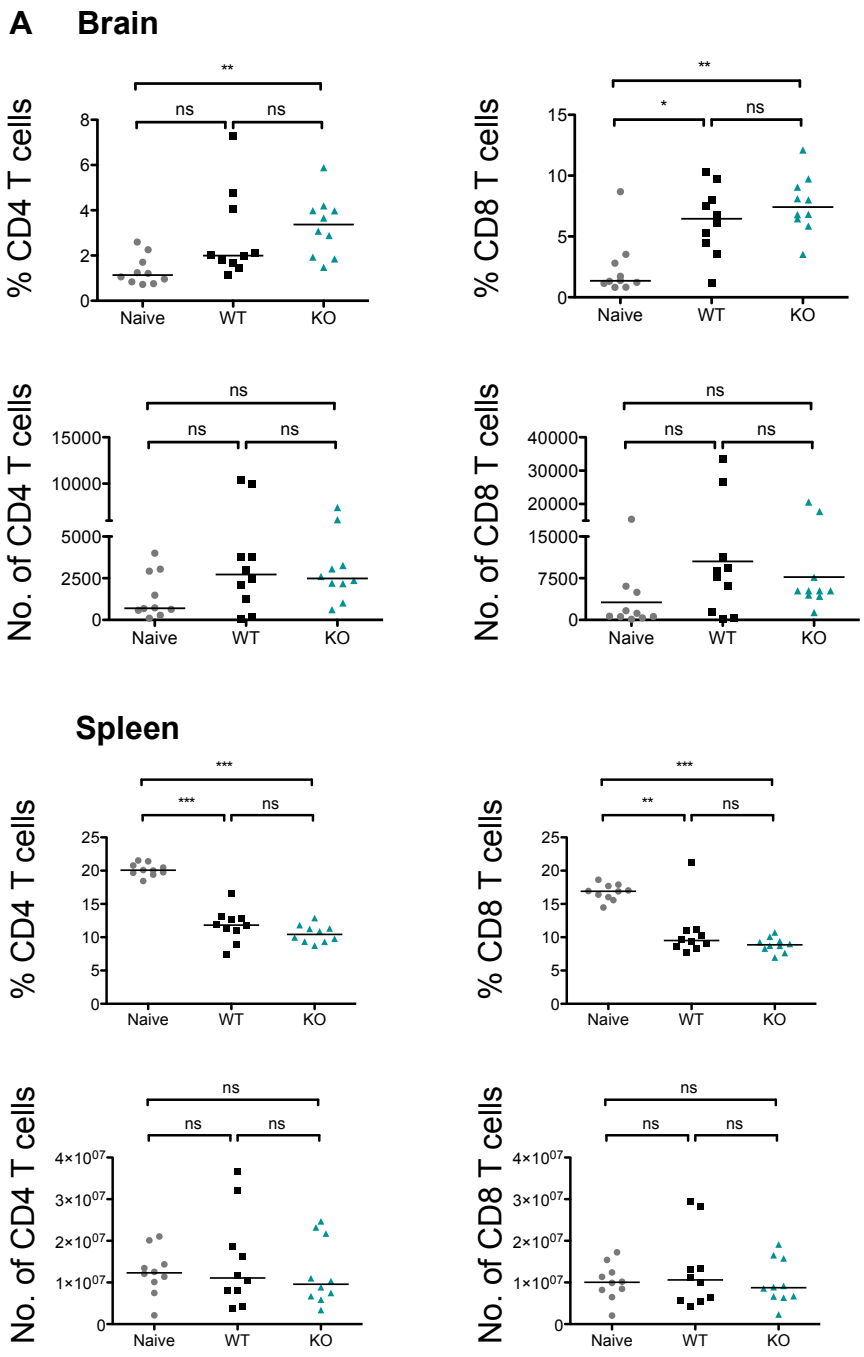

Figure 3.15. Activation of CD8⁺ T cells is comparable between *Pb*ANKA WT and *PbmaLS*_05 (-) infected mice post-injection of sporozoites. (A) Groups of 5 mice were infected with either *Pb*ANKA WT or *PbmaLS*_05 (-) sporozoites and sacrificed on day 8 p.i. along with 5 naïve mice (uninfected controls). After harvesting the brains and spleens, lymphocytes were isolated, stimulated *ex vivo* with the Pb1 epitope of GAP50 and then stained for CD8, CD4, CCR5 and IFN-γ. Quantification and phenotypic characterisation of T cells was done by flow cytometry. The percentages of CD8⁺ and CD4⁺ T cells were comparable between WT and KO infected mice in both organs. Statistical significance was determined by One-way Anova with Bonferonni's adjustment (***p<0.0001, ** p<0.001, * p<0.01; ns, not significant).

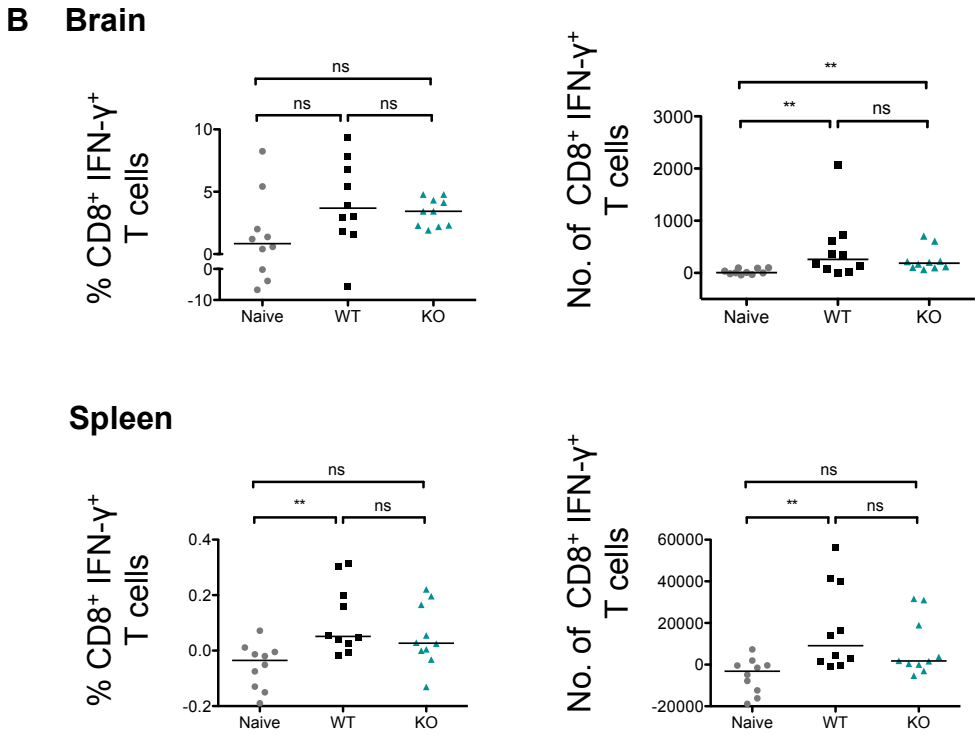

Figure 3.15. Activation of CD8⁺ T cells is comparable between *Pb*ANKA WT and *PbmaLS*_05 (-) infected mice post-injection of sporozoites. (B) The number of Pb1 (GAP50) specific IFN- γ⁺ CD8⁺ T cells is comparable in both brains and spleens of WT and KO infected mice, thus suggesting no difference in antigen recognition and T cell cytotoxity between both groups of mice. Represented results are from two independent experiments. Statistical significance was determined by One-way Anova with Bonferonni's adjustment (***p<0.0001, ** p<0.001, * p<0.01; ns, not significant).

3.10 Deletion of *PbmaLS*_05 reduces cross-presentation by brain endothelial cells, after iRBC infection, thereby abrogating the development of ECM

In spite of the discrepancies in the immune response between sporozoite and iRBC infections, none of the mice displayed any signs of ECM. Moreover, the immune response in the sporozoite-infected mice was comparable between WT and KO infected groups. I then proceeded to test for differences in cross-presentation by the brain endothelium after infection with either WT or KO parasites. Since the differences in immune response to WT or KO parasites in the brain differed after iRBC but not sporozoite infection, I hypothesised that activation of the endothelium and possibly cross-presentation of parasite antigens influencing the development of ECM might be different between the two modes of infection. In collaboration with Shanshan W. Howland and Laurent Renia (A*Star, Singapore) we measured differences in cross-presentation of Pb1 (GAP50) by the brain endothelial cells (209) after iRBC infection. In good agreement with the immunological data post iRBCs, the level of cross-presentation

of the GAP50 epitope was significantly lower in the KO infected mice, thus confirming a direct involvement of *Pb*maLS_05 in ECM progression **(Fig. 3.17)**.

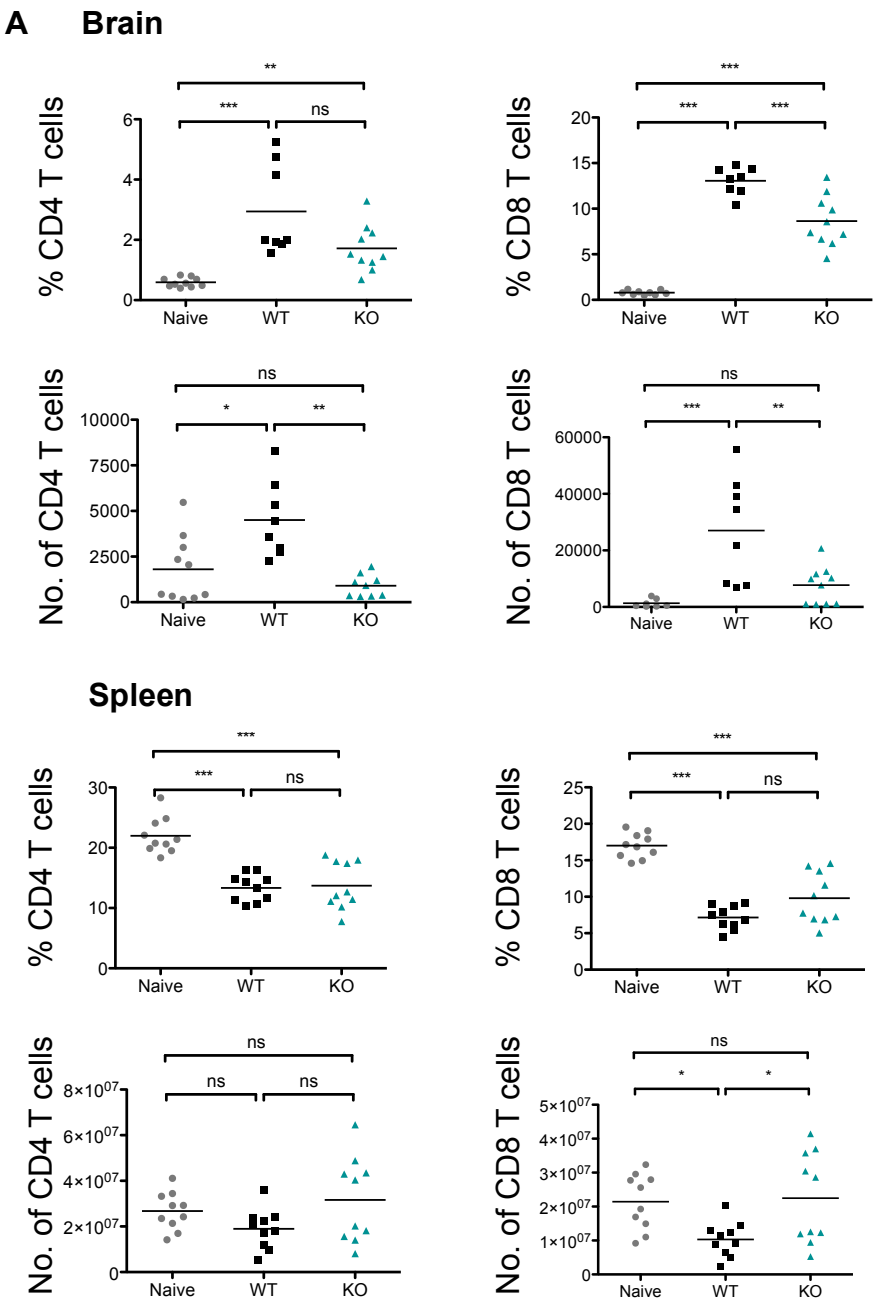

Figure 3.16. Mice infected with *PbmaLS*_05 (-) iRBCs have reduced infiltration of CD8⁺, CD4⁺ and IFN-γ⁺ CD8⁺ T cells in the brain, consistent with the non-ECM phenotype. (A) Groups of 5 mice were infected with 10^6 WT or KO iRBCs and sacrificed on day 5 p.i. along with 5 naïve mice (uninfected controls). Lymphocytes isolated from brains and spleens were stained with CD8, CD4 and IFN-γ antibodies for quantification and phenotypic analysis by flow cytometry. We observed a significant reduction in the percentage of $CD4^+$ and $CD8^+$ cells in the brains of KO infected mice, which is consistent with the non-ECM phenotype. Statistical significance was determined by One-way Anova with Bonferonni's adjustment (***$p<0.0001$, ** $p<0.001$, * $p<0.01$; ns, not significant).

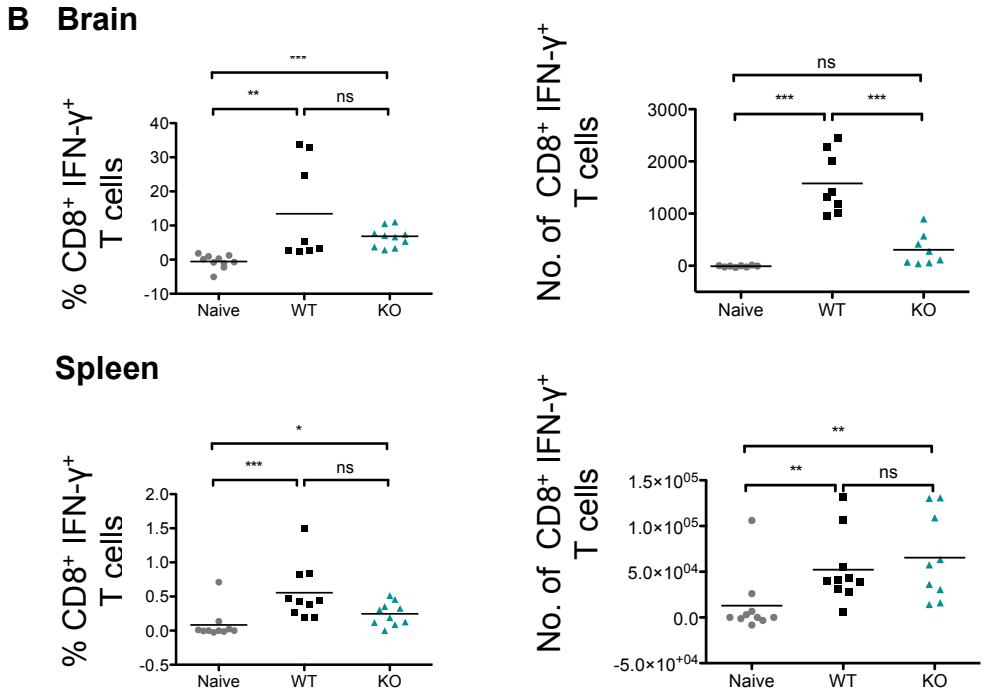

Figure 3.16. Mice infected with *PbmaLS*_05 (-) iRBCs have reduced infiltration of CD8⁺, CD4⁺ and IFN-γ⁺ CD8⁺ T cells in the brain, consistent with the non-ECM phenotype. (B) Interestingly, the number of Pb1 (GAP50) specific IFN- γ⁺ CD8⁺ T cells was also significantly lower in the brains of KO infected mice, thus suggesting inherent differences in priming or antigen recognition of CD8⁺ T cells in these mice. A One-way Anova with Bonferonni's adjustment was used to determine statistical significance (***p<0.0001, ** p<0.001, * p<0.01; ns, not significant).

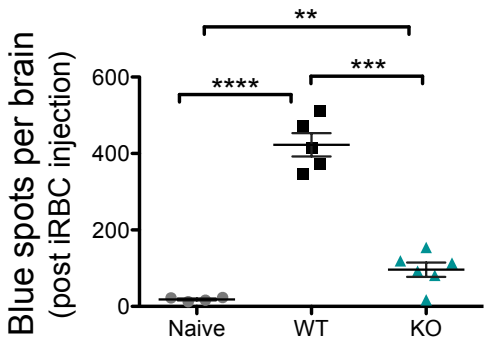

Figure 3.17. The cross-presentation of Pb1 (GAP50) is lower in the brains of *PbmaLS_05*(-) infected mice after iRBC injection (Performed by Shanshan W. Howland, A*Star, Singapore). C57BL/6 mice were infected intraperitoneally with 10^6 WT or KO iRBCs and harvested when the WT-infected mice exhibited neurological signs, along with naïve mice. Brain microvessel fragments were isolated and co-incubated with reporter cells that express lacZ upon detection of a parasite-derived peptide-MHC complex (*Pb*GAP50; SQLLNAKYL). Blue spots representing activated reporter cells were quantified following X-gal staining. **** p <0.0001, *** p <0.001, ** p<0.01, One-way ANOVA with Bonferroni's post-test on spot counts.

In order to determine if brain-infiltrating lymphocytes from WT infected mice could recognise and respond to *Pb*maLS_05, CD8 T cell epitopes were predicted for the full-length *Pb*maLS_05 protein, synthesised as peptides and used to pulse donor splenocytes from naïve mice. Both pulsed and unpulsed splenocytes were then used as antigen presenting cells and cultured with lymphocytes isolated from the brains of WT and KO sporozoite infected mice. The output of the experiment was the total number of IFN-γ

producing $CD8^+$ T cells, that were identified by the ELISpot assay as described in 2.2.8.5. Brain-infiltrating lymphocytes from WT infected mice recognised *Pb*maLS_05 epitopes in contrast to those isolated from *PbmaLS*_05 (-) sporozoite infected mice, thus confirming the *Pb*maLS_05 is indeed presented during a sporozoite infection **(Appendix Fig. 6.8)**.

3.11 MRI of the brains of infected mice support the existence of different mechanisms of ECM development between sporozoite and iRBC injections

In order to confirm the non-ECM phenotype through non-invasive methods, I infected mice with either WT or KO sporozoites or WT or KO iRBCs and imaged them *via* MRI, on the day when WT mice displayed signs of ECM (in collaboration with Dr. Angelika Hoffmann, Neuroradiology Unit, University Hospital Heidelberg). Previous research has shown that ECM initiates in the olfactory bulb (OB) (286) and spreads along the rostral migratory stream to the remaining parts of the brain (156). Moreover, activated perivascular $CD8^+$ T cells were shown to interact with brain endothelial cells cross-presenting parasite antigen, within the OB (215). Based on this information, we imaged the mice *via* an MRI scanner and typically looked at the OB of these mice. Interestingly, none of the KO infected mice showed a significant increase in brain volume, consistent with the non-ECM phenotype, when compared to the WT infected groups **(Fig. 3.18A)**. This observation was in agreement with the lack of haemorrhages and oedema within the OB of the KO iRBC mice in contrast to those infected with WT iRBC **(Fig. 3.18B)**. However, KO sporozoite infected mice still displayed haemorrhaging and oedema, though reduced in comparison to WT sporozoite infected mice **(Fig. 3.18B)**. These results conclude that while *Pb*maLS_05 could indeed play a crucial part in the induction of ECM in mice, at least two different mechanisms of ECM development exist, pertinent to sporozoites and iRBCs.

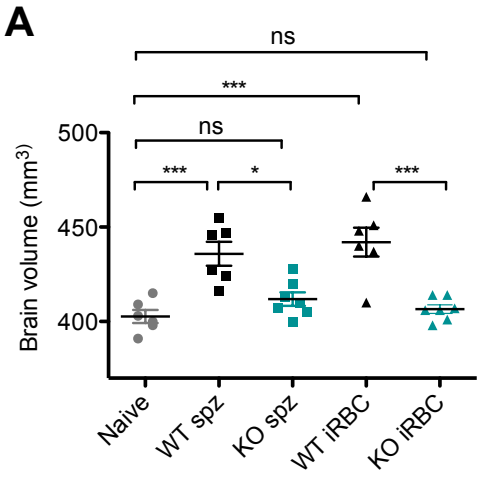

Group	Brain volume (mm³)	
	p.i.sporozoites	p.i.iRBC
Naïve	402.7±3.5	402.7±3.5
WT	435.8±6.3	442.0±7.6
KO	411.9±3.6	406.6±2.3

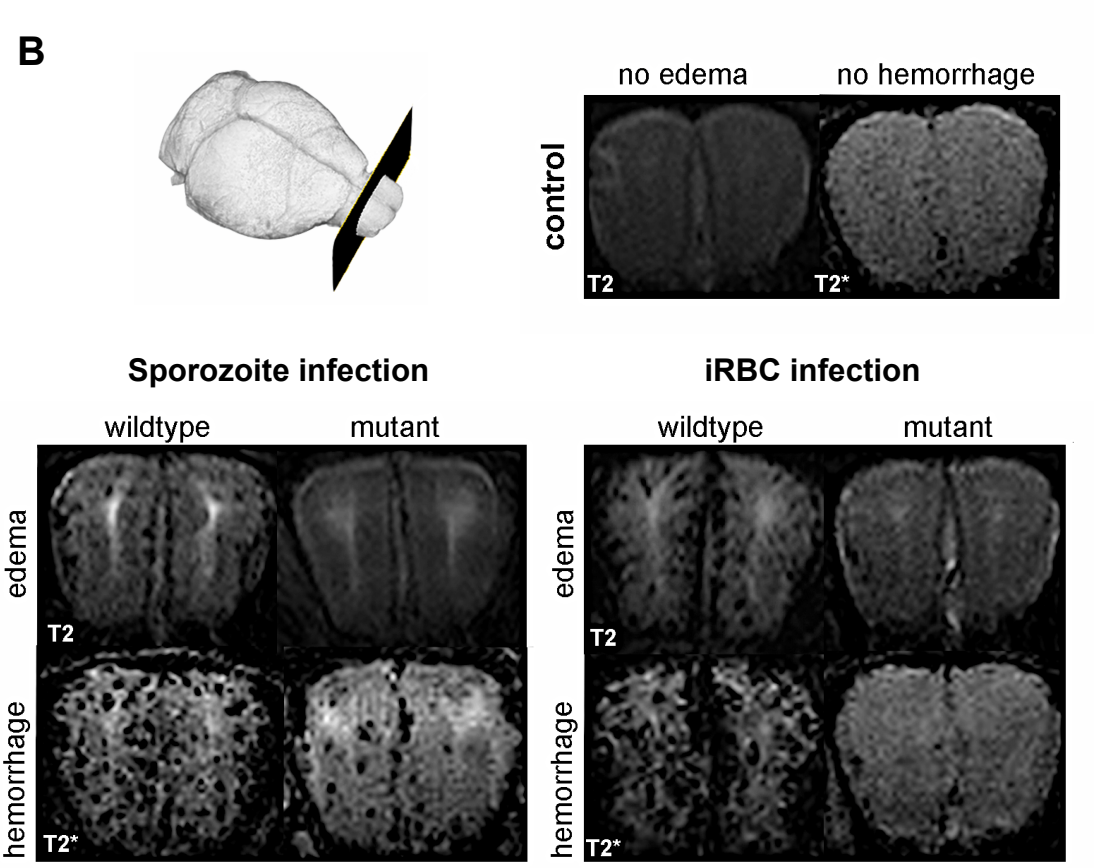

Groups	Oedema		Haemorrhages	
	p.i. sporozoites	p.i. iRBCs	p.i. sporozoites	p.i. iRBCs
	0		**0**	
WT	2.7±0.5	2.8±0.4	2.7±0.5	2.8±0.4
KO	1.1±0.6	0.7±0.3	1.2±0.6	0.5±0.4

Figure 3.18 MRI of WT and KO infected mice. (Imaging performed by Angelika Hoffmann, Neuroradiology Unit, University Hospital Heidelberg) (A) Mice infected with sporozoites or iRBCs of WT or KO parasites were imaged when WT mice displayed signs of ECM (7 d.p.i for sporozoites and 5 d.p.i. for iRBCs). All mice were anaesthetised and placed prone in an MRI scanner. A significant increase in the brain volumes of WT infected mice correlated with the ECM symptoms observed on the day of imaging. In contrast both KO sporozoite and KO iRBC infected mice showed no increase in the brain volume, which were in

fact comparable to the control (uninfected group). Statistical significance was determined using a One-Way ANOVA with Bonferroni's multiple comparison as a post-hoc test (***$p<0.0001$, **$p<0.001$, *$p<0.01$; ns, not significant). **(B)** Haemorrhages and Oedema were detected using the T2 and T2* protocol. The images displayed are representative of each group. Extensive haemorrhaging and oedema preceded signs of ECM in the WT infected mice and was more pronounced after iRBC infection compared to infection with sporozoites. In contrast, KO sporozoite infected mice showed minor oedema and haemorrhaging in the OB, both of which were absent after KO iRBC infection, thus further supporting the existence of two different mechanisms of ECM development. All images were analysed using the Amira 5.4 software.

Chapter 4

Discussion

Studies pertaining to sterile protection or protection from cerebral malaria have often stressed the importance of a broad antigenic repertoire in the induction of protective immunity (269, 270). Lessons learnt from the success of whole organism vaccines like CPS, RAS and GAP and failure of the RTS,S subunit vaccine, have moreover supported the view that 'the development of a successful vaccine against malaria is contingent upon the incorporation of multiple targets of protective immunity' (287). However, the identification of these targets is still under investigation.

Previous work identified a selection of *Plasmodium* transcripts, including *PfmaLS*_05, that were upregulated in intra-hepatic stages of RAS and hypothesised to contribute to protective immunity conferred by attenuated whole organism vaccines (280). The characterisation of *Pb*maLS_05 was thus initiated with the intention of determining its role in the parasite life cycle and its contribution to sterile protection.

4.1 Functional characterisation of *Pb*maLS_05 in the parasite life cycle.

*Pb*maLS_05 is relatively well conserved on both genomic and proteomic levels in all *Plasmodium* species. The orthologue in *P.yoelii* is comprised of two genes and each one aligns to one half of the orthologue in *P.falciparum,* thus suggesting the presence of spliced variants of the gene **(Fig. 3.1)**. The function of most of the orthologues of *Pb*maLS_05 is unknown, except for PY02854, where it is annotated as a SEN-1 related protein (PlasmoDB). Based on that *Pb*maLS_05 could be considered to function as an ATP-dependent helicase that is required for maturation of non-coding RNAs. However, this function seems unlikely since *Pb*maLS_05 localises to the apicoplast instead of the nucleus. A previous report hypothesised *Pf*maLS_05 to cluster with ABC transporters owing to the presence of the predicted P loop containing nucleoside domain (288). These data however, are solely based on sequence alignments and therefore necessitate further investigation.

*Pb*maLS_05 was first identified in pre-erythrocytic stages of *Pf*RAS, even though is transcribed throughout the parasite life cycle and alternatively spliced in two different

stages **(Fig. 3.2)**. Alternative splicing has often been observed for large multi-gene families of *Plasmodium* and hypothesised to play a role in evasion of host immunity (289). Interestingly, studies have shown that proteins encoded by *var* and *rif* genes are also expressed in sporozoites and gametocytes (290, 291), contrary to the assumption that multi-gene families are exclusively expressed during intra-erythrocytic stages of development, thus suggesting different roles in different stages of the life cycle (289). Similar studies from rodent *Plasmodium* strains have also proposed that the alternatively spliced forms play more diverse roles than previously thought in different stages of the parasite life cycle (272, 292). Indeed, splicing of *Plasmodium* genes like MAEBL, GRASP, CDPK6 and adenyl cyclase α (293-297) was shown to modify both their expression and localisation in the parasite life cycle. However, in contrast to MAEBL and GRASP where splicing exclusively modified the localisation of the protein from membrane to cytoplasm, isoforms of adenyl cyclase were suggested to perform different functions (293-297). It is thus likely that the alternatively spliced forms of *Pb*maLS_05 also fulfil "stage-specific" roles during the parasite life cycle.

Depletion of *PbmaLS*_05 in mid-gut sporozoites had no effect on sporogony, but significantly impacted the numbers of salivary gland sporozoites in KO infected mosquitoes **(Fig. 3.7)**. The reduction in salivary gland sporozoite numbers combined with the *in vitro* defect in motility **(Fig.3.7)** points to a function of *Pb*maLS_05 in salivary gland invasion (298, 299). This is based on the fact that sporozoite proteins CSP and TRAP also play dual roles in motility (300) and salivary gland invasion (301), indicating that both invasion and motility rely on a well conserved motor machinery (302, 303). The impairment in motility of *PbmaLS*_05 (-) sporozoites though striking *in vitro* was not reflected *in vivo* **(Fig. 3.8 & Table 1)**. This disparity could be explained by the spatial differences in a BSA-coated glass slide (2D) and the skin (3D), but has similarly been reported for other parasites lacking the transmembrane protein SSP3 (304) or the actin bundling protein coronin (305). However, undetectable expression levels of *Pb*maLS_05 in sporozoites by both C-terminal EGFP and N-terminal mCherry tagging strategies **(Fig. 3.4 & Appendix Fig. 6.5B)** together make it very unlikely, that *Pb*maLS_05 plays a role in motility in the skin.

Similarly, the transcription of a spliced isoform of *Pb*maLS_05 in parallel with delayed development of early liver stage KO parasites could suggest a role for *Pb*maLS_05 in intra-hepatic development **(Fig. 3.2 & 3.9)**. However, the function of *Pb*maLS_05 in

both mid-gut sporozoites and early liver stages can rather be considered descriptive due to undetectable protein levels or problems with tagging of the isoforms. A modest reduction in both sporozoite burden in salivary glands and sizes of early liver stages of KO parasites, indicate redundant roles for *Pb*maLS_05 in salivary gland invasion and early liver stage development.

One of the initial theories surrounding the transcriptional abundance of *maLS*_05 in *Pf*RAS liver stages, was its potential role in intra-hepatic development which was based on a previous study which suggested that hepatocyte invasion might trigger changes in transcription (306). However, deletion of *Pb*maLS_05 had no effect on intra-hepatic development, both *in vitro* and *in vivo.* While the data does not entirely exclude the use of *Pf*maLS_05 as a liver-stage antigen, it is plausible that transcriptional upregulation of maLS_05 in early liver stages might be induced in response to irradiation-induced stress (280).

In contrast to sporozoites and early liver stages, the full-length isoform of *Pb*maLS_05 is expressed in both later liver and blood stage parasites and localises to the apicoplast of both stages **(Fig. 3.4)**. The importance of the apicoplast in parasite growth and development has been highlighted through several studies (307-309), which makes it an attractive target for antimalarials. Parasites rely on the apicoplast for heme, isoprenoid and lipid synthesis (309), but the extent of reliance on the acquisition of these components is uncertain (310) and differs for liver- and blood stages (308). The process of replication and segregation of the apicoplast in *Plasmodium* parasites parallels with nuclear division and is completed before the formation of daughter merozoites, thus ensuring that every daughter cell inherits one apicoplast (311, 312). The expression of *Pb*maLS_05 exclusively during nuclear division in both liver and blood stages would thus imply an involvement of *Pb*maLS_05 in apicoplast division. Transfection of *Toxoplasma gondii* parasites with an ACP-GFP-mRON1 plasmid, disrupted apicoplast segregation resulting in parasites containing a single large apicoplast or parasites devoid of one. Parasites containing a single large apicoplast displayed reduced growth rates in comparison to those devoid of an apicoplast that survived for a short-term. This phenomenon is strikingly similar to the "delayed death" phenotype seen with antibiotics like azithromycin, clindamycin and doxycycline that affect biogenesis of the apicoplast (283, 313). It is thus conceivable that parasites lacking *Pb*maLS_05 have abnormal or inaccurately divided apicoplasts between daughter cells, consequently resulting in death

and elimination of parasites devoid of a functional apicoplast. This is supported by retarded growth rates of KO parasites in the blood and enhanced clearance by the spleen **(Fig. 3.11 & 3.12)**. Although abnormal apicoplast segregation sounds like a probable cause for the observed defect in blood stage growth, it warrants further confirmation with antibodies that stain the apicoplast. In contrast to blood stages, the timing of *Pb*maLS_05 expression in late liver stages would rather propose a role in transition of parasites from the liver to blood or the initiation of blood stage infection **(Fig. 3.4)**. The influence of these events on the disease progression and development of ECM is discussed below.

4.2 Characterisation of the role of *Pb*maLS_05 in the development of ECM.

Descriptions about ECM are mainly restricted to the intra-erythrocytic stages of the parasite life cycle. However, numerous studies in the past few years have provided evidence of a role for pre-erythrocytic immunity in modulating the development of ECM (section 1.3.2). The common theme between the different models of protection seems to be a modification in the immune response towards the initial inoculum of blood stage parasites that subsequently influences the outcome of ECM.

It is conceivable that an innate immune response developed during the liver or blood stages of infection, interferes with the priming of host immune responses that culminate in ECM. Indeed, hepatocytes recognise PAMPs such as parasite RNA, which activates the type 1 IFN response (314) and recruits NK and NKT cells that subsequently mediate control of parasite replication *via* IFN-γ secretion (315). An impaired release of merosomes could ideally prolong the time required for innate immunity against intra-erythrocytic stages of infection, to develop. The development of innate immune responses directed towards iRBCs was in fact demonstrated by immunisation of mice with a single dose of irradiated iRBCs. Protection against ECM was associated with antibody responses and reduced IFN-γ but intriguingly had no effect on the accumulation of $CD8^+$ T cells within the brains of infected mice (316). Indeed, infection of RBCs induces the up-regulation of TLRs and pro-inflammatory cytokine genes that are regulated by NF-κB. The activation of DCs through parasite DNA stimulation of TLR 9 promotes the secretion of cytokines that help control infection. For example, production of IL-12 by DCs in a MyD88 dependent fashion stimulates NK cells to

secrete IFN-γ that facilitates the activation of $CD4^+$ helper T cells (Th1). Th1 cells in turn promote the switch in class to IgG2a and IgG2b antibodies that are protective (317). The role of innate immunity in conferring protection therefore cannot be undermined.

Nevertheless, the immunopathological differences between WT and KO in relation to different experimental modes of infection (sporozoites versus iRBCs) that were investigated are discussed below.

A) Parasite sequestration and multiplication in the blood

The absence of ECM in mice infected with KO sporozoites could result from a 'trickling effect' or an impaired release of merozoites that initiate the first round of blood stage infection (240). However, the absence of any delay in intra-hepatic development or pre-patency after an infection with KO sporozoites, argues against the existence of a trickling effect **(Table 1)**. Moreover, infection of mice with KO iRBCs also reproduces the same phenotype, despite bypassing the pre-erythrocytic stage **(Table 3)**.

A common observation between KO sporozoites and iRBC infections was the retarded growth rates of intra-erythrocytic stages, which were more pronounced when WT infected mice display signs of ECM **(Fig. 3.11& 3.13)**. Moreover, the drop in peripheral parasitaemia of KO sporozoite infected mice correlated with increased amounts of parasite material in the spleen. Based on this observation, one could easily hypothesise that deletion of *Pb*maLS_05 weakens or reduces parasite sequestration by altering surface adhesion expression, thus leading to enhance clearance/accumulation of parasites by/in the spleen and a reduction in circulating parasites. This was indeed observed in a recent study by De Niz *et. al.* where virulence attenuated parasites displayed a reduction in sequestration and peripheral parasitaemias (180).

Intriguingly, the parasite load in the brains of KO infected mice was comparable to mice infected with WT sporozoites **(Fig. 3.12)**. To say that *Pb*maLS_05 influences surface adhesion expression is misleading because it is targeted to the apicoplast and therefore cannot regulate the transcription of *var* genes in the nucleus. Moreover, it is well known that the apicoplast imports several nuclear-encoded proteins (318, 319), but there is no evidence whatsoever to support the reverse. Still, it cannot be dismissed that the influence of the spleen on surface adhesion expression and subsequently sequestration differs between KO and WT infections, but this needs to be investigated further.

While these observations partially complement the importance of parasite fitness on the development of cerebral symptoms, the lack of any difference in parasite load in the brains of WT and KO sporozoite infected mice contradicts previous findings that organ-specific sequestration is critical for ECM immunopathogenesis **(Fig. 3.12)** (320). Moreover, in-depth analysis of endothelial activation in rodents has shown that sequestration alone is inadequate to cause localised inflammation and blood-brain barrier breakdown (209, 216).

B) T cell priming and activation in the spleen

In addition to parasitaemia, activated T cells play an important role in the development of ECM. Parasite sequestration in the spleen contributes to changes in splenic physiology and primes the immune response that is responsible for blood-brain barrier permeabilisation (discussed in 1.2.2.3). Priming of T cells within the spleen occurs in an antigen specific manner, in response to sequestration and phagocytosis of parasite material by splenic APCs. Studies have shown that both antigen availability and duration of antigen presentation affect the polarisation and switch between Th1- or Th2- T cell subsets (321). Moreover, excess antigen availability could either trigger apoptosis of T cells or make them unresponsive, thus creating either an anergic or tolerogenic environment (322). It is thus plausible that the excess parasite material within the spleen after injection with KO sporozoites triggers a hyporesponsive state in T cells, thereby reducing their antigen-specific activation and migration from the spleen. However, a comparable number of $CD4^+$ and $CD8^+$ T cells were isolated from the brains of KO and WT sporozoite infected mice even when WT infected mice succumbed to ECM **(Fig. 3.15A)**, thus suggesting that the priming of T cells per se was similar for both groups of infected mice.

In contrast to infection with sporozoites, KO iRBC infected mice displayed reduced parasite loads and reduced accumulation of $CD4^+$ and $CD8^+$ T cells in the brain, in spite of no difference in the spleen when compared to mice inoculated with WT iRBCs **(Fig. 3.16A)**. Although these results represent a more classical presentation of the non-ECM phenotype, they contradict observations made after sporozoite infections.

C) Antigen recognition

One could easily argue that sheer numbers of T cells do not contribute to ECM, but that the ability of $CD8^+$ T cells to produce cytotoxic molecules like IFN-γ upon recognition

of parasite antigens is of prime importance. This was indeed shown by two independent studies whereby equal numbers of $CD8^+$ T cells were isolated from the brains of ECM and non-ECM causing parasite strains (209, 216). It was therefore interesting to test if the $CD8^+$ T cells isolated from the brains and spleens of KO infected mice were capable of recognizing parasite antigens such as the Pb1 epitope of GAP50. Pb1 was classified as a dominant antigen that was recognised by a majority of $CD8^+$ T cells in the brains of ECM mice (209), and was therefore selected for this study. Interestingly, T cells isolated from the brains and spleens of both WT and KO sporozoite infected mice produced IFN-γ in response to Pb1 **(Fig. 3.15B)**. In contrast, the number of Pb1 specific IFN-γ^+ $CD8^+$ T cells isolated from the brains of KO iRBC infected mice was significantly lower compared to WT iRBC infected mice, thus indicating a reduction in activation of T cells after a KO iRBC infection **(Fig. 3.16B)**. These results, though contradictory to one another, emphasize that inherent differences in the recognition of parasite antigens by T cells exist between sporozoite and iRBC infections. In addition, it is possible that circumventing the liver leads to a change in the epitopes presented to T cells, thereby altering their specificities.

D) Cross-presentation and blood-brain barrier permeabilisation

Antigens recognised by cytotoxic T cells (CTLs) are mainly cross-presented during a malarial infection. $CD8\alpha^+$ DCs in the skin and spleen cross-present parasite antigen to naïve $CD8^+$ T cells, while $CD103^+$ DCs residing in non-lymphoid organs were shown to efficiently cross-present antigens to CTLs (323). In the context of ECM, phagocytosis of merozoites and cross-presentation of antigens by brain ECs critically facilitates an arrest of CTLs within the brain microvasculature (209, 216). In fact, cross-presentation of parasite antigens by APCs plays a very important part in ECM immunopathogenesis and is the key factor that distinguishes ECM from non-ECM parasite strains (209, 216). The intention of the cross-presentation assay was thus to dissect differences in cross-presentation of parasite antigens between WT and KO infected groups. The assay was performed (in collaboration with Shanshan W. Howland and Laurent Renia, A* Star, Singapore) with brain microvessel fragments isolated from mice, only after iRBC infections. Interestingly, endothelial cells of KO iRBC infected mice were less efficient at cross-presenting Pb1, which was in good agreement with the reduced numbers of IFN-γ^+ $CD8^+$ T cells in the brain and absence of ECM in these mice **(Fig. 3.17)**. Based on

this observation, the following hypothesis can be made to explain the non-ECM phenotype after infection with KO sporozoites.

1. It is plausible that cross-presentation by the activated endothelium is also impaired or reduced during an infection with KO sporozoites, which would explain why these mice do not develop ECM, despite the presence of a sufficient number of $CD8^+$ T cells in the brain that were capable of recognizing Pb1. However, priming of $CD8^+$ T cells first occurs in the spleen and is responsible for their activation and migration to other organs. Given that an equal number of $CD8^+$ T cells isolated from the brains of WT and KO sporozoite infected mice responded to Pb1 *in vitro*, it is quite unlikely that cross-presentation by endothelial cells in the brain is also impaired after sporozoite infection. Nevertheless, this has yet to be confirmed.

2. Alternatively, one could presume that the dominant role of Pb1 in inducing ECM as seen with iRBC infections, might not be reflected during a sporozoite infection. A study in 2013 showed that damage to the blood-brain barrier requires the synergistic effect of T cells with different antigen specificities (210). Based on the fact that mice do not develop ECM after a sporozoite infection, despite the presence of a comparable number of activated T cells to mice infected with WT sporozoites, it is tempting to speculate that *Pb*maLS_05 and not Pb1 might in fact be the dominant antigen that is cross-presented during a sporozoite infection.

The assumption that *Pb*maLS_05 could be cross-presented by endothelial cells in the brain is quite reasonable given that several differences exist between sporozoite and iRBC induced infections. In fact, studies have shown that variant surface antigens expressed by mosquito transmitted and blood-passaged parasites are significantly different (324). Inferences drawn from the study in rodents suggested that vector transmission favours a broader antigenic repertoire over a select subset of virulent genes, as seen for blood-passaged parasites (325). Hence, it is highly probable that the antigens expressed and presented by the immune system, may also vary between sporozoite induced and iRBC-induced infections. The disparity in the host immune response seen for KO sporozoite and KO iRBC infections are a testament to this difference. Indeed studies comparing immune responses between sporozoite and iRBC initiated infections, have demonstrated that both T cell activation and parasite dynamics in the blood vary between both groups (170, 171). Sporozoite infected mice were found to develop lower

parasitaemias apart from reduced frequencies and lower activation levels of $CD8^+$ T cells in the brain, compared to iRBC infections. The most interesting aspect however, is that both sporozoites and iRBCs are capable of inducing ECM in mice, thus suggesting that the priming of $CD8^+$ T cells is more efficient during a sporozoite-induced infection. It is thus very likely that mechanism of ECM development differs between sporozoite and iRBC infections.

It is interesting to note that Pb1 (GAP50) was identified during a screen for antigens cross-presented during an iRBC-initiated and not sporozoite induced infection (209, 210). *Pb*maLS_05 was not on the list of identified targets, most likely due to the presence of other dominant antigens. With that thought in mind, it was imperative to test if *Pb*maLS_05 was actually presented during a sporozoite infection. Predicted $CD8^+$ T cell epitopes for *Pb*maLS_05 were synthesised and used to stimulate brain-derived lymphocytes isolated from sporozoite infected mice, *in vitro*. Preliminary results indicated that $CD8^+$ T cells from WT sporozoite infected mice were indeed capable of recognising *Pb*maLS_05. More importantly, *Pb*maLS_05 was not recognised by brain-derived lymphocytes of KO sporozoite infected mice, judging by the absence of an IFN-γ^+ response **(Appendix Fig. 6.9)**, thus confirming significant differences in ECM pathogenesis, between sporozoites and blood-stage infections.

The data are thus supportive of an essential role of *Pb*maLS_05 in the development of ECM, particularly after a sporozoite infection and postulate the existence of at least two mechanisms of ECM development unique to sporozoites and iRBCs.

A summary of the key aspects and mechanisms of protection observed with KO parasites in contrast to a WT infection is depicted below **(Fig. 4.1 & Fig. 4.2)**. The following figures have been adapted from Howland, S. *et. al.,*2015 (179) to incorporate the role of *Pb*maLS_05 in the development of ECM.

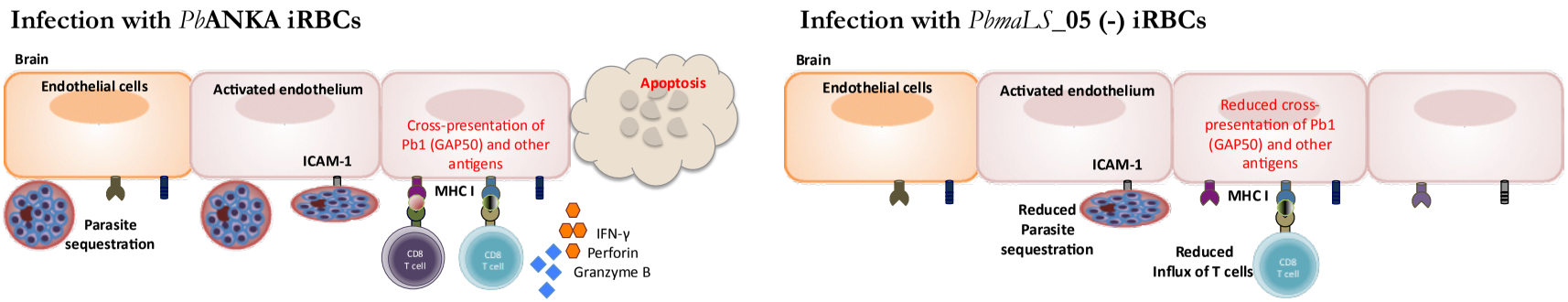

Figure 4.1A Mechanism of protection after infection with *PbmaLS*_05 (-) iRBCs.
In contrast to an infection with *Pb*ANKA iRBCs, mice infected with *PbmaLS*_05 (-) iRBCs feature less parasite sequestration and significantly reduced cross-presentation of potent parasite antigens like Pb1 (GAP50), thus preventing the onset of ECM and subsequent permeabilisation of the blood-brain barrier.

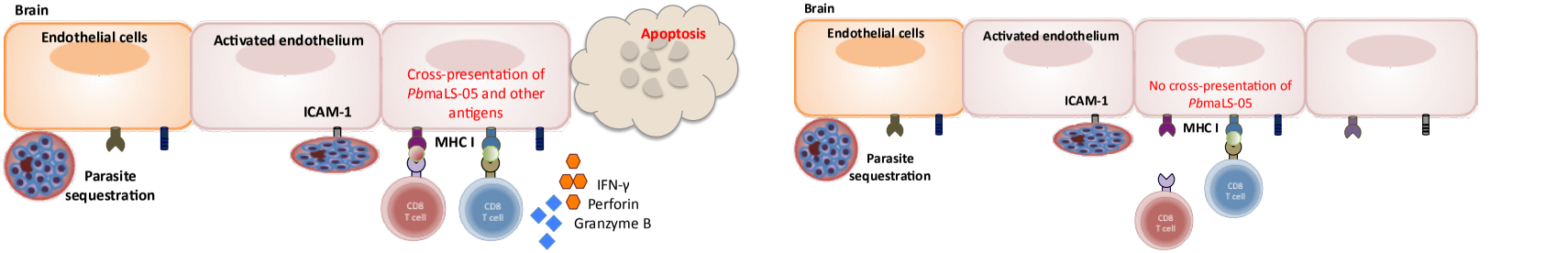

Figure 4.1B Mechanism of protection after infection with *PbmaLS*_05 (-) sporozoites.
Although parasite sequestration and $CD8^+$ T cell recruitment to the brain microvasculature is comparable between *Pb*ANKA and *PbmaLS*_05 (-) infected mice, the lack of cross-presentation of *Pb*maLS_05 during a sporozoite infection abrogates the development of ECM. Even though it is likely that Pb1 (GAP50) is still cross-presented, it does not play a dominant role in inducing ECM after a sporozoite infection. Hence *PbmaLS*_05 (-) infected mice display similar levels of IFN-γ^+ $CD8^+$ T cells within the brain, but are still protected from ECM.

4.3 A model to describe the process of ECM development after a sporozoite infection.

While the data implicates different mechanisms pertaining to ECM development after sporozoite and iRBC infections, it is still insufficient to describe the exact course of infection that occurs when parasites are transmitted *via* the natural route, i.e. transmitted by a mosquito during a blood meal. Nevertheless, based on the data described in this thesis and available literature, I herein propose a hypothetical model of ECM development after a sporozoite infection with modifications to the steps described in 1.2.2.2.

(1) Priming of the immune system in both skin and spleen

A proportion of sporozoites deposited in the skin during an infectious bite, enter the lymph nodes where they are captured by CD8α^+ DCs and presented to resident $CD8^+$ T cells (314). Priming of $CD8^+$ T cells first occurs in the skin followed by the spleen (33) and thus alerts the immune system before parasites reach the blood. The contribution of skin derived $CD8^+$ T cells in promoting ECM is however controversial, since bypassing the skin stage through intravenous injection of sporozoites also induces ECM in susceptible mice. Nevertheless, a proportion of sporozoites that fail to invade hepatocytes are cleared by the spleen, which primes both T cells and stimulates the production of antibodies against sporozoite proteins (326).

(2) Intra-hepatic development and initiation of blood stage infection

The exact role of the liver in influencing the development of ECM is practically unknown. Sporozoites traverse hepatocytes and leave a trail of CSP, which by unknown mechanisms lead to an influx of $CD8^+$ T cells and DCs that sample antigens expressed on MHC I. These T cells do not contribute to organ-associated pathology (327), possibly due to the fact that the liver is an immuno-privileged organ that might suppress any pro-inflammatory response. Nevertheless, it is possible that DCs, which have sampled antigenic material, migrate to the liver draining lymph nodes where they further prime T cells.

Parasite gradually egress from the liver, which leads to an increase in pro-inflammatory cytokines like IFN-γ and TNF-α. The number of merosomes released into the blood stream depends upon the number of sporozoites that successfully invaded hepatocytes, which might vary and thus modulate the outcome of infection. This initial inoculum

plays a critical role in the development of ECM based on the fact that both sporozoite and iRBC infections can cause ECM, even though iRBC infected mice develop significantly higher parasitaemias compared to mice infected with sporozoites (170).

The gradual release of merozoites into the blood stream permits the induction of innate immune mechanisms that involves NK cells that contribute to parasite clearance (96). Moreover, exposure to blood stages boosts the immune response towards antigens like GAP50 that are shared between sporozoites and blood stages. This in turn promotes DCs and other cells within the spleen phagocytose and clear a large proportion of parasites, thus preventing parasite growth from spiralling out of control and thereby reducing severe pathology.

(3) Sequestration and activation of immune effector cells

The steady increase in blood stage infection coupled to an increase in pro-inflammatory cytokines upregulates the expression of receptors on ECs in different organs. Parasites bind to these receptors by expressing variant surface ligands, which leads to sequestration. Because vector (mosquito) transmission attenuates virulence, iRBCs released from hepatocytes after a sporozoite infection express a broad range of virulent proteins, which affects the number of parasites sequestering within the spleen and other organs. The expression of more diverse ligands facilitates more efficient binding to endothelial cells, while evading immune responses. T cells within the spleen are primed against a broader antigenic repertoire with varying potencies. However, the low availability of antigen during the initial phase of infection might result in inefficient priming of T cells, thus reducing their activation.

(4) T cell migration to the brain and cross-presentation of parasite antigens

T cells of different specificities exit out of the spleen and migrate to different tissues *via* chemotaxis. Due to differences in activation levels, a lower proportion of T cells infiltrate the brain (170). ECs act as APCs and cross-present a broad range of parasite antigens that are recognised by T cells expressing the cognate receptor. The synergistic effects of T cells with varying specificities for their cognate antigens triggers the release of cytotoxic molecules and collectively leads to blood brain-barrier permeabilisation. The lower proportion of dominant antigens cross-presented however leads to localised BBB breakdown, as confirmed by the MRI images **(Fig. 3.18)**.

4.4 Implications of this study with relevance to HCM

Data about HCM is mainly gathered from clinical samples and post-mortem tissues. An overwhelming body of data related to *P.falciparum* infections however, has been acquired from *in vitro* cultured parasites, which do not always reflect the behaviour of the parasite as seen in endemic infections. The data presented herein adopts a similar view and challenges the pre-existing notion that HCM is exclusively a phenomenon that begins with the blood stage of the parasites. In addition to underlining the importance of studying CM in the context of sporozoite infections, which is the sole route of human malaria, this thesis proposes a new model of ECM development that can be used to further improve vaccination strategies against HCM and malaria in general.

Clinical studies on HCM have garnered a wealth of information from endemic and non-endemic regions of malaria and highlight three main findings pertaining to the HCM syndrome in individuals:

a) Younger children in malaria endemic areas, below the age group of 5, are particularly susceptible to developing HCM with high mortality rates, while older children and adults gradually acquire immune mechanisms to limit severe disease, but rarely achieve sterile immunity (328).

b) In contrast, individuals with no previous exposure to malaria are highly susceptible to developing severe disease symptoms, including CM, regardless of the age group.

c) Children rapidly acquire immunity to cerebral malaria after a single infection (329, 330), while immunity to febrile malaria is slow to develop (331) and quickly wanes in the absence of ongoing exposure (332, 333).

One of the confounding problems about HCM is the inconsistency in clinical presentation and pathology between individuals and typically between children and adults (described in 1.1). Even though factors influencing susceptibility to HCM are not completely known, the common consensus is that naturally acquired immunity to malaria affords the best level of protection against HCM. Naturally acquired immunity is rarely sterile and predominantly consists of antibody responses against intra-erythrocytic parasites (333, 334) with little or no involvement of responses to pre-erythrocytic stages (335). Individuals living in endemic regions gradually acquire antibodies that limit severe disease symptoms including CM and are classified as asymptomatic (336). Interestingly, protection in asymptomatic individuals relies on the acquisition of antibodies to a broader range of antigens in comparison to those found in symptomatic or more

susceptible individuals (337, 338). Vaccination approaches against malaria are therefore considering the incorporation of multiple antigens into vaccine design (339). A step further would be the inclusion of epitopes that are shared by multiple stages of the parasite life cycle, which could elicit cross-stage immunity (270).

*Pb*maLS_05 is one such antigen that is shared between late liver and blood stages and most likely expressed in sporozoites. Given the prominent role of *Pb*maLS_05 in ECM development and its conserved nature throughout the *Plasmodium* species, it was imperative to investigate if *Pf*maLS_05 also played similar roles. A study conducted by Kirsten Heiss, *et.al.* compared humoral immune responses to *Pf*maLS_05, between asymptomatic and symptomatic individuals and between children and adults. It was pleasing to see that asymptomatic children and adults had higher titres of antibodies to *Pf*maLS_05 compared to symptomatic children (Kirsten Heiss, *et al,* unpublished data), thus confirming an important role of *Pf*maLS_05 in CM.

While cross-presentation of *Pb*maLS_05 by brain endothelial cells awaits confirmation, there is no doubt that *Pb*maLS_05 epitopes are recognised by T cells. While the data are striking, there is paucity in the identification of $CD8^+$ T cell epitopes in humans. Moreover, pinpointing the exact role of $CD8^+$ T cells in the development of cerebral symptoms remains a distant possibility. In light of this reality, it would be tempting in to investigate peripheral $CD8^+$ T cells responses to *Pf*maLS_05 in both adults and children living in endemic regions.

In summary the overall data, though subject to reservations, are supportive of the use of the rodent model for HCM studies and propose a critical role for maLS_05 in severe disease progression. This study in general has greater implications for HCM, particularly in terms of translational aspects and vaccine design, especially in the context of antigens that are presented across the *Plasmodium* life cycle.

Chapter 5

References

1. Newton, C. R., T. T. Hien, and N. White. 2000. Cerebral malaria. *J Neurol Neurosurg Psychiatry* 69: 433-441.
2. Warrell, D. A., S. Looareesuwan, M. J. Warrell, P. Kasemsarn, R. Intaraprasert, D. Bunnag, and T. Harinasuta. 1982. Dexamethasone proves deleterious in cerebral malaria. A double-blind trial in 100 comatose patients. *N Engl J Med* 306: 313-319.
3. WHO. 2015. WHO malaria report.
4. Olliaro, P. 2008. Editorial commentary: mortality associated with severe Plasmodium falciparum malaria increases with age. *Clin Infect Dis* 47: 158-160.
5. Dondorp, A. M., S. J. Lee, M. A. Faiz, S. Mishra, R. Price, E. Tjitra, M. Than, Y. Htut, S. Mohanty, E. B. Yunus, R. Rahman, F. Nosten, N. M. Anstey, N. P. Day, and N. J. White. 2008. The relationship between age and the manifestations of and mortality associated with severe malaria. *Clin Infect Dis* 47: 151-157.
6. Hora, R., P. Kapoor, K. K. Thind, and P. C. Mishra. 2016. Cerebral malaria - clinical manifestations and pathogenesis. *Metab Brain Dis* 31: 225-237.
7. 1990. Severe and complicated malaria. World Health Organization, Division of Control of Tropical Diseases. *Trans R Soc Trop Med Hyg* 84 Suppl 2: 1-65.
8. Looareesuwan, S., D. A. Warrell, N. J. White, P. Chanthavanich, M. J. Warrell, S. Chantaratherakitti, S. Changswek, L. Chongmankongcheep, and C. Kanchanaranya. 1983. Retinal hemorrhage, a common sign of prognostic significance in cerebral malaria. *Am J Trop Med Hyg* 32: 911-915.
9. Artavanis-Tsakonas, K., J. E. Tongren, and E. M. Riley. 2003. The war between the malaria parasite and the immune system: immunity, immunoregulation and immunopathology. *Clin Exp Immunol* 133: 145-152.
10. Marsh, K., D. Forster, C. Waruiru, I. Mwangi, M. Winstanley, V. Marsh, C. Newton, P. Winstanley, P. Warn, N. Peshu, and et al. 1995. Indicators of life-threatening malaria in African children. *N Engl J Med* 332: 1399-1404.
11. Waruiru, C. M., C. R. Newton, D. Forster, L. New, P. Winstanley, I. Mwangi, V. Marsh, M. Winstanley, R. W. Snow, and K. Marsh. 1996. Epileptic seizures and malaria in Kenyan children. *Trans R Soc Trop Med Hyg* 90: 152-155.
12. Seydel, K. B., S. D. Kampondeni, C. Valim, M. J. Potchen, D. A. Milner, F. W. Muwalo, G. L. Birbeck, W. G. Bradley, L. L. Fox, S. J. Glover, C. A. Hammond, R. S. Heyderman, C. A. Chilingulo, M. E. Molyneux, and T. E. Taylor. 2015. Brain swelling and death in children with cerebral malaria. *N Engl J Med* 372: 1126-1137.
13. John, C. C., P. Bangirana, J. Byarugaba, R. O. Opoka, R. Idro, A. M. Jurek, B. Wu, and M. J. Boivin. 2008. Cerebral malaria in children is associated with long-term cognitive impairment. *Pediatrics* 122: e92-99.
14. Boivin, M. J., P. Bangirana, J. Byarugaba, R. O. Opoka, R. Idro, A. M. Jurek, and C. C. John. 2007. Cognitive impairment after cerebral malaria in children: a prospective study. *Pediatrics* 119: e360-366.
15. Idro, R., K. Marsh, C. C. John, and C. R. Newton. 2010. Cerebral malaria: mechanisms of brain injury and strategies for improved neurocognitive outcome. *Pediatr Res* 68: 267-274.

16. Gupta, H., P. Dhunputh, A. N. Bhatt, K. Satyamoorthy, and S. Umakanth. 2016. Cerebral malaria in a man with Plasmodium vivax mono-infection: a case report. *Trop Doct*.
17. Lakhotia, M., J. Singh, H. R. Pahadiya, H. Kumar, and P. K. Choudhary. 2015. Retinal Hemorrhages in Severe Non-cerebral Plasmodium vivax Malaria in an Adult. *J Clin Diagn Res* 9: OD01-03.
18. Pinzon, M. A., J. C. Pineda, F. Rosso, M. Shinchi, and F. Bonilla-Abadia. 2013. Plasmodium vivax cerebral malaria complicated with venous sinus thrombosis in Colombia. *Asian Pac J Trop Med* 6: 413-415.
19. Ozen, M., S. Gungor, M. Atambay, and N. Daldal. 2006. Cerebral malaria owing to Plasmodium vivax: case report. *Ann Trop Paediatr* 26: 141-144.
20. Manning, L., A. Rosanas-Urgell, M. Laman, H. Edoni, C. McLean, I. Mueller, P. Siba, and T. M. Davis. 2012. A histopathologic study of fatal paediatric cerebral malaria caused by mixed Plasmodium falciparum/Plasmodium vivax infections. *Malar J* 11: 107.
21. Borrmann, S., and K. Matuschewski. 2011. Targeting Plasmodium liver stages: better late than never. *Trends Mol Med* 17: 527-536.
22. Medica, D. L., and P. Sinnis. 2005. Quantitative dynamics of Plasmodium yoelii sporozoite transmission by infected anopheline mosquitoes. *Infect Immun* 73: 4363-4369.
23. Jin, Y., C. Kebaier, and J. Vanderberg. 2007. Direct microscopic quantification of dynamics of Plasmodium berghei sporozoite transmission from mosquitoes to mice. *Infect Immun* 75: 5532-5539.
24. Ponnudurai, T., A. H. Lensen, G. J. van Gemert, M. G. Bolmer, and J. H. Meuwissen. 1991. Feeding behaviour and sporozoite ejection by infected Anopheles stephensi. *Trans R Soc Trop Med Hyg* 85: 175-180.
25. Amino, R., S. Thiberge, B. Martin, S. Celli, S. Shorte, F. Frischknecht, and R. Menard. 2006. Quantitative imaging of Plasmodium transmission from mosquito to mammal. *Nat Med* 12: 220-224.
26. Vanderberg, J. P., and U. Frevert. 2004. Intravital microscopy demonstrating antibody-mediated immobilisation of Plasmodium berghei sporozoites injected into skin by mosquitoes. *Int J Parasitol* 34: 991-996.
27. Frevert, U., S. Engelmann, S. Zougbede, J. Stange, B. Ng, K. Matuschewski, L. Liebes, and H. Yee. 2005. Intravital observation of Plasmodium berghei sporozoite infection of the liver. *PLoS Biol* 3: e192.
28. Menard, R., J. Tavares, I. Cockburn, M. Markus, F. Zavala, and R. Amino. 2013. Looking under the skin: the first steps in malarial infection and immunity. *Nat Rev Microbiol* 11: 701-712.
29. Yamauchi, L. M., A. Coppi, G. Snounou, and P. Sinnis. 2007. Plasmodium sporozoites trickle out of the injection site. *Cell Microbiol* 9: 1215-1222.
30. Graewe, S., R. R. Stanway, A. Rennenberg, and V. T. Heussler. 2012. Chronicle of a death foretold: Plasmodium liver stage parasites decide on the fate of the host cell. *FEMS Microbiol Rev* 36: 111-130.
31. Gueirard, P., J. Tavares, S. Thiberge, F. Bernex, T. Ishino, G. Milon, B. Franke-Fayard, C. J. Janse, R. Menard, and R. Amino. 2010. Development of the malaria parasite in the skin of the mammalian host. *Proc Natl Acad Sci U S A* 107: 18640-18645.
32. Chakravarty, S., I. A. Cockburn, S. Kuk, M. G. Overstreet, J. B. Sacci, and F. Zavala. 2007. CD8+ T lymphocytes protective against malaria liver stages are primed in skin-draining lymph nodes. *Nat Med* 13: 1035-1041.

33. Obeid, M., J. F. Franetich, A. Lorthiois, A. Gego, A. C. Gruner, M. Tefit, C. Boucheix, G. Snounou, and D. Mazier. 2013. Skin-draining lymph node priming is sufficient to induce sterile immunity against pre-erythrocytic malaria. *EMBO Mol Med* 5: 250-263.
34. Sinnis, P., and F. Zavala. 2008. The skin stage of malaria infection: biology and relevance to the malaria vaccine effort. *Future Microbiol* 3: 275-278.
35. Pradel, G., S. Garapaty, and U. Frevert. 2004. Kupffer and stellate cell proteoglycans mediate malaria sporozoite targeting to the liver. *Comp Hepatol* 3 Suppl 1: S47.
36. Pradel, G., S. Garapaty, and U. Frevert. 2002. Proteoglycans mediate malaria sporozoite targeting to the liver. *Mol Microbiol* 45: 637-651.
37. Ying, P., M. Shakibaei, M. S. Patankar, P. Clavijo, R. C. Beavis, G. F. Clark, and U. Frevert. 1997. The malaria circumsporozoite protein: interaction of the conserved regions I and II-plus with heparin-like oligosaccharides in heparan sulfate. *Exp Parasitol* 85: 168-182.
38. Pinzon-Ortiz, C., J. Friedman, J. Esko, and P. Sinnis. 2001. The binding of the circumsporozoite protein to cell surface heparan sulfate proteoglycans is required for plasmodium sporozoite attachment to target cells. *J Biol Chem* 276: 26784-26791.
39. Tavares, J., P. Formaglio, S. Thiberge, E. Mordelet, N. Van Rooijen, A. Medvinsky, R. Menard, and R. Amino. 2013. Role of host cell traversal by the malaria sporozoite during liver infection. *J Exp Med* 210: 905-915.
40. Ishino, T., K. Yano, Y. Chinzei, and M. Yuda. 2004. Cell-passage activity is required for the malarial parasite to cross the liver sinusoidal cell layer. *PLoS Biol* 2: E4.
41. Kariu, T., T. Ishino, K. Yano, Y. Chinzei, and M. Yuda. 2006. CelTOS, a novel malarial protein that mediates transmission to mosquito and vertebrate hosts. *Mol Microbiol* 59: 1369-1379.
42. Bhanot, P., K. Schauer, I. Coppens, and V. Nussenzweig. 2005. A surface phospholipase is involved in the migration of plasmodium sporozoites through cells. *J Biol Chem* 280: 6752-6760.
43. Amino, R., D. Giovannini, S. Thiberge, P. Gueirard, B. Boisson, J. F. Dubremetz, M. C. Prevost, T. Ishino, M. Yuda, and R. Menard. 2008. Host cell traversal is important for progression of the malaria parasite through the dermis to the liver. *Cell Host Microbe* 3: 88-96.
44. Mota, M. M., G. Pradel, J. P. Vanderberg, J. C. Hafalla, U. Frevert, R. S. Nussenzweig, V. Nussenzweig, and A. Rodriguez. 2001. Migration of Plasmodium sporozoites through cells before infection. *Science* 291: 141-144.
45. Risco-Castillo, V., S. Topcu, C. Marinach, G. Manzoni, A. E. Bigorgne, S. Briquet, X. Baudin, M. Lebrun, J. F. Dubremetz, and O. Silvie. 2015. Malaria Sporozoites Traverse Host Cells within Transient Vacuoles. *Cell Host Microbe* 18: 593-603.
46. Risco-Castillo, V., S. Topcu, O. Son, S. Briquet, G. Manzoni, and O. Silvie. 2014. CD81 is required for rhoptry discharge during host cell invasion by Plasmodium yoelii sporozoites. *Cell Microbiol* 16: 1533-1548.
47. Foquet, L., C. C. Hermsen, L. Verhoye, G. J. van Gemert, R. Cortese, A. Nicosia, R. W. Sauerwein, G. Leroux-Roels, and P. Meuleman. 2015. Anti-CD81 but not anti-SR-BI blocks Plasmodium falciparum liver infection in a humanized mouse model. *J Antimicrob Chemother* 70: 1784-1787.
48. Kaushansky, A., A. N. Douglass, N. Arang, V. Vigdorovich, N. Dambrauskas, H. S. Kain, L. S. Austin, D. N. Sather, and S. H. Kappe. 2015. Malaria parasites

target the hepatocyte receptor EphA2 for successful host infection. *Science* 350: 1089-1092.

49. Matuschewski, K., A. C. Nunes, V. Nussenzweig, and R. Menard. 2002. Plasmodium sporozoite invasion into insect and mammalian cells is directed by the same dual binding system. *Embo J* 21: 1597-1606.
50. Silvie, O., J. F. Franetich, S. Charrin, M. S. Mueller, A. Siau, M. Bodescot, E. Rubinstein, L. Hannoun, Y. Charoenvit, C. H. Kocken, A. W. Thomas, G. J. Van Gemert, R. W. Sauerwein, M. J. Blackman, R. F. Anders, G. Pluschke, and D. Mazier. 2004. A role for apical membrane antigen 1 during invasion of hepatocytes by Plasmodium falciparum sporozoites. *J Biol Chem* 279: 9490-9496.
51. Ishino, T., Y. Chinzei, and M. Yuda. 2005. Two proteins with 6-cys motifs are required for malarial parasites to commit to infection of the hepatocyte. *Mol Microbiol* 58: 1264-1275.
52. Silvie, O., E. Rubinstein, J. F. Franetich, M. Prenant, E. Belnoue, L. Renia, L. Hannoun, W. Eling, S. Levy, C. Boucheix, and D. Mazier. 2003. Hepatocyte CD81 is required for Plasmodium falciparum and Plasmodium yoelii sporozoite infectivity. *Nat Med* 9: 93-96.
53. Gomes-Santos, C. S., M. A. Itoe, C. Afonso, R. Henriques, R. Gardner, N. Sepulveda, P. D. Simoes, H. Raquel, A. P. Almeida, L. F. Moita, F. Frischknecht, and M. M. Mota. 2012. Highly dynamic host actin reorganization around developing Plasmodium inside hepatocytes. *PLoS One* 7: e29408.
54. Gonzalez, V., A. Combe, V. David, N. A. Malmquist, V. Delorme, C. Leroy, S. Blazquez, R. Menard, and I. Tardieux. 2009. Host cell entry by apicomplexa parasites requires actin polymerization in the host cell. *Cell Host Microbe* 5: 259-272.
55. Stewart, M. J., S. Schulman, and J. P. Vanderberg. 1985. Rhoptry secretion of membranous whorls by Plasmodium berghei sporozoites. *J Protozool* 32: 280-283.
56. Kaushansky, A., A. S. Ye, L. S. Austin, S. A. Mikolajczak, A. M. Vaughan, N. Camargo, P. G. Metzger, A. N. Douglass, G. MacBeath, and S. H. Kappe. 2013. Suppression of host p53 is critical for Plasmodium liver-stage infection. *Cell Rep* 3: 630-637.
57. Kaushansky, A., P. G. Metzger, A. N. Douglass, S. A. Mikolajczak, V. Lakshmanan, H. S. Kain, and S. H. Kappe. 2013. Malaria parasite liver stages render host hepatocytes susceptible to mitochondria-initiated apoptosis. *Cell Death Dis* 4: e762.
58. van de Sand, C., S. Horstmann, A. Schmidt, A. Sturm, S. Bolte, A. Krueger, M. Lutgehetmann, J. M. Pollok, C. Libert, and V. T. Heussler. 2005. The liver stage of Plasmodium berghei inhibits host cell apoptosis. *Mol Microbiol* 58: 731-742.
59. Stanway, R. R., N. Mueller, B. Zobiak, S. Graewe, U. Froehlke, P. J. Zessin, M. Aepfelbacher, and V. T. Heussler. 2011. Organelle segregation into Plasmodium liver stage merozoites. *Cell Microbiol* 13: 1768-1782.
60. Itoe, M. A., J. L. Sampaio, G. G. Cabal, E. Real, V. Zuzarte-Luis, S. March, S. N. Bhatia, F. Frischknecht, C. Thiele, A. Shevchenko, and M. M. Mota. 2014. Host cell phosphatidylcholine is a key mediator of malaria parasite survival during liver stage infection. *Cell Host Microbe* 16: 778-786.
61. Mackellar, D. C., M. T. O'Neill, A. S. Aly, J. B. Sacci, Jr., A. F. Cowman, and S. H. Kappe. 2010. Plasmodium falciparum PF10_0164 (ETRAMP10.3) is an essential parasitophorous vacuole and exported protein in blood stages. *Eukaryot Cell* 9: 784-794.

62. Spielmann, T., D. L. Gardiner, H. P. Beck, K. R. Trenholme, and D. J. Kemp. 2006. Organization of ETRAMPs and EXP-1 at the parasite-host cell interface of malaria parasites. *Mol Microbiol* 59: 779-794.
63. Mikolajczak, S. A., V. Jacobs-Lorena, D. C. MacKellar, N. Camargo, and S. H. Kappe. 2007. L-FABP is a critical host factor for successful malaria liver stage development. *Int J Parasitol* 37: 483-489.
64. Nyboer, B. 2015. PhD Thesis.
65. Wickham, M. E., J. G. Culvenor, and A. F. Cowman. 2003. Selective inhibition of a two-step egress of malaria parasites from the host erythrocyte. *J Biol Chem* 278: 37658-37663.
66. Sturm, A., R. Amino, C. van de Sand, T. Regen, S. Retzlaff, A. Rennenberg, A. Krueger, J. M. Pollok, R. Menard, and V. T. Heussler. 2006. Manipulation of host hepatocytes by the malaria parasite for delivery into liver sinusoids. *Science* 313: 1287-1290.
67. Cowman, A. F., and S. H. Kappe. 2006. Microbiology. Malaria's stealth shuttle. *Science* 313: 1245-1246.
68. Graewe, S., K. E. Rankin, C. Lehmann, C. Deschermeier, L. Hecht, U. Froehlke, R. R. Stanway, and V. Heussler. 2011. Hostile takeover by Plasmodium: reorganization of parasite and host cell membranes during liver stage egress. *PLoS Pathog* 7: e1002224.
69. Baer, K., C. Klotz, S. H. Kappe, T. Schnieder, and U. Frevert. 2007. Release of hepatic Plasmodium yoelii merozoites into the pulmonary microvasculature. *PLoS Pathog* 3: e171.
70. Glushakova, S., D. Yin, T. Li, and J. Zimmerberg. 2005. Membrane transformation during malaria parasite release from human red blood cells. *Curr Biol* 15: 1645-1650.
71. Kerlin, D. H., and M. L. Gatton. 2013. Preferential invasion by Plasmodium merozoites and the self-regulation of parasite burden. *PLoS One* 8: e57434.
72. Mitchell, G. H., T. J. Hadley, M. H. McGinniss, F. W. Klotz, and L. H. Miller. 1986. Invasion of erythrocytes by Plasmodium falciparum malaria parasites: evidence for receptor heterogeneity and two receptors. *Blood* 67: 1519-1521.
73. Perkins, M. E., and E. H. Holt. 1988. Erythrocyte receptor recognition varies in Plasmodium falciparum isolates. *Mol Biochem Parasitol* 27: 23-34.
74. Cowman, A. F., D. Berry, and J. Baum. 2012. The cellular and molecular basis for malaria parasite invasion of the human red blood cell. *J Cell Biol* 198: 961-971.
75. Gruring, C., A. Heiber, F. Kruse, J. Ungefehr, T. W. Gilberger, and T. Spielmann. 2011. Development and host cell modifications of Plasmodium falciparum blood stages in four dimensions. *Nat Commun* 2: 165.
76. Tamez, P. A., S. Bhattacharjee, C. van Ooij, N. L. Hiller, M. Llinas, B. Balu, J. H. Adams, and K. Haldar. 2008. An erythrocyte vesicle protein exported by the malaria parasite promotes tubovesicular lipid import from the host cell surface. *PLoS Pathog* 4: e1000118.
77. Lauer, S. A., P. K. Rathod, N. Ghori, and K. Haldar. 1997. A membrane network for nutrient import in red cells infected with the malaria parasite. *Science* 276: 1122-1125.
78. Craig, A., and A. Scherf. 2001. Molecules on the surface of the Plasmodium falciparum infected erythrocyte and their role in malaria pathogenesis and immune evasion. *Mol Biochem Parasitol* 115: 129-143.
79. Goel, S., M. Palmkvist, K. Moll, N. Joannin, P. Lara, R. R. Akhouri, N. Moradi, K. Ojemalm, M. Westman, D. Angeletti, H. Kjellin, J. Lehtio, O. Blixt, L. Idestrom, C. G. Gahmberg, J. R. Storry, A. K. Hult, M. L. Olsson, G. von Heijne,

I. Nilsson, and M. Wahlgren. 2015. RIFINs are adhesins implicated in severe Plasmodium falciparum malaria. *Nat Med* 21: 314-317.

80. Deplaine, G., I. Safeukui, F. Jeddi, F. Lacoste, V. Brousse, S. Perrot, S. Biligui, M. Guillotte, C. Guitton, S. Dokmak, B. Aussilhou, A. Sauvanet, D. Cazals Hatem, F. Paye, M. Thellier, D. Mazier, G. Milon, N. Mohandas, O. Mercereau-Puijalon, P. H. David, and P. A. Buffet. 2011. The sensing of poorly deformable red blood cells by the human spleen can be mimicked in vitro. *Blood* 117: e88-95.
81. Nash, G. B., E. O'Brien, E. C. Gordon-Smith, and J. A. Dormandy. 1989. Abnormalities in the mechanical properties of red blood cells caused by Plasmodium falciparum. *Blood* 74: 855-861.
82. van der Heyde, H. C., J. Nolan, V. Combes, I. Gramaglia, and G. E. Grau. 2006. A unified hypothesis for the genesis of cerebral malaria: sequestration, inflammation and hemostasis leading to microcirculatory dysfunction. *Trends Parasitol* 22: 503-508.
83. O'Donnell, J. S., T. A. McKinnon, J. T. Crawley, D. A. Lane, and M. A. Laffan. 2005. Bombay phenotype is associated with reduced plasma-VWF levels and an increased susceptibility to ADAMTS13 proteolysis. *Blood* 106: 1988-1991.
84. Cox, J., S. Semoff, and M. Hommel. 1987. Plasmodium chabaudi: a rodent malaria model for in-vivo and in-vitro cytoadherence of malaria parasites in the absence of knobs. *Parasite Immunol* 9: 543-561.
85. Haldar, K., S. Kamoun, N. L. Hiller, S. Bhattacharje, and C. van Ooij. 2006. Common infection strategies of pathogenic eukaryotes. *Nat Rev Microbiol* 4: 922-931.
86. Kuehn, A., and G. Pradel. 2010. The coming-out of malaria gametocytes. *J Biomed Biotechnol* 2010: 976827.
87. Joice, R., S. K. Nilsson, J. Montgomery, S. Dankwa, E. Egan, B. Morahan, K. B. Seydel, L. Bertuccini, P. Alano, K. C. Williamson, M. T. Duraisingh, T. E. Taylor, D. A. Milner, and M. Marti. 2014. Plasmodium falciparum transmission stages accumulate in the human bone marrow. *Sci Transl Med* 6: 244re245.
88. Seydel, K. B., D. A. Milner, Jr., S. B. Kamiza, M. E. Molyneux, and T. E. Taylor. 2006. The distribution and intensity of parasite sequestration in comatose Malawian children. *J Infect Dis* 194: 208-205.
89. Lal, A. A., P. S. Patterson, J. B. Sacci, J. A. Vaughan, C. Paul, W. E. Collins, R. A. Wirtz, and A. F. Azad. 2001. Anti-mosquito midgut antibodies block development of Plasmodium falciparum and Plasmodium vivax in multiple species of Anopheles mosquitoes and reduce vector fecundity and survivorship. *Proc Natl Acad Sci U S A* 98: 5228-5233.
90. Sinden, R. E., and N. A. Croll. 1975. Cytology and kinetics of microgametogenesis and fertilization in Plasmodium yoelii nigeriensis. *Parasitology* 70: 53-65.
91. Angrisano, F., Y. H. Tan, A. Sturm, G. I. McFadden, and J. Baum. 2012. Malaria parasite colonisation of the mosquito midgut--placing the Plasmodium ookinete centre stage. *Int J Parasitol* 42: 519-527.
92. Cooke, G. S., and A. V. Hill. 2001. Genetics of susceptibility to human infectious disease. *Nat Rev Genet* 2: 967-977.
93. Erunkulu, O. A., A. V. Hill, D. P. Kwiatkowski, J. E. Todd, J. Iqbal, K. Berzins, E. M. Riley, and B. M. Greenwood. 1992. Severe malaria in Gambian children is not due to lack of previous exposure to malaria. *Clin Exp Immunol* 89: 296-300.
94. Dubos, F., A. Dauriac, L. El Mansouf, C. Courouble, M. Aurel, and A. Martinot. 2010. Imported malaria in children: incidence and risk factors for severity. *Diagn Microbiol Infect Dis* 66: 169-174.

95. Baird, J. K., S. Masbar, H. Basri, S. Tirtokusumo, B. Subianto, and S. L. Hoffman. 1998. Age-dependent susceptibility to severe disease with primary exposure to Plasmodium falciparum. *J Infect Dis* 178: 592-595.
96. Stevenson, M. M., and E. M. Riley. 2004. Innate immunity to malaria. *Nat Rev Immunol* 4: 169-180.
97. Day, N. P., T. T. Hien, T. Schollaardt, P. P. Loc, L. V. Chuong, T. T. Chau, N. T. Mai, N. H. Phu, D. X. Sinh, N. J. White, and M. Ho. 1999. The prognostic and pathophysiologic role of pro- and antiinflammatory cytokines in severe malaria. *J Infect Dis* 180: 1288-1297.
98. Dieye, Y., B. Mbengue, S. Dagamajalu, M. M. Fall, M. F. Loke, C. M. Nguer, A. Thiam, J. Vadivelu, and A. Dieye. 2016. Cytokine response during non-cerebral and cerebral malaria: evidence of a failure to control inflammation as a cause of death in African adults. *PeerJ* 4: e1965.
99. Conroy, A. L., H. Phiri, M. Hawkes, S. Glover, M. Mallewa, K. B. Seydel, T. E. Taylor, M. E. Molyneux, and K. C. Kain. 2010. Endothelium-based biomarkers are associated with cerebral malaria in Malawian children: a retrospective case-control study. *PLoS One* 5: e15291.
100. Erdman, L. K., A. Dhabangi, C. Musoke, A. L. Conroy, M. Hawkes, S. Higgins, N. Rajwans, K. T. Wolofsky, D. L. Streiner, W. C. Liles, C. M. Cserti-Gazdewich, and K. C. Kain. 2011. Combinations of host biomarkers predict mortality among Ugandan children with severe malaria: a retrospective case-control study. *PLoS One* 6: e17440.
101. Riley, E. M. 1999. Is T-cell priming required for initiation of pathology in malaria infections? *Immunol Today* 20: 228-233.
102. Jelinek, T., C. Schulte, R. Behrens, M. P. Grobusch, J. P. Coulaud, Z. Bisoffi, A. Matteelli, J. Clerinx, M. Corachan, S. Puente, I. Gjorup, G. Harms, H. Kollaritsch, A. Kotlowski, A. Bjorkmann, J. P. Delmont, J. Knobloch, L. N. Nielsen, J. Cuadros, C. Hatz, J. Beran, M. L. Schmid, M. Schulze, R. Lopez-Velez, K. Fleischer, A. Kapaun, P. McWhinney, P. Kern, J. Atougia, G. Fry, S. da Cunha, and G. Boecken. 2002. Imported Falciparum malaria in Europe: sentinel surveillance data from the European network on surveillance of imported infectious diseases. *Clin Infect Dis* 34: 572-576.
103. Deloron, P., and C. Chougnet. 1992. Is immunity to malaria really short-lived? *Parasitol Today* 8: 375-378.
104. Berendt, A. R., G. D. Tumer, and C. I. Newbold. 1994. Cerebral malaria: the sequestration hypothesis. *Parasitol Today* 10: 412-414.
105. Ponsford, M. J., I. M. Medana, P. Prapansilp, T. T. Hien, S. J. Lee, A. M. Dondorp, M. M. Esiri, N. P. Day, N. J. White, and G. D. Turner. 2012. Sequestration and microvascular congestion are associated with coma in human cerebral malaria. *J Infect Dis* 205: 663-671.
106. Dorovini-Zis, K., K. Schmidt, H. Huynh, W. Fu, R. O. Whitten, D. Milner, S. Kamiza, M. Molyneux, and T. E. Taylor. 2011. The neuropathology of fatal cerebral malaria in malawian children. *Am J Pathol* 178: 2146-2158.
107. Taylor, T. E., W. J. Fu, R. A. Carr, R. O. Whitten, J. S. Mueller, N. G. Fosiko, S. Lewallen, N. G. Liomba, and M. E. Molyneux. 2004. Differentiating the pathologies of cerebral malaria by postmortem parasite counts. *Nat Med* 10: 143-145.
108. Grau, G. E., C. D. Mackenzie, R. A. Carr, M. Redard, G. Pizzolato, C. Allasia, C. Cataldo, T. E. Taylor, and M. E. Molyneux. 2003. Platelet accumulation in brain microvessels in fatal pediatric cerebral malaria. *J Infect Dis* 187: 461-466.

109. Patnaik, J. K., B. S. Das, S. K. Mishra, S. Mohanty, S. K. Satpathy, and D. Mohanty. 1994. Vascular clogging, mononuclear cell margination, and enhanced vascular permeability in the pathogenesis of human cerebral malaria. *Am J Trop Med Hyg* 51: 642-647.
110. Silamut, K., N. H. Phu, C. Whitty, G. D. Turner, K. Louwrier, N. T. Mai, J. A. Simpson, T. T. Hien, and N. J. White. 1999. A quantitative analysis of the microvascular sequestration of malaria parasites in the human brain. *Am J Pathol* 155: 395-410.
111. Pongponratn, E., G. D. Turner, N. P. Day, N. H. Phu, J. A. Simpson, K. Stepniewska, N. T. Mai, P. Viriyavejakul, S. Looareesuwan, T. T. Hien, D. J. Ferguson, and N. J. White. 2003. An ultrastructural study of the brain in fatal Plasmodium falciparum malaria. *Am J Trop Med Hyg* 69: 345-359.
112. Dondorp, A. M., E. Pongponratn, and N. J. White. 2004. Reduced microcirculatory flow in severe falciparum malaria: pathophysiology and electron-microscopic pathology. *Acta Trop* 89: 309-317.
113. Turner, L., T. Lavstsen, S. S. Berger, C. W. Wang, J. E. Petersen, M. Avril, A. J. Brazier, J. Freeth, J. S. Jespersen, M. A. Nielsen, P. Magistrado, J. Lusingu, J. D. Smith, M. K. Higgins, and T. G. Theander. 2013. Severe malaria is associated with parasite binding to endothelial protein C receptor. *Nature* 498: 502-505.
114. Febbraio, M., D. P. Hajjar, and R. L. Silverstein. 2001. CD36: a class B scavenger receptor involved in angiogenesis, atherosclerosis, inflammation, and lipid metabolism. *J Clin Invest* 108: 785-791.
115. Montgomery, J., F. A. Mphande, M. Berriman, A. Pain, S. J. Rogerson, T. E. Taylor, M. E. Molyneux, and A. Craig. 2007. Differential var gene expression in the organs of patients dying of falciparum malaria. *Mol Microbiol* 65: 959-967.
116. Rogerson, S. J., S. C. Chaiyaroj, K. Ng, J. C. Reeder, and G. V. Brown. 1995. Chondroitin sulfate A is a cell surface receptor for Plasmodium falciparum-infected erythrocytes. *J Exp Med* 182: 15-20.
117. Fried, M., and P. E. Duffy. 1996. Adherence of Plasmodium falciparum to chondroitin sulfate A in the human placenta. *Science* 272: 1502-1504.
118. Robert, C., B. Pouvelle, P. Meyer, K. Muanza, H. Fujioka, M. Aikawa, A. Scherf, and J. Gysin. 1995. Chondroitin-4-sulphate (proteoglycan), a receptor for Plasmodium falciparum-infected erythrocyte adherence on brain microvascular endothelial cells. *Res Immunol* 146: 383-393.
119. Newbold, C., A. Craig, S. Kyes, A. Rowe, D. Fernandez-Reyes, and T. Fagan. 1999. Cytoadherence, pathogenesis and the infected red cell surface in Plasmodium falciparum. *Int J Parasitol* 29: 927-937.
120. Wassmer, S. C., C. Lepolard, B. Traore, B. Pouvelle, J. Gysin, and G. E. Grau. 2004. Platelets reorient Plasmodium falciparum-infected erythrocyte cytoadhesion to activated endothelial cells. *J Infect Dis* 189: 180-189.
121. Faille, D., V. Combes, A. J. Mitchell, A. Fontaine, I. Juhan-Vague, M. C. Alessi, G. Chimini, T. Fusai, and G. E. Grau. 2009. Platelet microparticles: a new player in malaria parasite cytoadherence to human brain endothelium. *Faseb J* 23: 3449-3458.
122. Turner, G. D., H. Morrison, M. Jones, T. M. Davis, S. Looareesuwan, I. D. Buley, K. C. Gatter, C. I. Newbold, S. Pukritayakamee, B. Nagachinta, and et al. 1994. An immunohistochemical study of the pathology of fatal malaria. Evidence for widespread endothelial activation and a potential role for intercellular adhesion molecule-1 in cerebral sequestration. *Am J Pathol* 145: 1057-1069.
123. Jambou, R., V. Combes, M. J. Jambou, B. B. Weksler, P. O. Couraud, and G. E. Grau. 2010. Plasmodium falciparum adhesion on human brain microvascular

endothelial cells involves transmigration-like cup formation and induces opening of intercellular junctions. *PLoS Pathog* 6: e1001021.

124. Wang, Q., and C. M. Doerschuk. 2000. Neutrophil-induced changes in the biomechanical properties of endothelial cells: roles of ICAM-1 and reactive oxygen species. *J Immunol* 164: 6487-6494.
125. Hubbard, A. K., and R. Rothlein. 2000. Intercellular adhesion molecule-1 (ICAM-1) expression and cell signaling cascades. *Free Radic Biol Med* 28: 1379-1386.
126. Adams, S., H. Brown, and G. Turner. 2002. Breaking down the blood-brain barrier: signaling a path to cerebral malaria? *Trends Parasitol* 18: 360-366.
127. Viebig, N. K., U. Wulbrand, R. Forster, K. T. Andrews, M. Lanzer, and P. A. Knolle. 2005. Direct activation of human endothelial cells by Plasmodium falciparum-infected erythrocytes. *Infect Immun* 73: 3271-3277.
128. Brown, H. C., T. T. Chau, N. T. Mai, N. P. Day, D. X. Sinh, N. J. White, T. T. Hien, J. Farrar, and G. D. Turner. 2000. Blood-brain barrier function in cerebral malaria and CNS infections in Vietnam. *Neurology* 55: 104-111.
129. Brown, H., S. Rogerson, T. Taylor, M. Tembo, J. Mwenechanya, M. Molyneux, and G. Turner. 2001. Blood-brain barrier function in cerebral malaria in Malawian children. *Am J Trop Med Hyg* 64: 207-213.
130. Medana, I. M., N. P. Day, N. Sachanonta, N. T. Mai, A. M. Dondorp, E. Pongponratn, T. T. Hien, N. J. White, and G. D. Turner. 2011. Coma in fatal adult human malaria is not caused by cerebral oedema. *Malar J* 10: 267.
131. Shinjo, K., S. Tsuda, T. Hayami, T. Asahi, and H. Kawaharada. 1989. Increase in permeability of human endothelial cell monolayer by recombinant human lymphotoxin. *Biochem Biophys Res Commun* 162: 1431-1437.
132. Cook-Mills, J. M., and T. L. Deem. 2005. Active participation of endothelial cells in inflammation. *J Leukoc Biol* 77: 487-495.
133. Feintuch, C. M., A. Saidi, K. Seydel, G. Chen, A. Goldman-Yassen, N. K. Mita-Mendoza, R. S. Kim, P. S. Frenette, T. Taylor, and J. P. Daily. 2016. Activated Neutrophils Are Associated with Pediatric Cerebral Malaria Vasculopathy in Malawian Children. *MBio* 7: e01300-01315.
134. Royall, J. A., R. L. Berkow, J. S. Beckman, M. K. Cunningham, S. Matalon, and B. A. Freeman. 1989. Tumor necrosis factor and interleukin 1 alpha increase vascular endothelial permeability. *Am J Physiol* 257: L399-410.
135. Mark, K. S., and D. W. Miller. 1999. Increased permeability of primary cultured brain microvessel endothelial cell monolayers following TNF-alpha exposure. *Life Sci* 64: 1941-1953.
136. Brown, H., G. Turner, S. Rogerson, M. Tembo, J. Mwenechanya, M. Molyneux, and T. Taylor. 1999. Cytokine expression in the brain in human cerebral malaria. *J Infect Dis* 180: 1742-1746.
137. Chakravorty, S. J., K. R. Hughes, and A. G. Craig. 2008. Host response to cytoadherence in Plasmodium falciparum. *Biochem Soc Trans* 36: 221-228.
138. Miller, D. W. 1999. Immunobiology of the blood-brain barrier. *J Neurovirol* 5: 570-578.
139. O'Sullivan, J. M., R. J. Preston, N. O'Regan, and J. S. O'Donnell. 2016. Emerging roles for hemostatic dysfunction in malaria pathogenesis. *Blood* 127: 2281-2288.
140. Pal, P., B. P. Daniels, A. Oskman, M. S. Diamond, R. S. Klein, and D. E. Goldberg. 2016. Plasmodium falciparum Histidine-Rich Protein II Compromises Brain Endothelial Barriers and May Promote Cerebral Malaria Pathogenesis. *MBio* 7.

141. Schofield, L., S. Novakovic, P. Gerold, R. T. Schwarz, M. J. McConville, and S. D. Tachado. 1996. Glycosylphosphatidylinositol toxin of Plasmodium up-regulates intercellular adhesion molecule-1, vascular cell adhesion molecule-1, and E-selectin expression in vascular endothelial cells and increases leukocyte and parasite cytoadherence via tyrosine kinase-dependent signal transduction. *J Immunol* 156: 1886-1896.
142. Prato, M., S. D'Alessandro, P. E. Van den Steen, G. Opdenakker, P. Arese, D. Taramelli, and N. Basilico. 2011. Natural haemozoin modulates matrix metalloproteinases and induces morphological changes in human microvascular endothelium. *Cell Microbiol* 13: 1275-1285.
143. Wyler, D. J., T. C. Quinn, and L. T. Chen. 1981. Relationship of alterations in splenic clearance function and microcirculation to host defense in acute rodent malaria. *J Clin Invest* 67: 1400-1404.
144. Looareesuwan, S., P. Suntharasamai, H. K. Webster, and M. Ho. 1993. Malaria in splenectomized patients: report of four cases and review. *Clin Infect Dis* 16: 361-366.
145. Chotivanich, K., R. Udomsangpetch, R. McGready, S. Proux, P. Newton, S. Pukrittayakamee, S. Looareesuwan, and N. J. White. 2002. Central role of the spleen in malaria parasite clearance. *J Infect Dis* 185: 1538-1541.
146. Hommel, M., P. H. David, and L. D. Oligino. 1983. Surface alterations of erythrocytes in Plasmodium falciparum malaria. Antigenic variation, antigenic diversity, and the role of the spleen. *J Exp Med* 157: 1137-1148.
147. David, P. H., M. Hommel, L. H. Miller, I. J. Udeinya, and L. D. Oligino. 1983. Parasite sequestration in Plasmodium falciparum malaria: spleen and antibody modulation of cytoadherence of infected erythrocytes. *Proc Natl Acad Sci U S A* 80: 5075-5079.
148. Ho, M., L. H. Bannister, S. Looareesuwan, and P. Suntharasamai. 1992. Cytoadherence and ultrastructure of Plasmodium falciparum-infected erythrocytes from a splenectomized patient. *Infect Immun* 60: 2225-2228.
149. Buffet, P. A., I. Safeukui, G. Deplaine, V. Brousse, V. Prendki, M. Thellier, G. D. Turner, and O. Mercereau-Puijalon. 2011. The pathogenesis of Plasmodium falciparum malaria in humans: insights from splenic physiology. *Blood* 117: 381-392.
150. Urban, B. C., T. T. Hien, N. P. Day, N. H. Phu, R. Roberts, E. Pongponratn, M. Jones, N. T. Mai, D. Bethell, G. D. Turner, D. Ferguson, N. J. White, and D. J. Roberts. 2005. Fatal Plasmodium falciparum malaria causes specific patterns of splenic architectural disorganization. *Infect Immun* 73: 1986-1994.
151. Mitchell, A. J., A. M. Hansen, L. Hee, H. J. Ball, S. M. Potter, J. C. Walker, and N. H. Hunt. 2005. Early cytokine production is associated with protection from murine cerebral malaria. *Infect Immun* 73: 5645-5653.
152. McNett, M. M., S. Amato, and S. A. Philippbar. 2016. A Comparative Study of Glasgow Coma Scale and Full Outline of Unresponsiveness Scores for Predicting Long-Term Outcome After Brain Injury. *J Neurosci Nurs* 48: 207-214.
153. Engwerda, C., E. Belnoue, A. C. Gruner, and L. Renia. 2005. Experimental models of cerebral malaria. *Curr Top Microbiol Immunol* 297: 103-143.
154. de Souza, J. B., J. C. Hafalla, E. M. Riley, and K. N. Couper. 2010. Cerebral malaria: why experimental murine models are required to understand the pathogenesis of disease. *Parasitology* 137: 755-772.
155. Haldar, K., S. C. Murphy, D. A. Milner, and T. E. Taylor. 2007. Malaria: mechanisms of erythrocytic infection and pathological correlates of severe disease. *Annu Rev Pathol* 2: 217-249.

156. Hoffmann, A., J. Pfeil, J. Alfonso, F. T. Kurz, F. Sahm, S. Heiland, H. Monyer, M. Bendszus, A. K. Mueller, X. Helluy, and M. Pham. 2016. Experimental Cerebral Malaria Spreads along the Rostral Migratory Stream. *PLoS Pathog* 12: e1005470.
157. Chang-Ling, T., A. L. Neill, and N. H. Hunt. 1992. Early microvascular changes in murine cerebral malaria detected in retinal wholemounts. *Am J Pathol* 140: 1121-1130.
158. de Souza, J. B., and E. M. Riley. 2002. Cerebral malaria: the contribution of studies in animal models to our understanding of immunopathogenesis. *Microbes Infect* 4: 291-300.
159. Riley, E. M., K. N. Couper, H. Helmby, J. C. Hafalla, J. B. de Souza, J. Langhorne, W. B. Jarra, and F. Zavala. 2010. Neuropathogenesis of human and murine malaria. *Trends Parasitol* 26: 277-278.
160. Baptista, F. G., A. Pamplona, A. C. Pena, M. M. Mota, S. Pied, and A. M. Vigario. 2010. Accumulation of Plasmodium berghei-infected red blood cells in the brain is crucial for the development of cerebral malaria in mice. *Infect Immun* 78: 4033-4039.
161. Hearn, J., N. Rayment, D. N. Landon, D. R. Katz, and J. B. de Souza. 2000. Immunopathology of cerebral malaria: morphological evidence of parasite sequestration in murine brain microvasculature. *Infect Immun* 68: 5364-5376.
162. Grau, G. E., L. F. Fajardo, P. F. Piguet, B. Allet, P. H. Lambert, and P. Vassalli. 1987. Tumor necrosis factor (cachectin) as an essential mediator in murine cerebral malaria. *Science* 237: 1210-1212.
163. Pais, T. F., and S. Chatterjee. 2005. Brain macrophage activation in murine cerebral malaria precedes accumulation of leukocytes and CD8+ T cell proliferation. *J Neuroimmunol* 163: 73-83.
164. McQuillan, J. A., A. J. Mitchell, Y. F. Ho, V. Combes, H. J. Ball, J. Golenser, G. E. Grau, and N. H. Hunt. 2011. Coincident parasite and CD8 T cell sequestration is required for development of experimental cerebral malaria. *Int J Parasitol* 41: 155-163.
165. Zhu, X., J. Liu, Y. Feng, W. Pang, Z. Qi, Y. Jiang, H. Shang, and Y. Cao. 2015. Phenylhydrazine administration accelerates the development of experimental cerebral malaria. *Exp Parasitol* 156: 1-11.
166. Schmidt, K. E., B. Schumak, S. Specht, B. Dubben, A. Limmer, and A. Hoerauf. 2011. Induction of pro-inflammatory mediators in Plasmodium berghei infected BALB/c mice breaks blood-brain-barrier and leads to cerebral malaria in an IL-12 dependent manner. *Microbes Infect* 13: 828-836.
167. Hafalla, J. C., C. Claser, K. N. Couper, G. E. Grau, L. Renia, J. B. de Souza, and E. M. Riley. 2012. The CTLA-4 and PD-1/PD-L1 inhibitory pathways independently regulate host resistance to Plasmodium-induced acute immune pathology. *PLoS Pathog* 8: e1002504.
168. Amani, V., A. M. Vigario, E. Belnoue, M. Marussig, L. Fonseca, D. Mazier, and L. Renia. 2000. Involvement of IFN-gamma receptor-medicated signaling in pathology and anti-malarial immunity induced by Plasmodium berghei infection. *Eur J Immunol* 30: 1646-1655.
169. Amani, V., M. I. Boubou, S. Pied, M. Marussig, D. Walliker, D. Mazier, and L. Renia. 1998. Cloned lines of Plasmodium berghei ANKA differ in their abilities to induce experimental cerebral malaria. *Infect Immun* 66: 4093-4099.
170. Bagot, S., F. Nogueira, A. Collette, V. do Rosario, F. Lemonier, P. A. Cazenave, and S. Pied. 2004. Comparative study of brain CD8+ T cells induced by

sporozoites and those induced by blood-stage Plasmodium berghei ANKA involved in the development of cerebral malaria. *Infect Immun* 72: 2817-2826.

171. Palomo, J., M. Fauconnier, L. Coquard, M. Gilles, S. Meme, F. Szeremeta, L. Fick, J. F. Franetich, M. Jacobs, D. Togbe, J. C. Beloeil, D. Mazier, B. Ryffel, and V. F. Quesniaux. 2013. Type I interferons contribute to experimental cerebral malaria development in response to sporozoite or blood-stage Plasmodium berghei ANKA. *Eur J Immunol* 43: 2683-2695.
172. deWalick, S., F. H. Amante, K. A. McSweeney, L. M. Randall, A. C. Stanley, A. Haque, R. D. Kuns, K. P. MacDonald, G. R. Hill, and C. R. Engwerda. 2007. Cutting edge: conventional dendritic cells are the critical APC required for the induction of experimental cerebral malaria. *J Immunol* 178: 6033-6037.
173. Piva, L., P. Tetlak, C. Claser, K. Karjalainen, L. Renia, and C. Ruedl. 2012. Cutting edge: Clec9A+ dendritic cells mediate the development of experimental cerebral malaria. *J Immunol* 189: 1128-1132.
174. Amante, F. H., A. Haque, A. C. Stanley, L. Rivera Fde, L. M. Randall, Y. A. Wilson, G. Yeo, C. Pieper, B. S. Crabb, T. F. de Koning-Ward, R. J. Lundie, M. F. Good, A. Pinzon-Charry, M. S. Pearson, M. G. Duke, D. P. McManus, A. Loukas, G. R. Hill, and C. R. Engwerda. 2010. Immune-mediated mechanisms of parasite tissue sequestration during experimental cerebral malaria. *J Immunol* 185: 3632-3642.
175. Lundie, R. J., L. J. Young, G. M. Davey, J. A. Villadangos, F. R. Carbone, W. R. Heath, and B. S. Crabb. 2010. Blood-stage Plasmodium berghei infection leads to short-lived parasite-associated antigen presentation by dendritic cells. *Eur J Immunol* 40: 1674-1681.
176. Tamura, T., K. Kimura, M. Yuda, and K. Yui. 2011. Prevention of experimental cerebral malaria by Flt3 ligand during infection with Plasmodium berghei ANKA. *Infect Immun* 79: 3947-3956.
177. Guermonprez, P., J. Helft, C. Claser, S. Deroubaix, H. Karanje, A. Gazumyan, G. Darasse-Jeze, S. B. Telerman, G. Breton, H. A. Schreiber, N. Frias-Staheli, E. Billerbeck, M. Dorner, C. M. Rice, A. Ploss, F. Klein, M. Swiecki, M. Colonna, A. O. Kamphorst, M. Meredith, R. Niec, C. Takacs, F. Mikhail, A. Hari, D. Bosque, T. Eisenreich, M. Merad, Y. Shi, F. Ginhoux, L. Renia, B. C. Urban, and M. C. Nussenzweig. 2013. Inflammatory Flt3l is essential to mobilize dendritic cells and for T cell responses during Plasmodium infection. *Nat Med* 19: 730-738.
178. Janssen, C. S., R. S. Phillips, C. M. Turner, and M. P. Barrett. 2004. Plasmodium interspersed repeats: the major multigene superfamily of malaria parasites. *Nucleic Acids Res* 32: 5712-5720.
179. Howland, S. W., C. Claser, C. M. Poh, S. Y. Gun, and L. Renia. 2015. Pathogenic CD8+ T cells in experimental cerebral malaria. *Semin Immunopathol* 37: 221-231.
180. De Niz, M., A. K. Ullrich, A. Heiber, A. Blancke Soares, C. Pick, R. Lyck, D. Keller, G. Kaiser, M. Prado, S. Flemming, H. Del Portillo, C. J. Janse, V. Heussler, and T. Spielmann. 2016. The machinery underlying malaria parasite virulence is conserved between rodent and human malaria parasites. *Nat Commun* 7: 11659.
181. Krishnegowda, G., A. M. Hajjar, J. Zhu, E. J. Douglass, S. Uematsu, S. Akira, A. S. Woods, and D. C. Gowda. 2005. Induction of proinflammatory responses in macrophages by the glycosylphosphatidylinositols of Plasmodium falciparum: cell signaling receptors, glycosylphosphatidylinositol (GPI) structural requirement, and regulation of GPI activity. *J Biol Chem* 280: 8606-8616.
182. Coban, C., K. J. Ishii, T. Kawai, H. Hemmi, S. Sato, S. Uematsu, M. Yamamoto, O. Takeuchi, S. Itagaki, N. Kumar, T. Horii, and S. Akira. 2005. Toll-like

receptor 9 mediates innate immune activation by the malaria pigment hemozoin. *J Exp Med* 201: 19-25.

183. Campanella, G. S., A. M. Tager, J. K. El Khoury, S. Y. Thomas, T. A. Abrazinski, L. A. Manice, R. A. Colvin, and A. D. Luster. 2008. Chemokine receptor CXCR3 and its ligands CXCL9 and CXCL10 are required for the development of murine cerebral malaria. *Proc Natl Acad Sci U S A* 105: 4814-4819.
184. Weiser, S., J. Miu, H. J. Ball, and N. H. Hunt. 2007. Interferon-gamma synergises with tumour necrosis factor and lymphotoxin-alpha to enhance the mRNA and protein expression of adhesion molecules in mouse brain endothelial cells. *Cytokine* 37: 84-91.
185. Schumak, B., K. Klocke, J. M. Kuepper, A. Biswas, A. Djie-Maletz, A. Limmer, N. van Rooijen, M. Mack, A. Hoerauf, and I. R. Dunay. 2015. Specific depletion of Ly6C(hi) inflammatory monocytes prevents immunopathology in experimental cerebral malaria. *PLoS One* 10: e0124080.
186. Villegas-Mendez, A., R. Greig, T. N. Shaw, J. B. de Souza, E. Gwyer Findlay, J. S. Stumhofer, J. C. Hafalla, D. G. Blount, C. A. Hunter, E. M. Riley, and K. N. Couper. 2012. IFN-gamma-producing CD4+ T cells promote experimental cerebral malaria by modulating CD8+ T cell accumulation within the brain. *J Immunol* 189: 968-979.
187. Renia, L., S. M. Potter, M. Mauduit, D. S. Rosa, M. Kayibanda, J. C. Deschemin, G. Snounou, and A. C. Gruner. 2006. Pathogenic T cells in cerebral malaria. *Int J Parasitol* 36: 547-554.
188. Couper, K. N., T. Barnes, J. C. Hafalla, V. Combes, B. Ryffel, T. Secher, G. E. Grau, E. M. Riley, and J. B. de Souza. 2010. Parasite-derived plasma microparticles contribute significantly to malaria infection-induced inflammation through potent macrophage stimulation. *PLoS Pathog* 6: e1000744.
189. Wassmer, S. C., V. Combes, and G. E. Grau. 2003. Pathophysiology of cerebral malaria: role of host cells in the modulation of cytoadhesion. *Ann N Y Acad Sci* 992: 30-38.
190. Belnoue, E., M. Kayibanda, A. M. Vigario, J. C. Deschemin, N. van Rooijen, M. Viguier, G. Snounou, and L. Renia. 2002. On the pathogenic role of brain-sequestered alphabeta CD8+ T cells in experimental cerebral malaria. *J Immunol* 169: 6369-6375.
191. van der Heyde, H. C., I. Gramaglia, G. Sun, and C. Woods. 2005. Platelet depletion by anti-CD41 (alphaIIb) mAb injection early but not late in the course of disease protects against Plasmodium berghei pathogenesis by altering the levels of pathogenic cytokines. *Blood* 105: 1956-1963.
192. Chen, L., Z. Zhang, and F. Sendo. 2000. Neutrophils play a critical role in the pathogenesis of experimental cerebral malaria. *Clin Exp Immunol* 120: 125-133.
193. Chen, L., and F. Sendo. 2001. Cytokine and chemokine mRNA expression in neutrophils from CBA/NSlc mice infected with Plasmodium berghei ANKA that induces experimental cerebral malaria. *Parasitol Int* 50: 139-143.
194. Lou, J., R. Lucas, and G. E. Grau. 2001. Pathogenesis of cerebral malaria: recent experimental data and possible applications for humans. *Clin Microbiol Rev* 14: 810-820, table of contents.
195. Lou, J., Y. R. Donati, P. Juillard, C. Giroud, C. Vesin, N. Mili, and G. E. Grau. 1997. Platelets play an important role in TNF-induced microvascular endothelial cell pathology. *Am J Pathol* 151: 1397-1405.
196. Claser, C., B. Malleret, S. Y. Gun, A. Y. Wong, Z. W. Chang, P. Teo, P. C. See, S. W. Howland, F. Ginhoux, and L. Renia. 2011. CD8+ T cells and IFN-gamma

mediate the time-dependent accumulation of infected red blood cells in deep organs during experimental cerebral malaria. *PLoS One* 6: e18720.

197. O'Regan, N., K. Gegenbauer, J. M. O'Sullivan, S. Maleki, T. M. Brophy, N. Dalton, A. Chion, P. G. Fallon, G. E. Grau, U. Budde, O. P. Smith, A. G. Craig, R. J. Preston, and J. S. O'Donnell. 2016. A novel role for von Willebrand factor in the pathogenesis of experimental cerebral malaria. *Blood* 127: 1192-1201.
198. Wassmer, S. C., J. B. de Souza, C. Frere, F. J. Candal, I. Juhan-Vague, and G. E. Grau. 2006. TGF-beta1 released from activated platelets can induce TNF-stimulated human brain endothelium apoptosis: a new mechanism for microvascular lesion during cerebral malaria. *J Immunol* 176: 1180-1184.
199. Sanni, L. A., S. Fu, R. T. Dean, G. Bloomfield, R. Stocker, G. Chaudhri, M. C. Dinauer, and N. H. Hunt. 1999. Are reactive oxygen species involved in the pathogenesis of murine cerebral malaria? *J Infect Dis* 179: 217-222.
200. Potter, S. M., A. J. Mitchell, W. B. Cowden, L. A. Sanni, M. Dinauer, J. B. de Haan, and N. H. Hunt. 2005. Phagocyte-derived reactive oxygen species do not influence the progression of murine blood-stage malaria infections. *Infect Immun* 73: 4941-4947.
201. Favre, N., B. Ryffel, and W. Rudin. 1999. The development of murine cerebral malaria does not require nitric oxide production. *Parasitology* 118 (Pt 2): 135-138.
202. Piguet, P. F., C. D. Kan, C. Vesin, A. Rochat, Y. Donati, and C. Barazzone. 2001. Role of CD40-CVD40L in mouse severe malaria. *Am J Pathol* 159: 733-742.
203. Grau, G. E., H. Heremans, P. F. Piguet, P. Pointaire, P. H. Lambert, A. Billiau, and P. Vassalli. 1989. Monoclonal antibody against interferon gamma can prevent experimental cerebral malaria and its associated overproduction of tumor necrosis factor. *Proc Natl Acad Sci U S A* 86: 5572-5574.
204. Rudin, W., N. Favre, G. Bordmann, and B. Ryffel. 1997. Interferon-gamma is essential for the development of cerebral malaria. *Eur J Immunol* 27: 810-815.
205. Randall, L. M., F. H. Amante, Y. Zhou, A. C. Stanley, A. Haque, F. Rivera, K. Pfeffer, S. Scheu, G. R. Hill, K. Tamada, and C. R. Engwerda. 2008. Cutting edge: selective blockade of LIGHT-lymphotoxin beta receptor signaling protects mice from experimental cerebral malaria caused by Plasmodium berghei ANKA. *J Immunol* 181: 7458-7462.
206. Fauconnier, M., J. Palomo, M. L. Bourigault, S. Meme, F. Szeremeta, J. C. Beloeil, A. Danneels, S. Charron, P. Rihet, B. Ryffel, and V. F. Quesniaux. 2012. IL-12Rbeta2 is essential for the development of experimental cerebral malaria. *J Immunol* 188: 1905-1914.
207. Kossodo, S., C. Monso, P. Juillard, T. Velu, M. Goldman, and G. E. Grau. 1997. Interleukin-10 modulates susceptibility in experimental cerebral malaria. *Immunology* 91: 536-540.
208. Wu, J. J., G. Chen, J. Liu, T. Wang, W. Zheng, and Y. M. Cao. 2010. Natural regulatory T cells mediate the development of cerebral malaria by modifying the pro-inflammatory response. *Parasitol Int* 59: 232-241.
209. Howland, S. W., C. M. Poh, S. Y. Gun, C. Claser, B. Malleret, N. Shastri, F. Ginhoux, G. M. Grotenbreg, and L. Renia. 2013. Brain microvessel cross-presentation is a hallmark of experimental cerebral malaria. *EMBO Mol Med* 5: 916-931.
210. Poh, C. M., S. W. Howland, G. M. Grotenbreg, and L. Renia. 2014. Damage to the blood-brain barrier during experimental cerebral malaria results from synergistic effects of CD8+ T cells with different specificities. *Infect Immun* 82: 4854-4864.

211. Belnoue, E., M. Kayibanda, J. C. Deschemin, M. Viguier, M. Mack, W. A. Kuziel, and L. Renia. 2003. CCR5 deficiency decreases susceptibility to experimental cerebral malaria. *Blood* 101: 4253-4259.
212. Van den Steen, P. E., K. Deroost, I. Van Aelst, N. Geurts, E. Martens, S. Struyf, C. Q. Nie, D. S. Hansen, P. Matthys, J. Van Damme, and G. Opdenakker. 2008. CXCR3 determines strain susceptibility to murine cerebral malaria by mediating T lymphocyte migration toward IFN-gamma-induced chemokines. *Eur J Immunol* 38: 1082-1095.
213. Hansen, D. S., N. J. Bernard, C. Q. Nie, and L. Schofield. 2007. NK cells stimulate recruitment of CXCR3+ T cells to the brain during Plasmodium berghei-mediated cerebral malaria. *J Immunol* 178: 5779-5788.
214. Mai, J., A. Virtue, J. Shen, H. Wang, and X. F. Yang. 2013. An evolving new paradigm: endothelial cells--conditional innate immune cells. *J Hematol Oncol* 6: 61.
215. Howland, S. W., C. M. Poh, and L. Renia. 2015. Activated Brain Endothelial Cells Cross-Present Malaria Antigen. *PLoS Pathog* 11: e1004963.
216. Shaw, T. N., P. J. Stewart-Hutchinson, P. Strangward, D. B. Dandamudi, J. A. Coles, A. Villegas-Mendez, J. Gallego-Delgado, N. van Rooijen, E. Zindy, A. Rodriguez, J. M. Brewer, K. N. Couper, and M. L. Dustin. 2015. Perivascular Arrest of CD8+ T Cells Is a Signature of Experimental Cerebral Malaria. *PLoS Pathog* 11: e1005210.
217. Grau, G. E., P. Pointaire, P. F. Piguet, C. Vesin, H. Rosen, I. Stamenkovic, F. Takei, and P. Vassalli. 1991. Late administration of monoclonal antibody to leukocyte function-antigen 1 abrogates incipient murine cerebral malaria. *Eur J Immunol* 21: 2265-2267.
218. Haque, A., S. E. Best, K. Unosson, F. H. Amante, F. de Labastida, N. M. Anstey, G. Karupiah, M. J. Smyth, W. R. Heath, and C. R. Engwerda. 2011. Granzyme B expression by CD8+ T cells is required for the development of experimental cerebral malaria. *J Immunol* 186: 6148-6156.
219. Nitcheu, J., O. Bonduelle, C. Combadiere, M. Tefit, D. Seilhean, D. Mazier, and B. Combadiere. 2003. Perforin-dependent brain-infiltrating cytotoxic CD8+ T lymphocytes mediate experimental cerebral malaria pathogenesis. *J Immunol* 170: 2221-2228.
220. Taylor, S. M., C. Cerami, and R. M. Fairhurst. 2013. Hemoglobinopathies: slicing the Gordian knot of Plasmodium falciparum malaria pathogenesis. *PLoS Pathog* 9: e1003327.
221. Bauduer, F. 2012. Red cell polymorphisms and malaria : an evolutionary approach. In *Société d'Anthropologie de Paris*. Springer, Paris. 55-64.
222. Krause, M. A., S. A. Diakite, T. M. Lopera-Mesa, C. Amaratunga, T. Arie, K. Traore, S. Doumbia, D. Konate, J. R. Keefer, M. Diakite, and R. M. Fairhurst. 2012. alpha-Thalassemia impairs the cytoadherence of Plasmodium falciparum-infected erythrocytes. *PLoS One* 7: e37214.
223. Roberts, D. J., and T. N. Williams. 2003. Haemoglobinopathies and resistance to malaria. *Redox Rep* 8: 304-310.
224. Rowe, J. A., I. G. Handel, M. A. Thera, A. M. Deans, K. E. Lyke, A. Kone, D. A. Diallo, A. Raza, O. Kai, K. Marsh, C. V. Plowe, O. K. Doumbo, and J. M. Moulds. 2007. Blood group O protects against severe Plasmodium falciparum malaria through the mechanism of reduced rosetting. *Proc Natl Acad Sci U S A* 104: 17471-17476.
225. Luzzatto, L., F. A. Usanga, and S. Reddy. 1969. Glucose-6-phosphate dehydrogenase deficient red cells: resistance to infection by malarial parasites. *Science* 164: 839-842.

226. Ouma, C., G. C. Davenport, T. Were, M. F. Otieno, J. B. Hittner, J. M. Vulule, J. Martinson, J. M. Ong'echa, R. E. Ferrell, and D. J. Perkins. 2008. Haplotypes of IL-10 promoter variants are associated with susceptibility to severe malarial anemia and functional changes in IL-10 production. *Hum Genet* 124: 515-524.
227. Hansson, H. H., L. Turner, L. Moller, C. W. Wang, D. T. Minja, S. Gesase, B. Mmbando, I. C. Bygbjerg, T. G. Theander, J. P. Lusingu, M. Alifrangis, and T. Lavstsen. 2015. Haplotypes of the endothelial protein C receptor (EPCR) gene are not associated with severe malaria in Tanzania. *Malar J* 14: 474.
228. Luoni, D. P. K. a. G. 2005. Host Genetic Factors in Resistance and Susceptibility to Malaria. In *Molecular Approaches to Malaria*, 2005 ed. I. W. Sherman, ed. ASM Press, Washington, D.C. 462-475.
229. Marsh, K., L. Otoo, R. J. Hayes, D. C. Carson, and B. M. Greenwood. 1989. Antibodies to blood stage antigens of Plasmodium falciparum in rural Gambians and their relation to protection against infection. *Trans R Soc Trop Med Hyg* 83: 293-303.
230. Carlson, J., H. Helmby, A. V. Hill, D. Brewster, B. M. Greenwood, and M. Wahlgren. 1990. Human cerebral malaria: association with erythrocyte rosetting and lack of anti-rosetting antibodies. *Lancet* 336: 1457-1460.
231. Barragan, A., P. G. Kremsner, W. Weiss, M. Wahlgren, and J. Carlson. 1998. Age-related buildup of humoral immunity against epitopes for rosette formation and agglutination in African areas of malaria endemicity. *Infect Immun* 66: 4783-4787.
232. Joos, C., L. Marrama, H. E. Polson, S. Corre, A. M. Diatta, B. Diouf, J. F. Trape, A. Tall, S. Longacre, and R. Perraut. 2010. Clinical protection from falciparum malaria correlates with neutrophil respiratory bursts induced by merozoites opsonized with human serum antibodies. *PLoS One* 5: e9871.
233. Bull, P. C., B. S. Lowe, M. Kortok, C. S. Molyneux, C. I. Newbold, and K. Marsh. 1998. Parasite antigens on the infected red cell surface are targets for naturally acquired immunity to malaria. *Nat Med* 4: 358-360.
234. Casals-Pascual, C., R. Idro, N. Gicheru, S. Gwer, B. Kitsao, E. Gitau, R. Mwakesi, D. J. Roberts, and C. R. Newton. 2008. High levels of erythropoietin are associated with protection against neurological sequelae in African children with cerebral malaria. *Proc Natl Acad Sci U S A* 105: 2634-2639.
235. Casals-Pascual, C., R. Idro, S. Picot, D. J. Roberts, and C. R. Newton. 2009. Can erythropoietin be used to prevent brain damage in cerebral malaria? *Trends Parasitol* 25: 30-36.
236. Shabani, E., R. O. Opoka, R. Idro, R. Schmidt, G. S. Park, P. Bangirana, G. M. Vercellotti, J. S. Hodges, J. A. Widness, and C. C. John. 2015. High plasma erythropoietin levels are associated with prolonged coma duration and increased mortality in children with cerebral malaria. *Clin Infect Dis* 60: 27-35.
237. Kester, K. E., J. F. Cummings, O. Ofori-Anyinam, C. F. Ockenhouse, U. Krzych, P. Moris, R. Schwenk, R. A. Nielsen, Z. Debebe, E. Pinelis, L. Juompan, J. Williams, M. Dowler, V. A. Stewart, R. A. Wirtz, M. C. Dubois, M. Lievens, J. Cohen, W. R. Ballou, and D. G. Heppner, Jr. 2009. Randomized, double-blind, phase 2a trial of falciparum malaria vaccines RTS,S/AS01B and RTS,S/AS02A in malaria-naive adults: safety, efficacy, and immunologic associates of protection. *J Infect Dis* 200: 337-346.
238. Moorthy, V. S., and W. R. Ballou. 2009. Immunological mechanisms underlying protection mediated by RTS,S: a review of the available data. *Malar J* 8: 312.
239. Bejon, P., L. Andrews, R. F. Andersen, S. Dunachie, D. Webster, M. Walther, S. C. Gilbert, T. Peto, and A. V. Hill. 2005. Calculation of liver-to-blood inocula,

parasite growth rates, and preerythrocytic vaccine efficacy, from serial quantitative polymerase chain reaction studies of volunteers challenged with malaria sporozoites. *J Infect Dis* 191: 619-626.

240. Guinovart, C., J. J. Aponte, J. Sacarlal, P. Aide, A. Leach, Q. Bassat, E. Macete, C. Dobano, M. Lievens, C. Loucq, W. R. Ballou, J. Cohen, and P. L. Alonso. 2009. Insights into long-lasting protection induced by RTS,S/AS02A malaria vaccine: further results from a phase IIb trial in Mozambican children. *PLoS One* 4: e5165.
241. Schellenberg, D., C. Menendez, E. Kahigwa, J. Aponte, J. Vidal, M. Tanner, H. Mshinda, and P. Alonso. 2001. Intermittent treatment for malaria and anaemia control at time of routine vaccinations in Tanzanian infants: a randomised, placebo-controlled trial. *Lancet* 357: 1471-1477.
242. Sutherland, C. J., C. J. Drakeley, and D. Schellenberg. 2007. How is childhood development of immunity to Plasmodium falciparum enhanced by certain antimalarial interventions? *Malar J* 6: 161.
243. Yanez, D. M., D. D. Manning, A. J. Cooley, W. P. Weidanz, and H. C. van der Heyde. 1996. Participation of lymphocyte subpopulations in the pathogenesis of experimental murine cerebral malaria. *J Immunol* 157: 1620-1624.
244. Baccarella, A., B. W. Huang, M. F. Fontana, and C. C. Kim. 2014. Loss of Toll-like receptor 7 alters cytokine production and protects against experimental cerebral malaria. *Malar J* 13: 354.
245. Zhu, X., Y. Pan, Y. Li, Y. Jiang, H. Shang, D. C. Gowda, L. Cui, and Y. Cao. 2012. Targeting Toll-like receptors by chloroquine protects mice from experimental cerebral malaria. *Int Immunopharmacol* 13: 392-397.
246. Besnard, A. G., R. Guabiraba, W. Niedbala, J. Palomo, F. Reverchon, T. N. Shaw, K. N. Couper, B. Ryffel, and F. Y. Liew. 2015. IL-33-mediated protection against experimental cerebral malaria is linked to induction of type 2 innate lymphoid cells, M2 macrophages and regulatory T cells. *PLoS Pathog* 11: e1004607.
247. Hempel, C., V. Combes, N. H. Hunt, J. A. Kurtzhals, and G. E. Grau. 2011. CNS hypoxia is more pronounced in murine cerebral than noncerebral malaria and is reversed by erythropoietin. *Am J Pathol* 179: 1939-1950.
248. Wei, X., Y. Li, X. Sun, X. Zhu, Y. Feng, J. Liu, Y. Jiang, H. Shang, L. Cui, and Y. Cao. 2014. Erythropoietin protects against murine cerebral malaria through actions on host cellular immunity. *Infect Immun* 82: 165-173.
249. Van Den Ham, K. M., M. T. Shio, A. Rainone, S. Fournier, C. M. Krawczyk, and M. Olivier. 2015. Iron prevents the development of experimental cerebral malaria by attenuating CXCR3-mediated T cell chemotaxis. *PLoS One* 10: e0118451.
250. Val, C. H., F. Brant, A. S. Miranda, F. G. Rodrigues, B. C. Oliveira, E. A. Santos, D. R. Assis, L. Esper, B. C. Silva, M. A. Rachid, H. B. Tanowitz, A. L. Teixeira, M. M. Teixeira, W. C. Regis, and F. S. Machado. 2015. Effect of mushroom Agaricus blazei on immune response and development of experimental cerebral malaria. *Malar J* 14: 311.
251. Grau, G. E., D. Gretener, and P. H. Lambert. 1987. Prevention of murine cerebral malaria by low-dose cyclosporin A. *Immunology* 61: 521-525.
252. de Souza, J. B., U. Okomo, N. D. Alexander, N. Aziz, B. M. Owens, H. Kaur, M. Jasseh, S. Muangnoicharoen, P. F. Sumariwalla, D. C. Warhurst, S. A. Ward, D. J. Conway, L. Ulloa, K. J. Tracey, B. M. Foxwell, P. M. Kaye, and M. Walther. 2010. Oral activated charcoal prevents experimental cerebral malaria in mice and in a randomized controlled clinical trial in man did not interfere with the pharmacokinetics of parenteral artesunate. *PLoS One* 5: e9867.
253. Haque, A., S. E. Best, F. H. Amante, S. Mustafah, L. Desbarrieres, F. de Labastida, T. Sparwasser, G. R. Hill, and C. R. Engwerda. 2010. CD4+ natural

regulatory T cells prevent experimental cerebral malaria via CTLA-4 when expanded in vivo. *PLoS Pathog* 6: e1001221.

254. Amante, F. H., A. C. Stanley, L. M. Randall, Y. Zhou, A. Haque, K. McSweeney, A. P. Waters, C. J. Janse, M. F. Good, G. R. Hill, and C. R. Engwerda. 2007. A role for natural regulatory T cells in the pathogenesis of experimental cerebral malaria. *Am J Pathol* 171: 548-559.
255. Nie, C. Q., N. J. Bernard, L. Schofield, and D. S. Hansen. 2007. CD4+ CD25+ regulatory T cells suppress CD4+ T-cell function and inhibit the development of Plasmodium berghei-specific TH1 responses involved in cerebral malaria pathogenesis. *Infect Immun* 75: 2275-2282.
256. Shan, Y., J. Liu, Y. Y. Pan, Y. J. Jiang, H. Shang, and Y. M. Cao. 2013. Age-related CD4(+)CD25(+)Foxp3(+) regulatory T-cell responses during Plasmodium berghei ANKA infection in mice susceptible or resistant to cerebral malaria. *Korean J Parasitol* 51: 289-295.
257. Liu, Y., Y. Chen, Z. Li, Y. Han, Y. Sun, Q. Wang, B. Liu, and Z. Su. 2013. Role of IL-10-producing regulatory B cells in control of cerebral malaria in Plasmodium berghei infected mice. *Eur J Immunol* 43: 2907-2918.
258. Niikura, M., S. Kamiya, A. Nakane, K. Kita, and F. Kobayashi. 2010. IL-10 plays a crucial role for the protection of experimental cerebral malaria by co-infection with non-lethal malaria parasites. *Int J Parasitol* 40: 101-108.
259. Specht, S., D. F. Ruiz, B. Dubben, S. Deininger, and A. Hoerauf. 2010. Filaria-induced IL-10 suppresses murine cerebral malaria. *Microbes Infect* 12: 635-642.
260. Wang, M. L., Y. H. Feng, W. Pang, Z. M. Qi, Y. Zhang, Y. J. Guo, E. J. Luo, and Y. M. Cao. 2014. Parasite densities modulate susceptibility of mice to cerebral malaria during co-infection with Schistosoma japonicum and Plasmodium berghei. *Malar J* 13: 116.
261. Settles, E. W., L. A. Moser, T. H. Harris, and L. J. Knoll. 2014. Toxoplasma gondii upregulates interleukin-12 to prevent Plasmodium berghei-induced experimental cerebral malaria. *Infect Immun* 82: 1343-1353.
262. Haussig, J. M., K. Matuschewski, and T. W. Kooij. 2011. Inactivation of a Plasmodium apicoplast protein attenuates formation of liver merozoites. *Mol Microbiol* 81: 1511-1525.
263. Lewis, M. D., J. Behrends, E. C. C. Sa, A. M. Mendes, F. Lasitschka, J. M. Sattler, K. Heiss, T. W. Kooij, M. Prudencio, G. Bringmann, F. Frischknecht, and A. K. Mueller. 2015. Chemical attenuation of Plasmodium in the liver modulates severe malaria disease progression. *J Immunol* 194: 4860-4870.
264. Spaccapelo, R., C. J. Janse, S. Caterbi, B. Franke-Fayard, J. A. Bonilla, L. M. Syphard, M. Di Cristina, T. Dottorini, A. Savarino, A. Cassone, F. Bistoni, A. P. Waters, J. B. Dame, and A. Crisanti. 2010. Plasmepsin 4-deficient Plasmodium berghei are virulence attenuated and induce protective immunity against experimental malaria. *Am J Pathol* 176: 205-217.
265. Perlmann, P., and M. Troye-Blomberg. 2000. Malaria blood-stage infection and its control by the immune system. *Folia Biol (Praha)* 46: 210-218.
266. Bijker, E. M., G. J. Bastiaens, A. C. Teirlinck, G. J. van Gemert, W. Graumans, M. van de Vegte-Bolmer, R. Siebelink-Stoter, T. Arens, K. Teelen, W. Nahrendorf, E. J. Remarque, W. Roeffen, A. Jansens, D. Zimmerman, M. Vos, B. C. van Schaijk, J. Wiersma, A. J. van der Ven, Q. de Mast, L. van Lieshout, J. J. Verweij, C. C. Hermsen, A. Scholzen, and R. W. Sauerwein. 2013. Protection against malaria after immunization by chloroquine prophylaxis and sporozoites is mediated by preerythrocytic immunity. *Proc Natl Acad Sci U S A* 110: 7862-7867.

267. Behet, M. C., L. Foquet, G. J. van Gemert, E. M. Bijker, P. Meuleman, G. Leroux-Roels, C. C. Hermsen, A. Scholzen, and R. W. Sauerwein. 2014. Sporozoite immunization of human volunteers under chemoprophylaxis induces functional antibodies against pre-erythrocytic stages of Plasmodium falciparum. *Malar J* 13: 136.
268. Sahu, T., L. Lambert, J. Herrod, S. Conteh, S. Orr-Gonzalez, D. Carter, and P. E. Duffy. 2015. Chloroquine neither eliminates liver stage parasites nor delays their development in a murine Chemoprophylaxis Vaccination model. *Front Microbiol* 6: 283.
269. Snow, R. W., J. A. Omumbo, B. Lowe, C. S. Molyneux, J. O. Obiero, A. Palmer, M. W. Weber, M. Pinder, B. Nahlen, C. Obonyo, C. Newbold, S. Gupta, and K. Marsh. 1997. Relation between severe malaria morbidity in children and level of Plasmodium falciparum transmission in Africa. *Lancet* 349: 1650-1654.
270. Nahrendorf, W., A. Scholzen, R. W. Sauerwein, and J. Langhorne. 2015. Cross-stage immunity for malaria vaccine development. *Vaccine* 33: 7513-7517.
271. Pesce, E. R., P. Acharya, U. Tatu, W. S. Nicoll, A. Shonhai, H. C. Hoppe, and G. L. Blatch. 2008. The Plasmodium falciparum heat shock protein 40, Pfj4, associates with heat shock protein 70 and shows similar heat induction and localisation patterns. *Int J Biochem Cell Biol* 40: 2914-2926.
272. Hall, N., M. Karras, J. D. Raine, J. M. Carlton, T. W. Kooij, M. Berriman, L. Florens, C. S. Janssen, A. Pain, G. K. Christophides, K. James, K. Rutherford, B. Harris, D. Harris, C. Churcher, M. A. Quail, D. Ormond, J. Doggett, H. E. Trueman, J. Mendoza, S. L. Bidwell, M. A. Rajandream, D. J. Carucci, J. R. Yates, 3rd, F. C. Kafatos, C. J. Janse, B. Barrell, C. M. Turner, A. P. Waters, and R. E. Sinden. 2005. A comprehensive survey of the Plasmodium life cycle by genomic, transcriptomic, and proteomic analyses. *Science* 307: 82-86.
273. Nakabayashi, H., K. Taketa, K. Miyano, T. Yamane, and J. Sato. 1982. Growth of human hepatoma cells lines with differentiated functions in chemically defined medium. *Cancer Res* 42: 3858-3863.
274. Kooij, T. W., M. M. Rauch, and K. Matuschewski. 2012. Expansion of experimental genetics approaches for Plasmodium berghei with versatile transfection vectors. *Mol Biochem Parasitol* 185: 19-26.
275. Silvie, O., K. Goetz, and K. Matuschewski. 2008. A sporozoite asparagine-rich protein controls initiation of Plasmodium liver stage development. *PLoS Pathog* 4: e1000086.
276. Hulier, E., P. Petour, G. Snounou, M. P. Nivez, F. Miltgen, D. Mazier, and L. Renia. 1996. A method for the quantitative assessment of malaria parasite development in organs of the mammalian host. *Mol Biochem Parasitol* 77: 127-135.
277. Janse, C. J., J. Ramesar, and A. P. Waters. 2006. High-efficiency transfection and drug selection of genetically transformed blood stages of the rodent malaria parasite Plasmodium berghei. *Nat Protoc* 1: 346-356.
278. Carroll, R. W., M. S. Wainwright, K. Y. Kim, T. Kidambi, N. D. Gomez, T. Taylor, and K. Haldar. 2010. A rapid murine coma and behavior scale for quantitative assessment of murine cerebral malaria. *PLoS One* 5.
279. van der Heyde, H. C., P. Bauer, G. Sun, W. L. Chang, L. Yin, J. Fuseler, and D. N. Granger. 2001. Assessing vascular permeability during experimental cerebral malaria by a radiolabeled monoclonal antibody technique. *Infect Immun* 69: 3460-3465.
280. Frank, R. 2014. PhD Thesis.

281. Nussenzweig, R. S., J. Vanderberg, H. Most, and C. Orton. 1967. Protective immunity produced by the injection of x-irradiated sporozoites of plasmodium berghei. *Nature* 216: 160-162.
282. Hoffman, S. L., L. M. Goh, T. C. Luke, I. Schneider, T. P. Le, D. L. Doolan, J. Sacci, P. de la Vega, M. Dowler, C. Paul, D. M. Gordon, J. A. Stoute, L. W. Church, M. Sedegah, D. G. Heppner, W. R. Ballou, and T. L. Richie. 2002. Protection of humans against malaria by immunization with radiation-attenuated Plasmodium falciparum sporozoites. *J Infect Dis* 185: 1155-1164.
283. Dahl, E. L., and P. J. Rosenthal. 2007. Multiple antibiotics exert delayed effects against the Plasmodium falciparum apicoplast. *Antimicrob Agents Chemother* 51: 3485-3490.
284. Friesen, J., O. Silvie, E. D. Putrianti, J. C. Hafalla, K. Matuschewski, and S. Borrmann. 2010. Natural immunization against malaria: causal prophylaxis with antibiotics. *Sci Transl Med* 2: 40ra49.
285. El-Assaad, F., C. Hempel, V. Combes, A. J. Mitchell, H. J. Ball, J. A. Kurtzhals, N. H. Hunt, J. M. Mathys, and G. E. Grau. 2011. Differential microRNA expression in experimental cerebral and noncerebral malaria. *Infect Immun* 79: 2379-2384.
286. Zhao, H., T. Aoshi, S. Kawai, Y. Mori, A. Konishi, M. Ozkan, Y. Fujita, Y. Haseda, M. Shimizu, M. Kohyama, K. Kobiyama, K. Eto, J. Nabekura, T. Horii, T. Ishino, M. Yuda, H. Hemmi, T. Kaisho, S. Akira, M. Kinoshita, K. Tohyama, Y. Yoshioka, K. J. Ishii, and C. Coban. 2014. Olfactory plays a key role in spatiotemporal pathogenesis of cerebral malaria. *Cell Host Microbe* 15: 551-563.
287. Long, C. A., and F. Zavala. 2016. Malaria vaccines and human immune responses. *Curr Opin Microbiol* 32: 96-102.
288. Gangwar, D., M. K. Kalita, D. Gupta, V. S. Chauhan, and A. Mohmmed. 2009. A systematic classification of Plasmodium falciparum P-loop NTPases: structural and functional correlation. *Malar J* 8: 69.
289. Cunningham, D., J. Lawton, W. Jarra, P. Preiser, and J. Langhorne. 2010. The pir multigene family of Plasmodium: antigenic variation and beyond. *Mol Biochem Parasitol* 170: 65-73.
290. Wang, C. W., S. B. Mwakalinga, C. J. Sutherland, S. Schwank, S. Sharp, C. C. Hermsen, R. W. Sauerwein, T. G. Theander, and T. Lavstsen. 2010. Identification of a major rif transcript common to gametocytes and sporozoites of Plasmodium falciparum. *Malar J* 9: 147.
291. Florens, L., M. P. Washburn, J. D. Raine, R. M. Anthony, M. Grainger, J. D. Haynes, J. K. Moch, N. Muster, J. B. Sacci, D. L. Tabb, A. A. Witney, D. Wolters, Y. Wu, M. J. Gardner, A. A. Holder, R. E. Sinden, J. R. Yates, and D. J. Carucci. 2002. A proteomic view of the Plasmodium falciparum life cycle. *Nature* 419: 520-526.
292. Fonager, J., D. Cunningham, W. Jarra, S. Koernig, A. A. Henneman, J. Langhorne, and P. Preiser. 2007. Transcription and alternative splicing in the yir multigene family of the malaria parasite Plasmodium y. yoelii: identification of motifs suggesting epigenetic and post-transcriptional control of RNA expression. *Mol Biochem Parasitol* 156: 1-11.
293. Pham, J. S., R. Sakaguchi, L. M. Yeoh, N. S. De Silva, G. I. McFadden, Y. M. Hou, and S. A. Ralph. 2014. A dual-targeted aminoacyl-tRNA synthetase in Plasmodium falciparum charges cytosolic and apicoplast tRNACys. *Biochem J* 458: 513-523.
294. Struck, N. S., S. Herrmann, C. Langer, A. Krueger, B. J. Foth, K. Engelberg, A. L. Cabrera, S. Haase, M. Treeck, M. Marti, A. F. Cowman, T. Spielmann, and T. W.

Gilberger. 2008. Plasmodium falciparum possesses two GRASP proteins that are differentially targeted to the Golgi complex via a higher- and lower-eukaryote-like mechanism. *J Cell Sci* 121: 2123-2129.

295. Muhia, D. K., C. A. Swales, U. Eckstein-Ludwig, S. Saran, S. D. Polley, J. M. Kelly, P. Schaap, S. Krishna, and D. A. Baker. 2003. Multiple splice variants encode a novel adenylyl cyclase of possible plastid origin expressed in the sexual stage of the malaria parasite Plasmodium falciparum. *J Biol Chem* 278: 22014-22022.
296. Saenz, F. E., B. Balu, J. Smith, S. R. Mendonca, and J. H. Adams. 2008. The transmembrane isoform of Plasmodium falciparum MAEBL is essential for the invasion of Anopheles salivary glands. *PLoS One* 3: e2287.
297. Ghai, M., S. Dutta, T. Hall, D. Freilich, and C. F. Ockenhouse. 2002. Identification, expression, and functional characterization of MAEBL, a sporozoite and asexual blood stage chimeric erythrocyte-binding protein of Plasmodium falciparum. *Mol Biochem Parasitol* 123: 35-45.
298. Ghosh, A. K., M. Devenport, D. Jethwaney, D. E. Kalume, A. Pandey, V. E. Anderson, A. A. Sultan, N. Kumar, and M. Jacobs-Lorena. 2009. Malaria parasite invasion of the mosquito salivary gland requires interaction between the Plasmodium TRAP and the Anopheles saglin proteins. *PLoS Pathog* 5: e1000265.
299. Mikolajczak, S. A., H. Silva-Rivera, X. Peng, A. S. Tarun, N. Camargo, V. Jacobs-Lorena, T. M. Daly, L. W. Bergman, P. de la Vega, J. Williams, A. S. Aly, and S. H. Kappe. 2008. Distinct malaria parasite sporozoites reveal transcriptional changes that cause differential tissue infection competence in the mosquito vector and mammalian host. *Mol Cell Biol* 28: 6196-6207.
300. Sultan, A. A., V. Thathy, U. Frevert, K. J. Robson, A. Crisanti, V. Nussenzweig, R. S. Nussenzweig, and R. Menard. 1997. TRAP is necessary for gliding motility and infectivity of plasmodium sporozoites. *Cell* 90: 511-522.
301. Myung, J. M., P. Marshall, and P. Sinnis. 2004. The Plasmodium circumsporozoite protein is involved in mosquito salivary gland invasion by sporozoites. *Mol Biochem Parasitol* 133: 53-59.
302. Kappe, S., T. Bruderer, S. Gantt, H. Fujioka, V. Nussenzweig, and R. Menard. 1999. Conservation of a gliding motility and cell invasion machinery in Apicomplexan parasites. *J Cell Biol* 147: 937-944.
303. Baum, J., D. Richard, J. Healer, M. Rug, Z. Krnajski, T. W. Gilberger, J. L. Green, A. A. Holder, and A. F. Cowman. 2006. A conserved molecular motor drives cell invasion and gliding motility across malaria life cycle stages and other apicomplexan parasites. *J Biol Chem* 281: 5197-5208.
304. Harupa, A., B. K. Sack, V. Lakshmanan, N. Arang, A. N. Douglass, B. G. Oliver, A. B. Stuart, D. N. Sather, S. E. Lindner, K. Hybiske, M. Torii, and S. H. Kappe. 2014. SSP3 is a novel Plasmodium yoelii sporozoite surface protein with a role in gliding motility. *Infect Immun* 82: 4643-4653.
305. Bane, K. S., S. Lepper, J. Kehrer, J. M. Sattler, M. Singer, M. Reinig, D. Klug, K. Heiss, J. Baum, A. K. Mueller, and F. Frischknecht. 2016. The Actin Filament-Binding Protein Coronin Regulates Motility in Plasmodium Sporozoites. *PLoS Pathog* 12: e1005710.
306. Siau, A., O. Silvie, J. F. Franetich, S. Yalaoui, C. Marinach, L. Hannoun, G. J. van Gemert, A. J. Luty, E. Bischoff, P. H. David, G. Snounou, C. Vaquero, P. Froissard, and D. Mazier. 2008. Temperature shift and host cell contact up-regulate sporozoite expression of Plasmodium falciparum genes involved in hepatocyte infection. *PLoS Pathog* 4: e1000121.

307. Fleige, T., J. Limenitakis, and D. Soldati-Favre. 2010. Apicoplast: keep it or leave it. *Microbes Infect* 12: 253-262.
308. Lim, L., and G. I. McFadden. 2010. The evolution, metabolism and functions of the apicoplast. *Philos Trans R Soc Lond B Biol Sci* 365: 749-763.
309. Waller, R. F., and G. I. McFadden. 2005. The apicoplast: a review of the derived plastid of apicomplexan parasites. *Curr Issues Mol Biol* 7: 57-79.
310. Shears, M. J., C. Y. Botte, and G. I. McFadden. 2015. Fatty acid metabolism in the Plasmodium apicoplast: Drugs, doubts and knockouts. *Mol Biochem Parasitol* 199: 34-50.
311. Stanway, R. R., T. Witt, B. Zobiak, M. Aepfelbacher, and V. T. Heussler. 2009. GFP-targeting allows visualization of the apicoplast throughout the life cycle of live malaria parasites. *Biol Cell* 101: 415-430, 415 p following 430.
312. van Dooren, G. G., M. Marti, C. J. Tonkin, L. M. Stimmler, A. F. Cowman, and G. I. McFadden. 2005. Development of the endoplasmic reticulum, mitochondrion and apicoplast during the asexual life cycle of Plasmodium falciparum. *Mol Microbiol* 57: 405-419.
313. He, C. Y., M. K. Shaw, C. H. Pletcher, B. Striepen, L. G. Tilney, and D. S. Roos. 2001. A plastid segregation defect in the protozoan parasite Toxoplasma gondii. *Embo J* 20: 330-339.
314. Radtke, A. J., W. Kastenmuller, D. A. Espinosa, M. Y. Gerner, S. W. Tse, P. Sinnis, R. N. Germain, F. P. Zavala, and I. A. Cockburn. 2015. Lymph-node resident CD8alpha+ dendritic cells capture antigens from migratory malaria sporozoites and induce CD8+ T cell responses. *PLoS Pathog* 11: e1004637.
315. Miller, J. L., B. K. Sack, M. Baldwin, A. M. Vaughan, and S. H. Kappe. 2014. Interferon-mediated innate immune responses against malaria parasite liver stages. *Cell Rep* 7: 436-447.
316. Gerald, N. J., V. Majam, B. Mahajan, Y. Kozakai, and S. Kumar. 2011. Protection from experimental cerebral malaria with a single dose of radiation-attenuated, blood-stage Plasmodium berghei parasites. *PLoS One* 6: e24398.
317. Gazzinelli, R. T., P. Kalantari, K. A. Fitzgerald, and D. T. Golenbock. 2014. Innate sensing of malaria parasites. *Nat Rev Immunol* 14: 744-757.
318. Agrawal, S., D. W. Chung, N. Ponts, G. G. van Dooren, J. Prudhomme, C. F. Brooks, E. M. Rodrigues, J. C. Tan, M. T. Ferdig, B. Striepen, and K. G. Le Roch. 2013. An apicoplast localized ubiquitylation system is required for the import of nuclear-encoded plastid proteins. *PLoS Pathog* 9: e1003426.
319. Zuegge, J., S. Ralph, M. Schmuker, G. I. McFadden, and G. Schneider. 2001. Deciphering apicoplast targeting signals--feature extraction from nuclear-encoded precursors of Plasmodium falciparum apicoplast proteins. *Gene* 280: 19-26.
320. Schofield, L. 2007. Intravascular infiltrates and organ-specific inflammation in malaria pathogenesis. *Immunol Cell Biol* 85: 130-137.
321. Kapsenberg, M. L. 2003. Dendritic-cell control of pathogen-driven T-cell polarization. *Nat Rev Immunol* 3: 984-993.
322. Redmond, W. L., B. C. Marincek, and L. A. Sherman. 2005. Distinct requirements for deletion versus anergy during CD8 T cell peripheral tolerance in vivo. *J Immunol* 174: 2046-2053.
323. Amorim, K. N., D. C. Chagas, F. B. Sulczewski, and S. B. Boscardin. 2016. Dendritic Cells and Their Multiple Roles during Malaria Infection. *J Immunol Res* 2016: 2926436.
324. Bachmann, A., M. Petter, R. Krumkamp, M. Esen, J. Held, J. A. Scholz, T. Li, B. K. Sim, S. L. Hoffman, P. G. Kremsner, B. Mordmuller, M. F. Duffy, and E.

Tannich. 2016. Mosquito Passage Dramatically Changes var Gene Expression in Controlled Human Plasmodium falciparum Infections. *PLoS Pathog* 12: e1005538.
325. Spence, P. J., W. Jarra, P. Levy, A. J. Reid, L. Chappell, T. Brugat, M. Sanders, M. Berriman, and J. Langhorne. 2013. Vector transmission regulates immune control of Plasmodium virulence. *Nature* 498: 228-231.
326. Stewart, M. J., R. J. Nawrot, S. Schulman, and J. P. Vanderberg. 1986. Plasmodium berghei sporozoite invasion is blocked in vitro by sporozoite-immobilizing antibodies. *Infect Immun* 51: 859-864.
327. Haque, A., S. E. Best, F. H. Amante, A. Ammerdorffer, F. de Labastida, T. Pereira, G. A. Ramm, and C. R. Engwerda. 2011. High parasite burdens cause liver damage in mice following Plasmodium berghei ANKA infection independently of CD8(+) T cell-mediated immune pathology. *Infect Immun* 79: 1882-1888.
328. Snow, R. W., J. F. Trape, and K. Marsh. 2001. The past, present and future of childhood malaria mortality in Africa. *Trends Parasitol* 17: 593-597.
329. Gupta, S., R. W. Snow, C. A. Donnelly, K. Marsh, and C. Newbold. 1999. Immunity to non-cerebral severe malaria is acquired after one or two infections. *Nat Med* 5: 340-343.
330. Gupta, S., R. W. Snow, C. Donnelly, and C. Newbold. 1999. Acquired immunity and postnatal clinical protection in childhood cerebral malaria. *Proc Biol Sci* 266: 33-38.
331. Baird, J. K. 1998. Age-dependent characteristics of protection v. susceptibility to Plasmodium falciparum. *Ann Trop Med Parasitol* 92: 367-390.
332. Dorfman, J. R., P. Bejon, F. M. Ndungu, J. Langhorne, M. M. Kortok, B. S. Lowe, T. W. Mwangi, T. N. Williams, and K. Marsh. 2005. B cell memory to 3 Plasmodium falciparum blood-stage antigens in a malaria-endemic area. *J Infect Dis* 191: 1623-1630.
333. Beeson, J. G., F. H. Osier, and C. R. Engwerda. 2008. Recent insights into humoral and cellular immune responses against malaria. *Trends Parasitol* 24: 578-584.
334. Astagneau, P., J. M. Roberts, R. W. Steketee, J. J. Wirima, J. P. Lepers, and P. Deloron. 1995. Antibodies to a Plasmodium falciparum blood-stage antigen as a tool for predicting the protection levels of two malaria-exposed populations. *Am J Trop Med Hyg* 53: 23-28.
335. Offeddu, V., V. Thathy, K. Marsh, and K. Matuschewski. 2012. Naturally acquired immune responses against Plasmodium falciparum sporozoites and liver infection. *Int J Parasitol* 42: 535-548.
336. Farouk, S. E., A. Dolo, S. Bereczky, B. Kouriba, B. Maiga, A. Farnert, H. Perlmann, M. Hayano, S. M. Montgomery, O. K. Doumbo, and M. Troye-Blomberg. 2005. Different antibody- and cytokine-mediated responses to Plasmodium falciparum parasite in two sympatric ethnic tribes living in Mali. *Microbes Infect* 7: 110-117.
337. Daou, M., B. Kouriba, N. Ouedraogo, I. Diarra, C. Arama, Y. Keita, S. Sissoko, B. Ouologuem, S. Arama, T. Bousema, O. K. Doumbo, R. W. Sauerwein, and A. Scholzen. 2015. Protection of Malian children from clinical malaria is associated with recognition of multiple antigens. *Malar J* 14: 56.
338. Addai-Mensah, O., M. Seidel, N. Amidu, D. J. Maskus, S. Kapelski, G. Breuer, C. Franken, E. Owusu-Dabo, M. Frempong, R. Rakotozandrindrainy, H. Schinkel, A. Reimann, T. Klockenbring, S. Barth, R. Fischer, and R. Fendel. 2016. Acquired immune responses to three malaria vaccine candidates and their

relationship to invasion inhibition in two populations naturally exposed to malaria. *Malar J* 15: 65.

339. Riley, E. M., and V. A. Stewart. 2013. Immune mechanisms in malaria: new insights in vaccine development. *Nat Med* 19: 168-178.

Chapter 6

Appendices

6.1 Vector maps

The vectors used to generate the constructs for gene deletion (*PbmaLS*_05 (-)), C-terminal tagging (*Pb*maLS_05 CT EGFP) and N-terminal tagging (*Pb*maLS_05 NT mCherry) are listed below. All vectors contain a gene (*Tg*DHFR/TS) coding for pyrimethamine resistance and an ampicillin resistance cassette. The b3D+ (275) vector contains an additional 3'UTR for C-terminal tagging. All vector maps were prepared using the Ape Plasmid Editor v2.0.49 software.

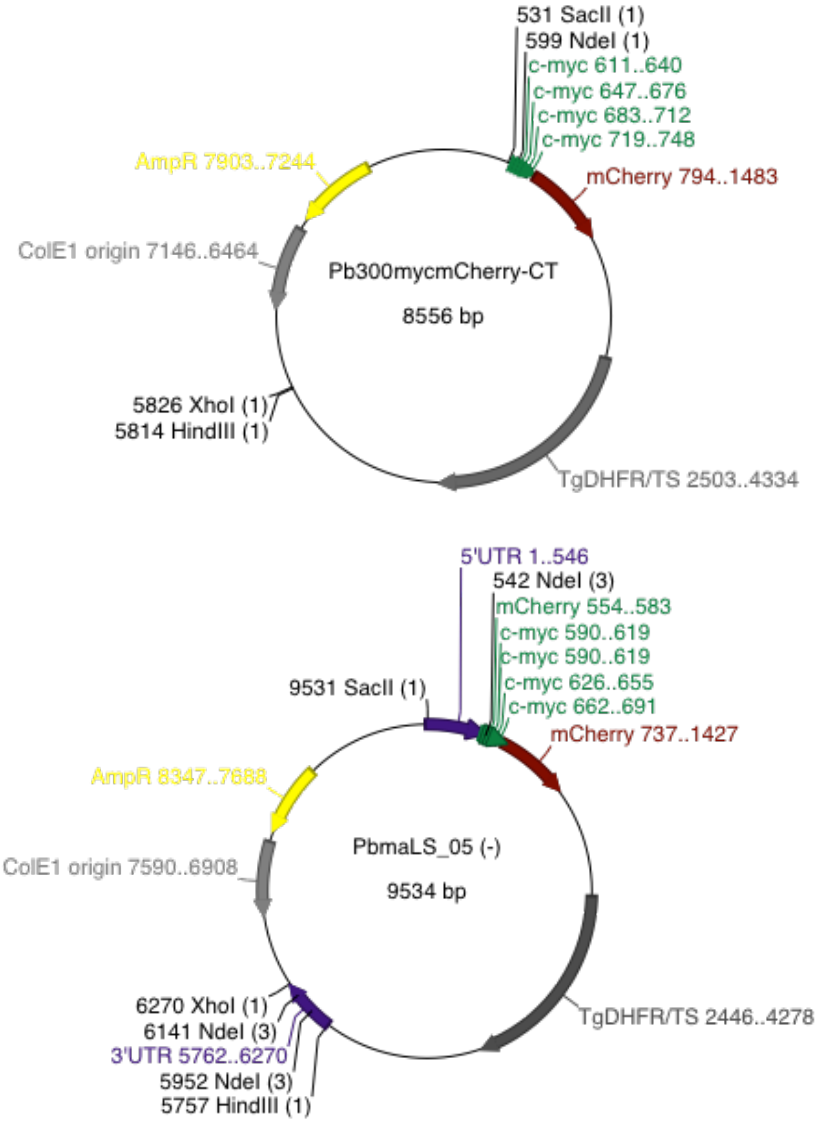

Figure 6.1A *PbmaLS*_05 (-) targeting vector. The *PbmaLS*_05 (-) targeting construct was prepared as described in 2.2.1.6, by insertion of 5'UTR and 3'UTR fragments (amplified using primers listed in 2.1.14.1) into the Pb300mycmCherry-CT vector.

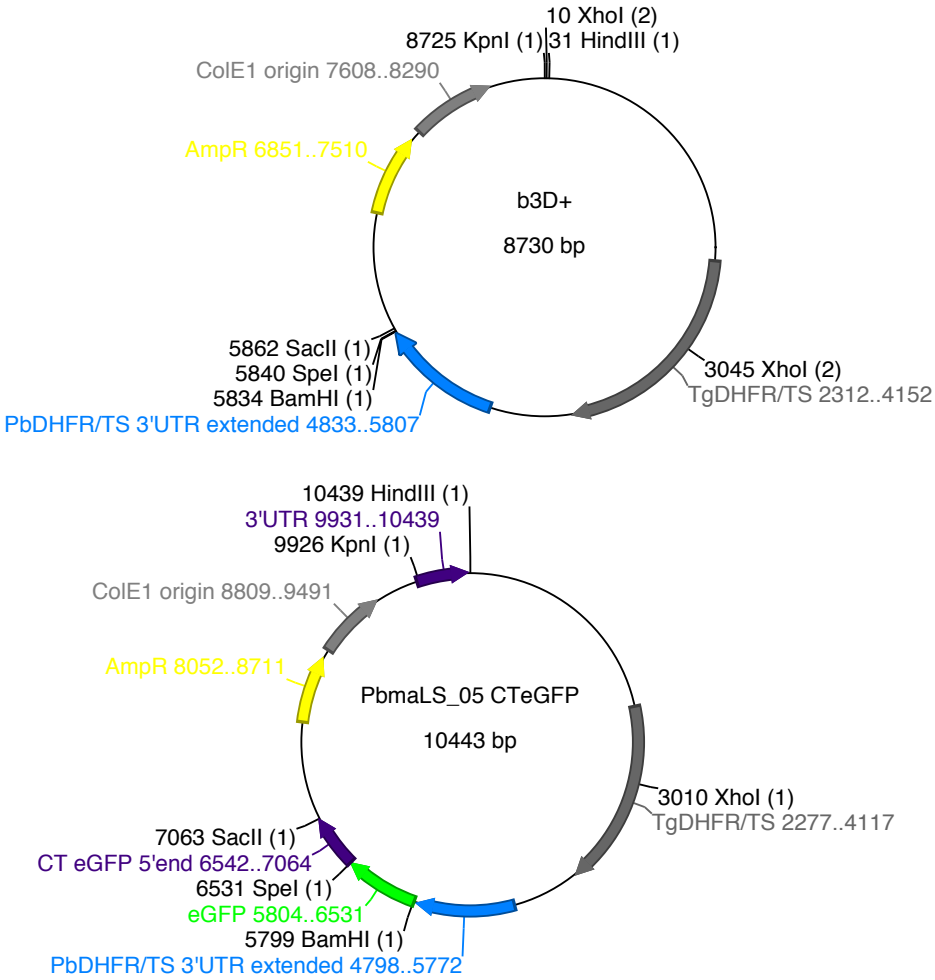

Figure 6.1B *Pb*maLS_05 CT EGFP tagging vector. The *Pb*maLS_05 CT EGFP construct was prepared as described in 2.2.1.7, by insertion of 3'UTR, CTEGFP 5'end and EGFP PCR fragments (amplified using primers listed in 2.1.14.2) into the b3D+ vector.

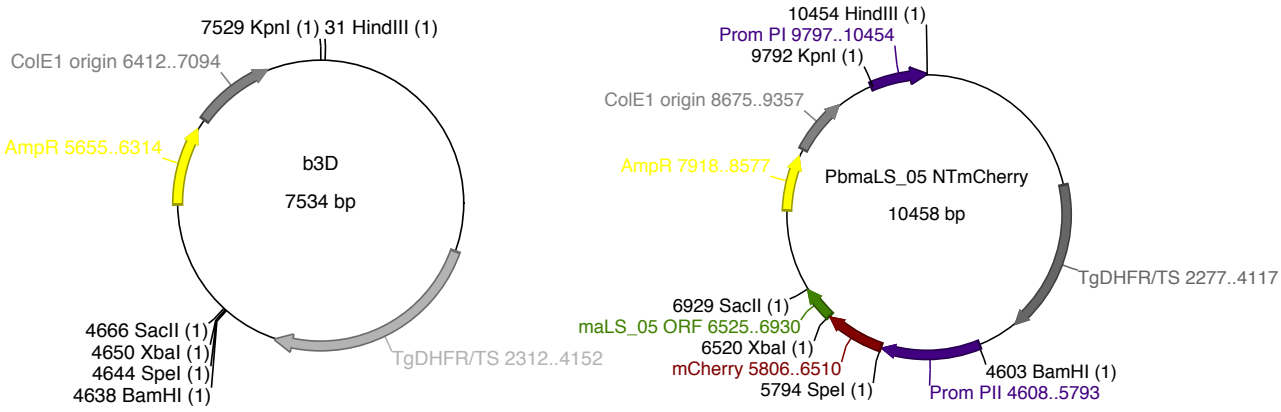

Figure 6.1C *Pb*maLS_05 NT mCherry tagging vector. The *Pb*maLS_05 NT mCherry construct was prepared as described in 2.2.1.8, by insertion of Prom PI, Prom PII, maLS_05 ORF and mCherry PCR fragments (amplified using primers listed in 2.1.14.3) into the b3D vector.

6.2 The Rapid Murine Coma and Behaviour Scale (RMCBS)

Label	Score	Description
Coordination		
Gait	0-2	Non-ataxic-normal
Balance	0-2	Non body extension-extends front feet on wall-entire body life
Exploratory Behaviour		
Motor Performance	0-2	None-2-3 corners explored in 90 seconds-explores 4 corners in 15 seconds
Strength and Tone		
Body Position	0-2	On side-hunched-full extension
Limb Strength	0-2	Hypotonic, no grasp-weak pull-back (front paw grasp only)-strong pull-back (active pull away, jerk away)
Reflexes and Self-Preservation		
Touch Escape	0-2	None-unilateral-instant and bilateral; 3 attempts
Pinna Reflex	0-2	None-unilateral-instant and bilateral; 3 attempts
Toe Pinch	0-2	None-unilateral-instant and bilateral; 3 attempts
Aggression	0-2	None-bite attempt with tail cut-bite attempt prior to tail cut, in 5 seconds
Hygiene-Related Behaviour		
Grooming	0-2	Ruffled, with swaths of hair out of place-dusty/piloerection-normal/clean with sheen

Figure 6.2. Rapid Murine Coma and Behavioural Scale (RMCBS). The RMCBS consists of 10 different parameters (each with a score of 0-2) and is used to grade mice, with 0 being the lowest and 2 being the highest. A mouse can receive a minimum score of 0 and a maximum score of 20 depending on the severity of disease symptoms.

6.3 Sequence alignment of maLS_05 in all Apicomplexan parasites

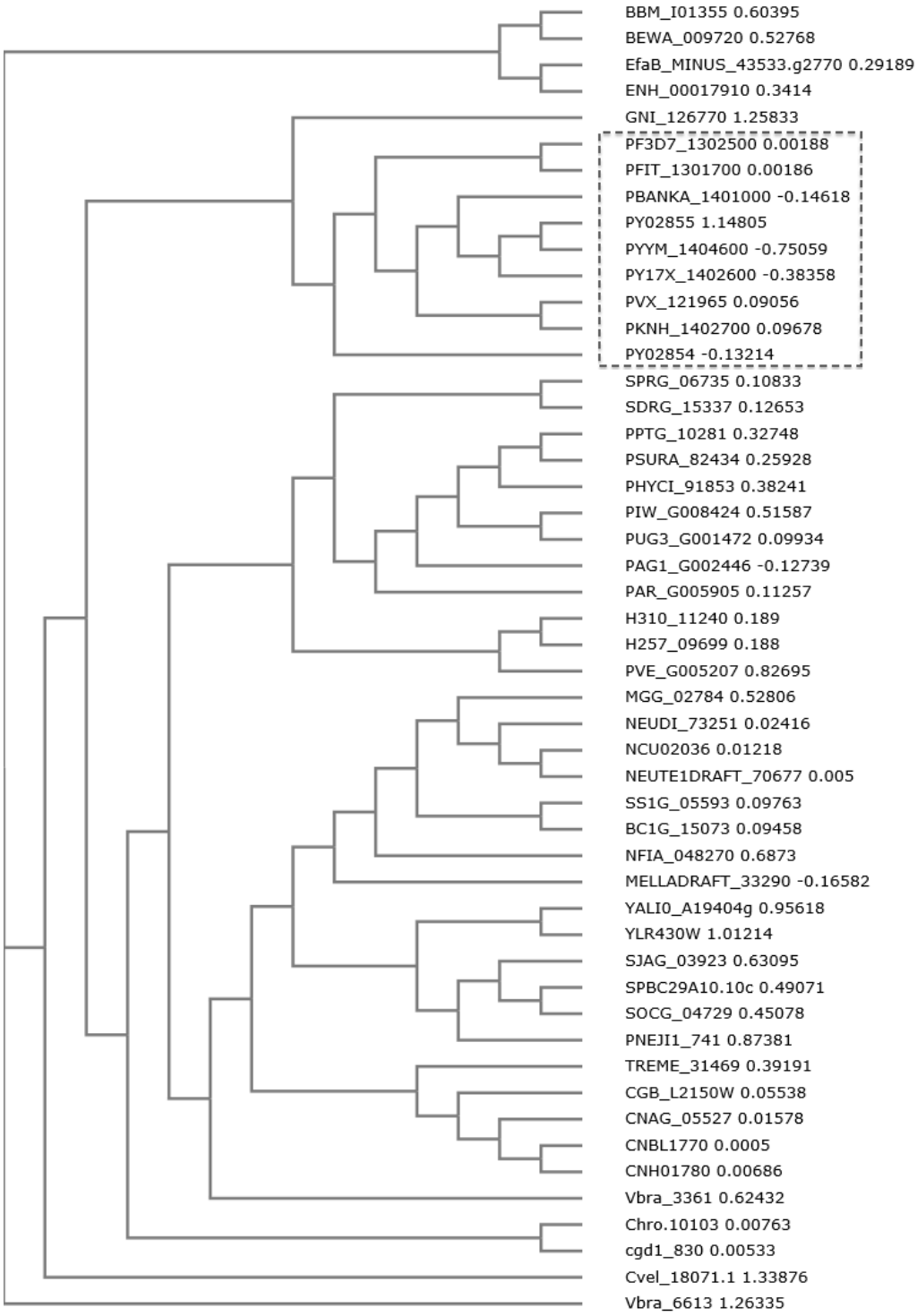

Figure 6.3 Sequence alignment of maLS_05 in all Apicomplexan parasites. The sequence alignment of protein sequences of maLS_05 in all species of Apicomplexa, was done using the online tool MUSCLE, from EMBL-EBI. The clustering of maLS_05 sequences from all *Plasmodium* species (highlighted by a box) suggests that it well conserved in *Plasmodium*.

6.4 Detection of the full-length *Pb*maLS_05 protein by Western Blotting.

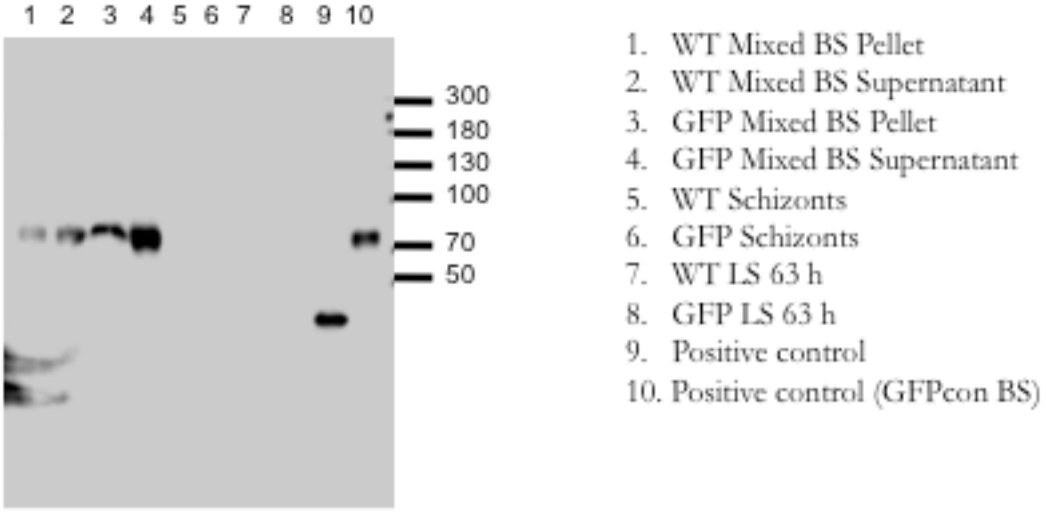

Figure 6.4. *Pb*maLS_05 could be detected *via* Western Blotting. Anti-GFP antibodies were used to detect and determine the size of the full length *Pb*maLS_05 protein. Protein extracts from all stages of the parasite life cycle were loaded onto a gradient gel along with a protein ladder and positive controls (extracts from *Pb*ANKA GFPcon blood stage parasites and sporozoites with CSP tagged GFP). Although free GFP was detected in the positive controls, no band corresponding to the predicted size of 303 kDa, was visible.

6.5 Cloning and transfection of *Pb*maLS_05 NT mCherry parasites and visualisation of *Pb*maLS_05 expression by live microscopy

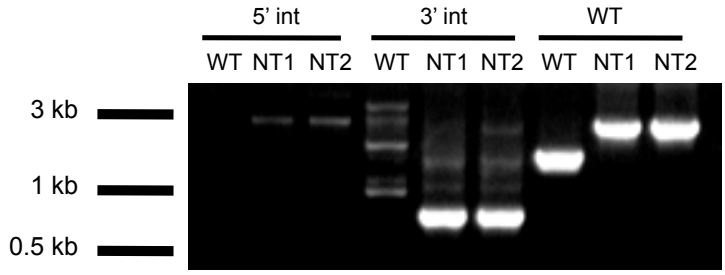

Figure 6.5A Cloning of *Pb*maLS_05 NT mCherry transfected parasites. Clonal populations of *Pb*maLS_05 NT mCherry parasites were isolated by limiting dilution of transfected parasites. Purity of the clones was established by PCR amplification of the WT genomic locus, i.e. primers binding to the genomic regions flanking the mCherry tag. Thus absence of a tag as seen in WT parasites results in a smaller fragment compared to that observed for NT1 and NT2 clones.

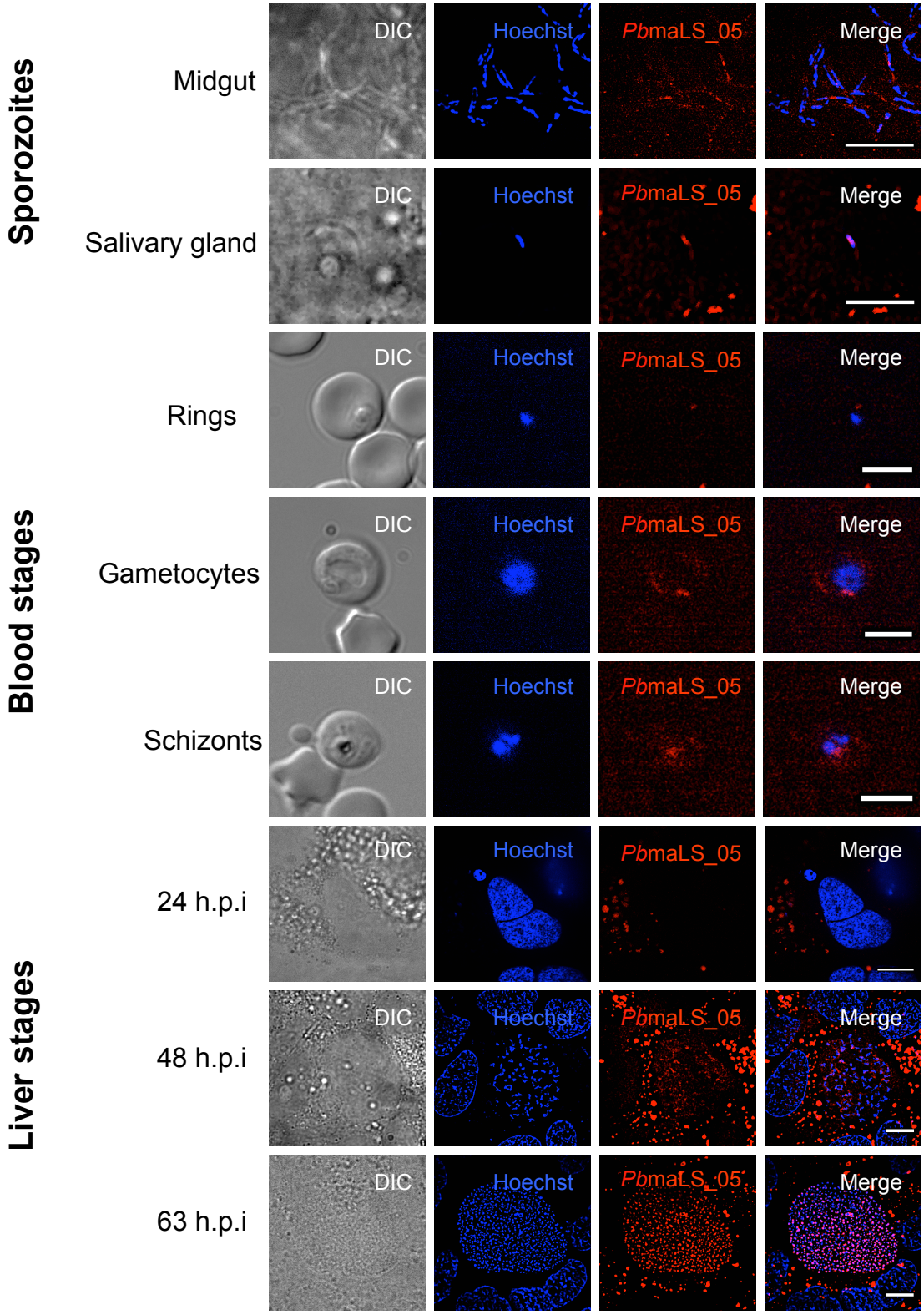

Figure 6.5B Live imaging of *Pb*maLS_05 NT mCherry parasites. Live imaging of *Pb*maLS_05 NT mCherry parasites showed a different expression and localisation pattern compared to *Pb*maLS_05 CT EGFP parasites. Although expression of *Pb*maLS_05 was again detected in liver and blood stage schizonts, the localisation was more punctuate as opposed to branched in the liver, and more cytoplasmic as opposed to organelle-specific in the blood. No expression was detected in sporozoites, early and mid-liver stages (24 and 48 h.p.i respectively). Scale bar = 10 μm.

6.6 Effect of azithromycin treatment on intra-hepatic stages of *Pb*ANKA WT parasites

*Pb*maLS_05 EGFP liver stage parasites treated with azithromycin displayed incomplete, abnormal nuclear division, unlike untreated controls. Based on previous studies, treatment of parasites with azithromycin specifically affects apicoplast inheritance and biogenesis (283). In order to validate my observation and exclude any effect of the of a C-terminal EGFP tag on nuclear division, *Pb*ANKA WT liver stages were treated with azithromycin. However, the nuclei were similar to that observed for *Pb*maLS_05 EGFP parasites, thus confirming that azithromycin does indeed have an effect on nuclear division.

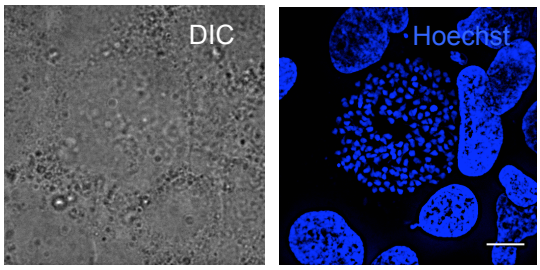

Figure 6.6 Live imaging of azithromycin treated *Pb*ANKA WT parasites. Liver stages of *Pb*ANKA WT parasites were treated with azithromycin for 52 hours and then imaged live. Hoechst was used for visualization of the nuclei. Azithromycin treated liver stage parasites display abnormal nuclear division in contrast to untreated parasites, thus suggesting an effect of azithromycin treatment on nuclear division. Scale bar = 10 μm.

6.7 Control experiments to test if tagging *Pb*maLS_05 has an effect on ECM outcome

As additional control experiments, mice were injected with 10^4 sporozoites of *Pb*maLS_05 CT myc, *Pb*maLS_05 CT EGFP or *Pb*maLS_05 NT mCherry tagged parasites, in order to verify if the absence of ECM was exclusively due to deletion of *PbmaLS*_05. Moreover, the experiment validated the integrity of the transfection procedure and verified if tagging interfered with parasite growth. Interestingly, all infected mice except those injected with *Pb*maLS_05 NT mCherry parasites developed ECM, on days similar to WT infected mice thus excluding any effect of the C-terminal tag on parasite viability. However, the effect of the N-terminal tag on ECM outcome coupled to miss-targeting of the *Pb*maLS_05 protein in blood stages, further implicated a role for *Pb*maLS_05 in the development of ECM.

Parasite line injected	No. of sporozoites injected i.v.	No. of mice	ECM (%)
*Pb*maLS_05 CT myc	10^4	6	5/6 (83 %)
*Pb*maLS_05 CT EGFP	10^4	4	2/4 (50 %)
*Pb*maLS_05 NT mCherry	10^4	3	0/3 (0%)

6.8 Gating strategy for lymphocytes, CD4$^+$ T cells, CD8$^+$ T cells and IFN-γ$^+$ CD8$^+$ T cells.

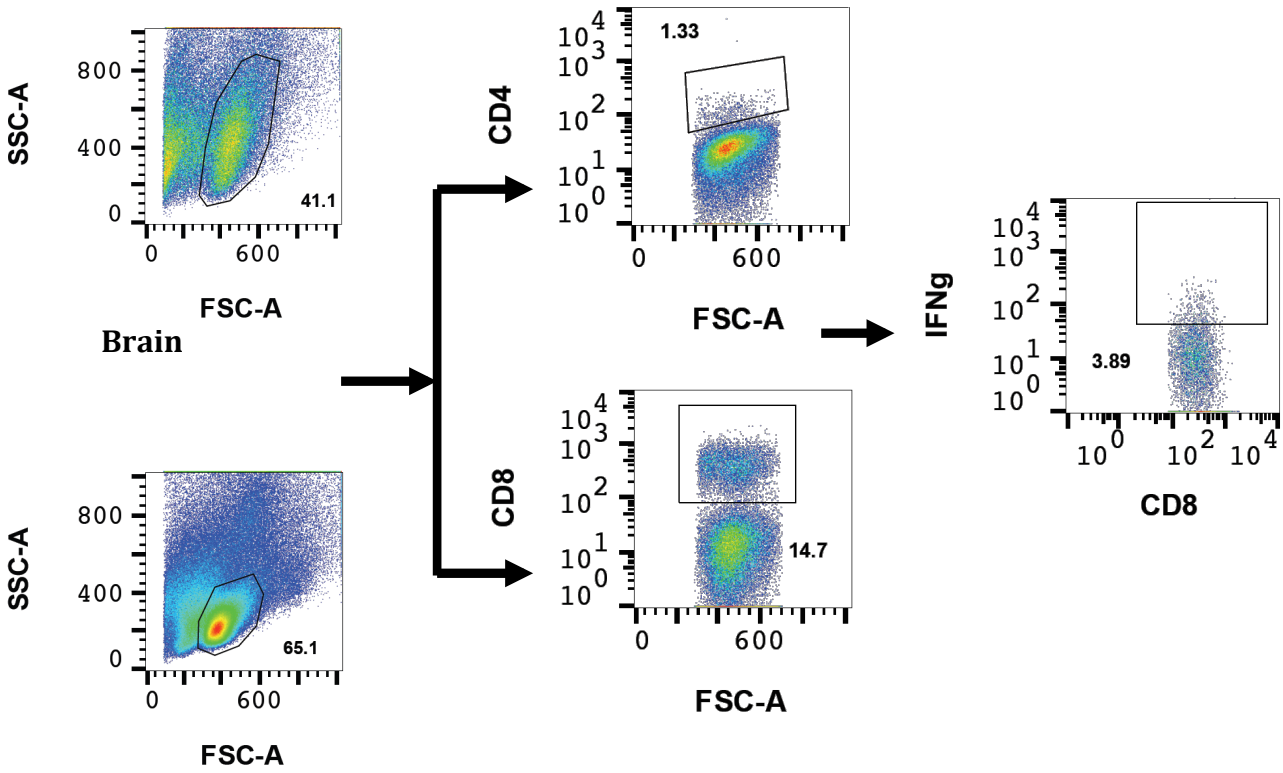

Figure 6.7 Gating strategies for lymphocytes and T cell subsets. Lymphocytes from the brains and spleens of infected mice were isolated and stained for CD4, CD8 and IFN-γ. FSC versus SSC was used to first gate on the lymphocyte population. Lymphocytes were sub-gated for T cells by plotting FSC with either CD4 or CD8. In order to determine the percentage of IFN-γ$^+$ CD8$^+$ T cells, total CD8 T cells were plotted against IFN-γ. The FACS analysis was performed using FlowJo v10.

6.9 ELISpot with predicted CD8 T cell epitopes of *Pb*maLS_05.

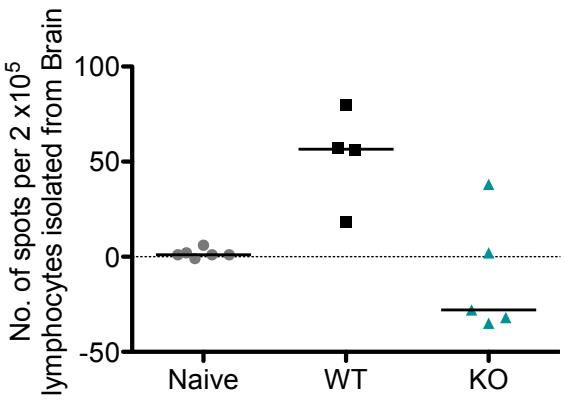

Figure 6.8. *Pb*maLS_05 is presented during a sporozoite infection. Naïve splenocytes were pulsed with *Pb*maLS_05 peptides or unpulsed and cultured *ex vivo* with brain-infiltrating lymphocytes of WT and KO sporozoite infected mice. Brain derived lymphocytes of WT infected mice responded to *Pb*maLS_05 epitopes by producing IFN- γ$^+$ and were identified by the assay. Each blue spot represents one IFN-γ$^+$ producing cell. In contrast to WT, lymphocytes isolated from KO sporozoite infected mice did not respond to stimulation with *Pb*maLS_05 epitopes.

Acknowledgements

I would like to express my gratitude to the following people, who have in some way or another contributed to the completion of this thesis;

-My supervisor, **Ann-Kristin Mueller** for her constant support and guidance throughout the duration of my PhD. Thank you for your encouragement and positivity, especially when experiments did not work out as planned.

-My TAC members, **Prof. Michael Lanzer**, **Prof. Philipp Wiedemann** and **Prof. Frederich Frischknecht** for their advice on experiments.

-Prof. Alexander Dalpke and **Prof. Viktor Umansky** for agreeing to be a part of my defence committee.

-Shanshan Howland and **Laurent Renia** for enthusiastically collaborating on the cross-presentation assay.

-Angelika Hoffmann and **Manuel Fischer** for the MRI imaging and analysis.

-HBIGS for the courses and **Miriam Griesheimer** for help with all the administrative paperwork.

-Jenny and **Miriam** for the mosquito breeding and squeezing in cages at the last minute.

All the former and current members of the lab;

-Britta, for the initial help with cloning and transfections. Thank you for all your help during my first year in Heidelberg, especially with the endless list of German translations.

-Kirsten, for being the 'go to' person whenever there were questions. Thank you for your willingness to discuss data and help with experiments. You're literally the nicest 'Freiburger' I know!

-Klara, for proofreading parts of this thesis and making useful suggestions. Thank you for your innovative ideas, 'blah blah blah' conversations and weekend plans.

-Maria, I'd probably still be sitting under the hood harvesting mice, if you weren't around. Thank you for always sticking until the end of the experiment, even if the end was at 7 am. And thanks for all the crazy times outside the lab.

-Matt, for patiently introducing me to ECM. Thank you for all the lengthy discussions about the data and immunology in general.

-Roland, for critical discussions about data interpretation and the importance of paying attention to detail.

-Julia, for all the funny stories and constant supply of stamps.

-Christianne, **Aina**, **Yvonne**, **Florian**, **Franzi, Johannes** and **Kamil**, for the good times both in an outside the lab.

-Vera Mitesser and **Roos de Jong**, for their valuable help on different experiments.

Special thanks to;

-Martin Dittmer, for the dumbed down version of statistics. Thanks to you my data actually has stars!

-Tina, for all the discussions on HCM and for being so spontaneous.

-Vihang and Kartik, for the Indian dinners, nostalgic talks about Mumbai and the constant reminder about my 'incorrect' Marathi accent.

-Simon & Mercine Dias and Sheena Pinto for never letting me miss home. Thanks to Sheena for help with proofreading and formatting of this thesis along with scientific discussions on just about anything and for helping me keep my sanity this past year!

- Dr. Deshpande, Dr. Shastry and **Dr. Swammy** for inspiring my interest in malaria.

-Dogel Lepcha for inspiring my interest in science.

-My family and **friends** in India for keeping me grounded.

-This thesis is dedicated to my mum and dad.